12-5-2018 5:30 PM

Acromial Insufficiency Fractures in Reverse Total Shoulder Arthroplasty: A Biomechanical Study

Alicia Kerrigan, *The University of Western Ontario*

Supervisor: Athwal, George, *The University of Western Ontario*
: Johnson, Jim, *The University of Western Ontario*

A thesis submitted in partial fulfillment of the requirements for the Master of Science degree in Surgery

Abstract

Reverse total shoulder arthroplasty (RTSA) is becoming increasingly utilized in the aging population, with a growing list of surgical indications including rotator cuff tear arthropathy, proximal humerus fractures, and revision arthroplasty. Acromial insufficiency fractures following RTSA are poorly understood, difficult to diagnose, and associated with inferior clinical outcomes. There exists a lack of knowledge in the literature regarding the etiology of post-operative acromial fractures. The purpose of this study is to evaluate the role of implant parameters on acromial strain following RTSA.

Using a cadaveric model, a custom designed modular RTSA system was implanted that allowed for evaluation of modifiable parameters including glenoid lateralization, humeral lateralization, and neck-shaft angle. Acromial strain was measured by 4 strain gauges placed along the acromion and scapular spine. Total deltoid force was measured as a secondary outcome. All specimens were tested in 4 planes of elevation including 0° and 90° abduction and 0° and 90° forward flexion.

Lateralization of the glenoid component was found to increase acromial strain with the arm in 0° forward flexion. Lateralization of the humeral component was found to decrease acromial strain with the arm in abduction. Neck-shaft angle had no significant effect on acromial strain. Disruption of the coracoacromial (CA) ligament had no significant effect on acromial strain. The findings of this study have clinical importance in the future research and design of RTSA implants. A continued focus needs to be placed on the evaluation of additional implant parameters and their role on acromial fractures following RTSA.

Keywords

Reverse total shoulder arthroplasty, biomechanics, acromial fracture, glenoid lateralization, humeral lateralization, neck-shaft angle, coracoacromial ligament.

Co-Authorship Statement

Chapter 1: Alicia Kerrigan – sole author

Chapter 2: Alicia Kerrigan – study design, data collection, statistical analysis, manuscript preparation

Jason Lockhart – study design, data collection, statistical analysis

Jacob Reeves – study design, data collection, statistical analysis,

Dan Langohr – study design, data collection, statistical analysis, reviewed manuscript

Jim Johnson – study design, reviewed manuscript

George Athwal – study design, specimen preparation, reviewed manuscript

Chapter 3: Alicia Kerrigan – study design, data collection, statistical analysis, manuscript preparation

Jason Lockhart – study design, data collection, statistical analysis

Jacob Reeves – study design, data collection, statistical analysis

Dan Langohr – study design, data collection, statistical analysis, reviewed manuscript

Jim Johnson – study design, reviewed manuscript

George Athwal – study design, specimen preparation, reviewed manuscript

Chapter 4: Alicia Kerrigan – study design, data collection, statistical analysis, manuscript preparation

Jason Lockhart – study design, data collection, statistical analysis

Jacob Reeves – study design, data collection, statistical analysis

Dan Langohr – study design, data collection, statistical analysis, reviewed manuscript

Jim Johnson – study design, reviewed manuscript

George Athwal – study design, specimen preparation, reviewed manuscript

Chapter 5: Alicia Kerrigan – sole author

Acknowledgments

This Master's thesis would not have been possible without the support and hard work of many people. I'd like to acknowledge and thank my main supervisors, Dr. George Athwal and Dr. Jim Johnson for their guidance, support, and undeniable expertise. The Hand and Upper Limb biomechanics research lab provided me with all the resources necessary to complete this project. Thank you to Dan Langohr, Jacob Reeves and Jason Lockhart for their commitment to this project and countless hours spent testing in the lab. And finally, a huge thank you to my family, friends and loved ones who provided me with unwavering support and sanity as I completed this Master's thesis while undergoing my Orthopaedic Surgery residency training.

Table of Contents

Abstract ii

Co-Authorship Statement iii

Acknowledgments iv

Table of Contents v

List of Tables ix

List of Figures x

Chapter 1 1

1 Introduction 1

1.1 The Shoulder 1

1.1.1 Osteology 1

1.1.2 Kinematics of the Shoulder 6

1.1.3 Static Stabilizers of the Shoulder 7

1.1.4 Dynamic Stabilizers of the Shoulder 9

1.2 Rotator Cuff Tear Arthropathy 13

1.2.1 Overview 13

1.2.2 Clinical Manifestations 15

1.2.3 Treatment Options 15

1.3 Reverse Total Shoulder Arthroplasty 15

1.3.1 Overview 15

1.3.2 Importance of Deltoid 17

1.3.3 Indications 18

1.3.4 Outcomes 19

1.3.5 Complications 20

1.3.6 RTSA Surgical and Implant Considerations 25

1.4 Thesis Rationale 31

1.5 Thesis Objectives 32

1.6 Thesis Hypothesis 33

1.7 Thesis Overview 33

1.8 References 34

Chapter 2 47

2 The Role of Glenoid and Humeral Lateralization on Acromial Strain 47

2.1 Introduction 47

2.2 Materials and Methods 50

2.2.1 Specimen Preparation 50

2.2.2 Shoulder Simulator 56

2.2.3 Testing Protocol 57

2.2.4 Outcome Variables 58

2.2.5 Statistical Analysis 58

2.3 Results 59

2.3.1 Acromial Strain 59

2.3.2 Total Deltoid Force 64

2.4 Discussion 66

2.4.1 Glenoid Lateralization 67

2.4.2 Humeral Lateralization 68

2.4.3 Strengths and Limitations 69

2.5 Conclusions 70

2.6 References 71

Chapter 3 80

3 The Role of Neck-Shaft Angle on Acromial Strain 80

3.1 Introduction 80

3.2 Materials and Methods 82
3.2.1 Specimen Preparation 82
3.2.2 Shoulder Simulator 84
3.2.3 Testing Protocol 85
3.2.4 Outcome Variables 85
3.2.5 Statistical Analysis 86
3.3 Results 86
3.3.1 Acromial Strain 86
3.3.2 Total Deltoid Force 88
3.4 Discussion 89
3.4.1 Strengths and Limitations 90
3.5 Conclusions 91
3.6 References 92
Chapter 4 100
4 The Effect of Coracoacromial Ligament State on Acromial Strain 100
4.1 Introduction 100
4.2 Materials and Methods 103
4.2.1 Specimen Preparation 103
4.2.2 Shoulder Simulator 105
4.2.3 Testing Protocol 106
4.2.4 Outcome Variables 107
4.2.5 Statistical Analysis 107
4.3 Results 108
4.3.1 Acromial Strain 108
4.3.2 Total Deltoid Force 110
4.4 Discussion 111

4.4.1 Strengths and Limitations ... 112

4.5 Conclusions ... 113

4.6 References ... 114

Chapter 5 ... 120

5 Thesis Conclusions ... 120

5.1 *Summary of Chapter 2:* The Role of Glenoid and Humeral Lateralization on Acromial Strain ... 121

5.2 *Summary of Chapter 3*: The Role of Neck-Shaft Angle on Acromial Strain ... 122

5.3 *Summary of Chapter 4:* The Effect of Coracoacromial Ligament State on Acromial Strain ... 123

5.4 Future Directions ... 123

5.5 Significance ... 124

APPENDIX A: Glossary of Terms ... 126

Curriculum Vitae ... 132

List of Tables

Table 5-1: Commercial Implant Parameters..125

List of Figures

Figure 1-1: The Shoulder Joint 2

Figure 1-2: Osseous Anatomy of the Humerus..3

Figure 1-3: Anterior View of the Scapula 4

Figure 1-4: Posterior View of the Scapula 4

Figure 1-5: Overview of Acromial Morphology..5

Figure 1-6: Soft Tissue Stabilizers of the Shoulder 7

Figure 1-7: Dynamic Stabilizers of the Shoulder...9

Figure 1-8: Anatomical Segments of the Deltoid Muscle Origin 12

Figure 1-9: Rotator Cuff Tear Arthropathy (early) 14

Figure 1-10: Rotator Cuff Tear Arthropathy (advanced) 14

Figure 1-11: Reverse Total Shoulder Arthroplasty 16

Figure 1-12: Deltoid Biomechanics Following RTSA Implantation 17

Figure 1-13: Levy Classification of Acromial Fractures..23

Figure 1-14: Glenoid Lateralization...29

Figure 1-15: Humeral Lateralization..29

Figure 1-16: Neck-shaft Angle 30

Figure 2-1: Tagged Rotator Cuff Tendons 51

Figure 2-2: Tagged Heads of Deltoid Origin..52

Figure 2-3: Illustration depicting the anatomic location of the strain gauges on a right scapula 55

Figure 2-4: Strain gauge placement as seen on the right scapular spine and acromion of a study specimen 55

Figure 2-5: Shoulder Simulator Setup 56

Figure 2-6: Averaged Acromial Strain for All Strain Gauges 59

Figure 2-7: The Effect of Glenoid Lateralization on Acromial Strain 61

Figure 2-8: The Effect of Humeral Lateralization on Acromial Strain 63

Figure 2-9: The Effect of Glenoid Lateralization on Total Deltoid Force 64

Figure 2-10: The Effect of Humeral Lateralization on Total Deltoid Force 65

Figure 3-1: Strain Gauge Placement 84

Figure 3-2: The Effect of Neck-Shaft Angle on Acromial Strain 87

Figure 3-3: The Effect of Neck-Shaft Angle on Total Deltoid Force 88

Figure 4-1: Anatomy of the Coracoacromial Ligament 101

Figure 4-2: Strain Gauge Placement 105

Figure 4-3: The Effect of Coracoacromial Ligament State on Acromial Strain 109

Figure 4-4: The Effect of Coracoacromial Ligament State on Total Deltoid Force 110

Chapter 1

1 Introduction

The purpose of this thesis is to biomechanically assess the effect of reverse shoulder arthroplasty implant parameters on acromial strain and acromial fractures. This chapter will focus on providing an overview of the anatomy of the shoulder, including shoulder biomechanics. The concept of rotator cuff arthropathy and its treatments options will be introduced. A focus will be placed on reverse total shoulder arthroplasty, including its indications and complications. Finally, the rationale, objectives, and thesis hypothesis will also be reviewed.

1.1 The Shoulder

The shoulder, most commonly thought of as the glenohumeral joint, is a diarthrodial multi-axial joint with the greatest mobility of any joint in the body. It is made up of the articulation of a large humeral head and a relatively small glenoid fossa and relies on a complex network of ligamentous and muscular stabilizers. As a ball-in-socket-like joint, it affords a large arc of motion including forward flexion, extension, internal rotation, external rotation, abduction and adduction and circumduction (Rockwood & Matsen, 2017).

1.1.1 Osteology

The osteology of the shoulder girdle as a whole includes the humerus, scapula, and clavicle (Figure 1-1). This includes four major articulations: the glenohumeral joint – between the humeral head and glenoid; the acromioclavicular joint – between the scapula and clavicle; the sternoclavicular joint – between the clavicle and sternum; and the scapulothoracic articulation – between the scapula and the posterior thoracic rib cage (Terry & Chopp, 2000).

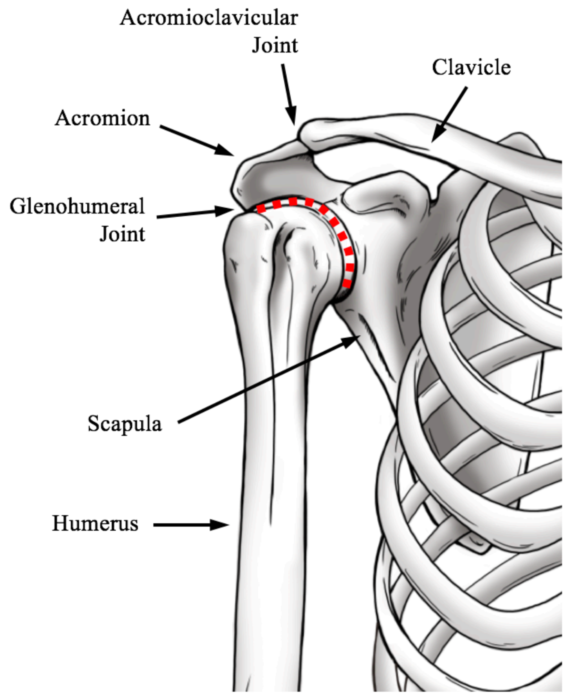

Figure 1-1: The Shoulder Joint

This illustration depicts the pertinent osteology of the shoulder girdle including the glenohumeral joint (red dashed line).

1.1.1.1 The Humerus

The humerus is the largest and longest bone of the upper extremity. Anatomically, the proximal humerus is made up of the humeral head, the greater and lesser tuberosities, the bicipital groove, and the proximal humeral shaft. The anatomical neck of the humerus is defined by the junction of the articular surface of the head and the greater and lesser tuberosities. At the anatomical neck, the head is angled at an average of 135° relative to the shaft (neck-shaft angle) and is retroverted relative to the transepicondylar axis of the distal humerus (Jeong, Bryan & Iannotti, 2009). The surgical neck lies just below the greater and lesser tuberosities. The tuberosities are important osseous landmarks for the insertion of the rotator cuff tendons. Between them lies the bicipital groove, which serves as the tract for the long head of the biceps. Finally, the deltoid muscle inserts distally into the deltoid tuberosity, a prominence along the anterolateral surface of the humeral shaft (Swarm, Mahar, Weichel & Pedowitz, 2007).

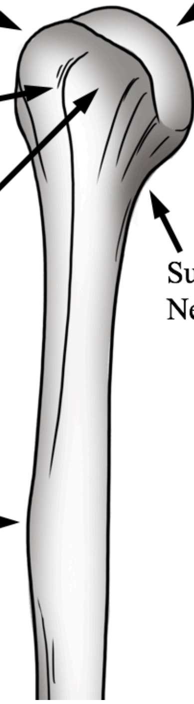

Figure 1-2: Osseous Anatomy of the Humerus

Illustration depicting the relevant osseous anatomy of the proximal humerus.

1.1.1.2 The Scapula

The scapula is a broad, triangular shaped bone located along the posterolateral aspect of the thorax. It makes up the posterior aspect of the shoulder girdle. Its main function serves as muscular attachment. Along its anterior surface lies the subscapular fossa, and posteriorly the scapular spine separates the supraspinous fossa superiorly and the infraspinous fossa inferiorly (Figures 1-2 & 1-3). The scapular spine serves as a site of insertion for the trapezius muscle, and laterally as a site of origin for the posterior third of the deltoid muscle. The scapular spine then continues superiorly and laterally to form the base of the acromion (Swarm, Mahar, Weichel & Pedowitz, 2007).

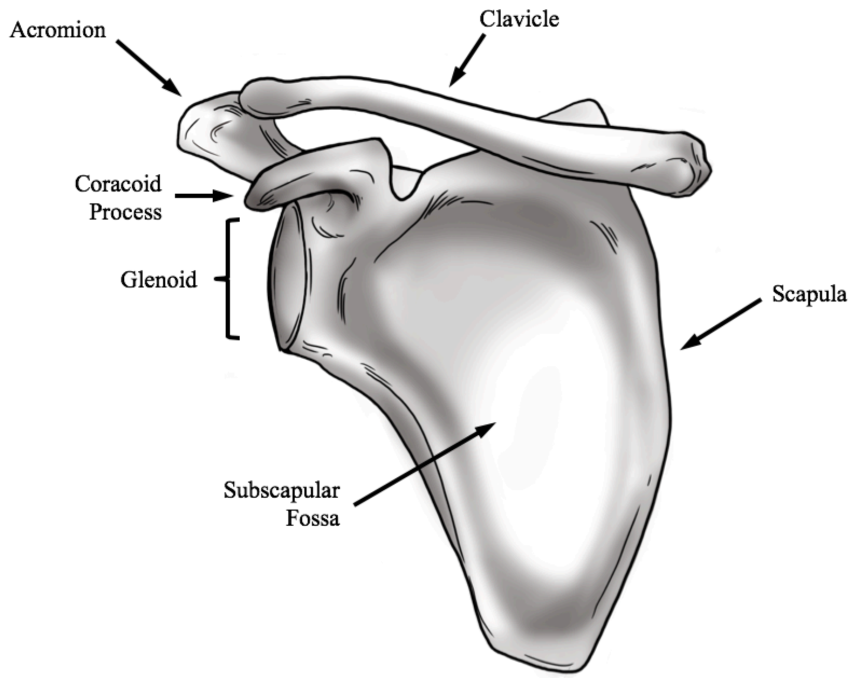

Figure 1-3: Anterior View of the Scapula

Illustration depicting the osseous anatomy of the anterior right scapula and clavicle.

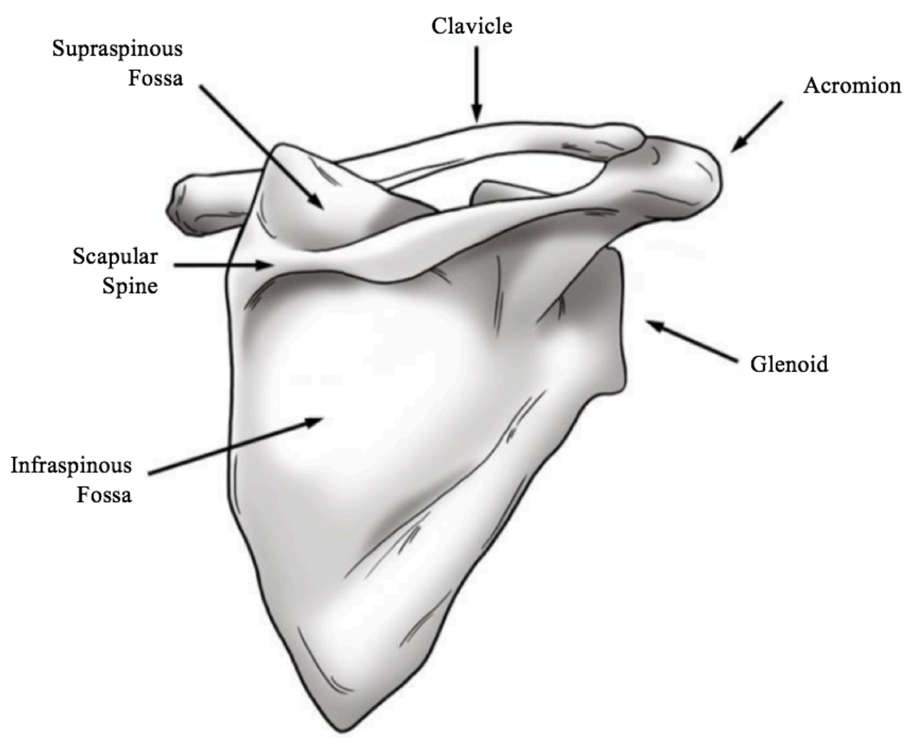

Figure 1-4: Posterior View of the Scapula

Illustration depicting the osseous anatomy of the posterior right scapula and clavicle.

The glenoid fossa is located laterally along the scapula, inferior to the acromion. In relation to the scapular plane, the glenoid fossa is retroverted an average of 2° to 10° and tilted superiorly an average of 5°. The scapular plane itself lies 30° to 45° anterior to the coronal plane of the body. The glenoid fossa acts as the articulating surface of the glenohumeral joint and is covered in hyaline cartilage. The articular surface is concave to accommodate the spherical humeral head, although it is only one third to one fourth the size of the humeral head. This stability of the glenohumeral joint relies heavily on the surrounding complex static and dynamic soft tissue stabilizers. (Terry & Chopp, 2000).

The acromion – the structure of primary interest in this work – forms a flat, lateral projection that acts as a portion of the roof overlying the space for the rotator cuff. Laterally, it articulates with the distal clavicle through the acromioclavicular (AC) ligament, forming the AC joint. It serves as a site of attachment for the trapezius muscle superiorly, and laterally as the origin of the middle third of the deltoid muscle. It serves as a prominent lever arm for deltoid muscle function. Three different acromial morphologies have been described including type I (flat), type II (curved), and type III (hooked). The variations in morphology have implications in subacromial impingement and rotator cuff pathology (Balke et al., 2013).

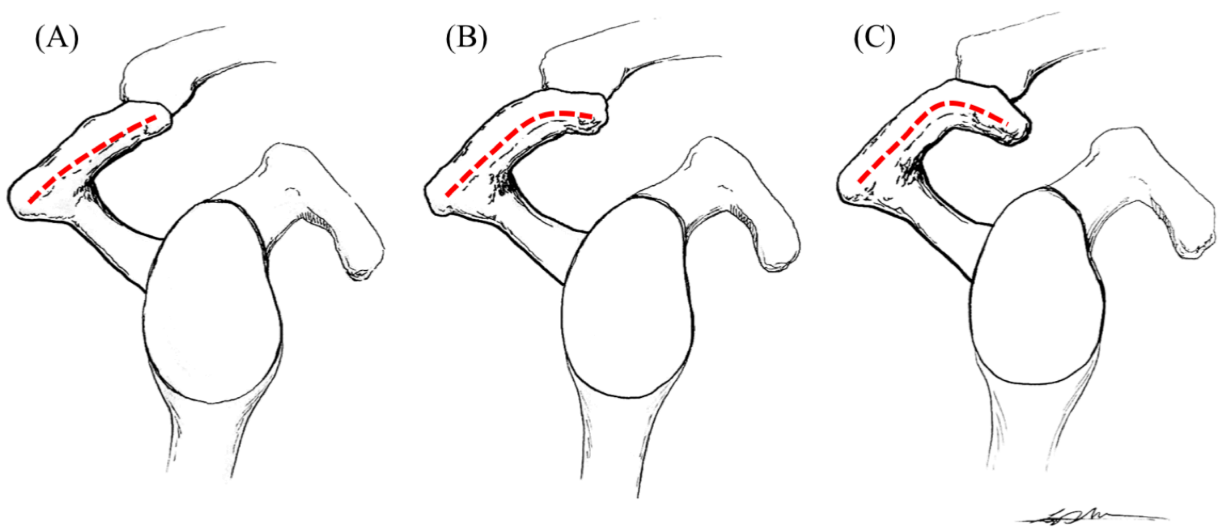

Figure 1-5: Overview of Acromial Morphology

Illustration depicting variations in acromial morphology including (A) type I (flat), (B) type II (curved), and (C) type III (hooked).

1.1.1.3 The Clavicle

The clavicle is an "S-shaped" bone that connects to the shoulder girdle laterally via the acromioclavicular joint, and to the axial skeleton medially via the sternoclavicular joint. It serves as a site of muscular attachment, including the anterior third of the deltoid muscle and the pectoralis major. It has multiple ligamentous attachment sites, which aid in its function as a strut to stabilize the shoulder from inferior migration (Terry & Chopp, 2000).

1.1.2 Kinematics of the Shoulder

The shoulder is one of the most mobile joints in the body. As previously described, the articulation of the large humeral head with the small glenoid fossa allows for a large arc of motion. Again, as discussed, this articulation relies heavily on the complex network of surrounding soft tissues which affords the shoulder joint stability.

Motion through the glenohumeral joint is achieved through both glenohumeral and scapulothoracic motion, a concept known as scapulohumeral rhythm. Inman et al. defined the ratio of glenohumeral to scapulothoracic motion to be 2:1, although a wide range of ratios have been reported (Inman, Saunders & Abbott, 1996).

Planes of motion of the shoulder include forward flexion and extension in the sagittal plane, abduction and adduction in the coronal plane, and internal and external rotation in the axial plane. The humerus can also be abducted in the scapular plane, known as "scaption". Through the intricate network of static and dynamic stabilizers, the healthy shoulder affords a large arc of motion without compromising stability (Lippitt et al., 1993; Abboud & Soslowsky, 2002; Hurov, 2009).

1.1.3 Static Stabilizers of the Shoulder

The glenohumeral joint of the shoulder, as noted earlier, is inherently unstable given the large spherical humeral head that articulates with the small glenoid fossa. As such, this joint relies heavily on surrounding soft tissue stabilizers. During range of motion, static stabilizers of the shoulder come under tension and limit any extreme joint angles. Static soft tissue stabilizers of the shoulder include the glenoid labrum, the joint capsule, and the ligaments (Terry & Chopp, 2000). Figure 1-6 illustrates the soft tissue anatomy of the glenohumeral joint and surrounding stabilizers of the shoulder.

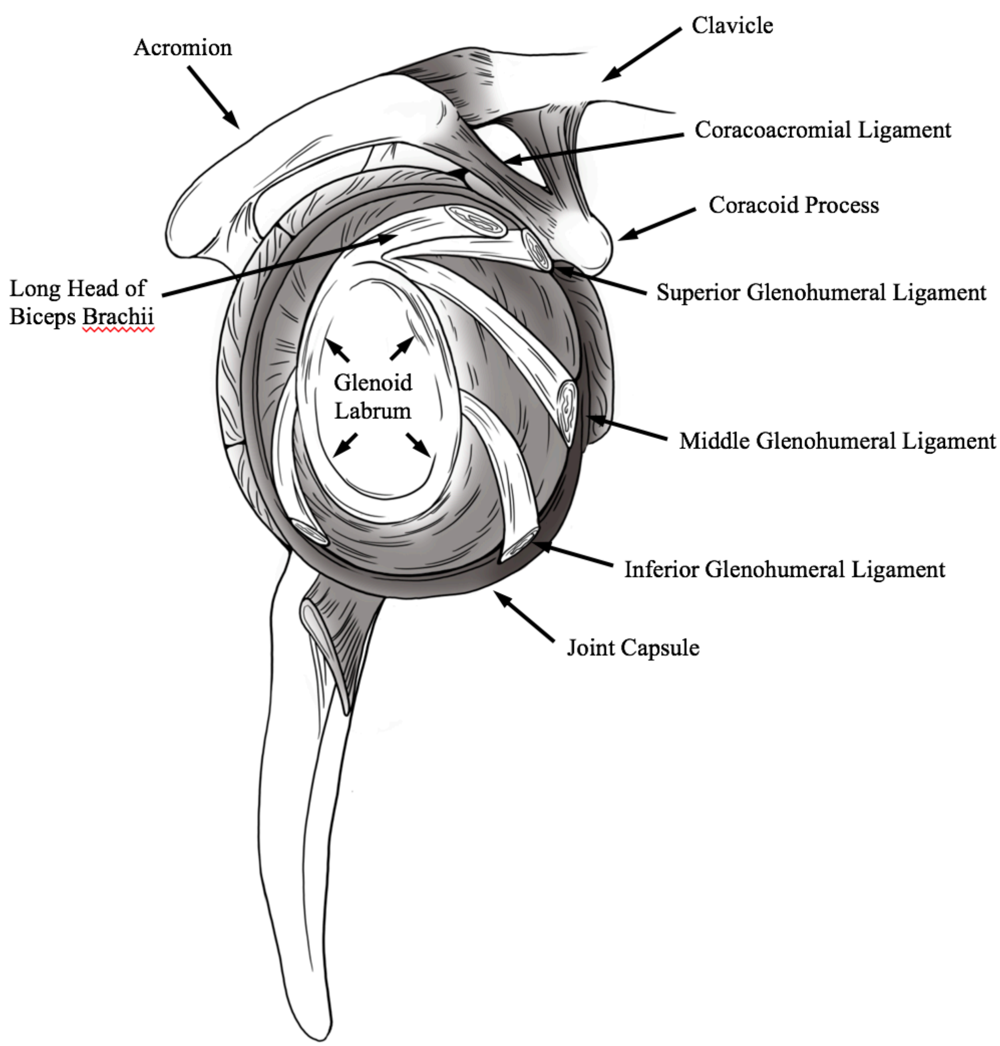

Figure 1-6: Soft Tissue Stabilizers of the Shoulder

Illustration depicting a sagittal view of the right scapula and soft tissue stabilizers surrounding the glenohumeral joint.

The glenoid labrum is a circumferential fibrous ring attached to the glenoid articular margin. The labrum serves to deepen the glenoid socket, increasing the contact surface area of the glenohumeral joint, thereby enhancing stability. The labrum also serves as an anchor point for numerus glenohumeral ligaments, as well as the long head of the biceps tendon (Swarm, Mahar, Weichel & Pedowitz, 2007).

The joint capsule is a continuous fibrous cylinder surrounding the glenohumeral joint that extends from the glenoid labrum down to the neck of the humerus. At rest, it is a relatively loose, redundant structure that variably tightens upon glenohumeral range of motion. The joint capsule is intimately related to the glenohumeral ligaments, which arise from three focal areas of capsular thickening. These ligaments provide additional stability to the glenohumeral joint during range of motion (Clark & Harryman, 1992).

The superior glenohumeral ligament (GHL) extends from the supraglenoid fossa to the lesser tuberosity, running in line with the coracohumeral ligament. It functions to stabilize the humeral head from inferior and posterior translation while the arm is adducted. The middle glenohumeral ligament has more variable anatomy, most commonly running from the supraglenoid tubercle and inserting onto the lesser tuberosity. It becomes taut as the arm abducts, at which time is resists both anterior and posterior translation of the humeral head. The inferior glenohumeral ligament is made up of both an anterior and posterior band. It extends from the anteroinferior labrum and inferior aspect of the glenoid and inserts into the inferior lesser tuberosity. In a position of abduction and external rotation, the inferior glenohumeral ligament prevents anterior translation of the humeral head (Terry & Chopp, 2000). Finally, the coracoacromial (CA) ligament has been shown to provide static stability to the glenohumeral joint, specifically with anterior and superior translation of the humeral head (Lee, Black, Tibone & McMahon, 2001; Wellmann et al., 2008).

1.1.4 Dynamic Stabilizers of the Shoulder

Dynamic stabilizers of the shoulder play an important role during functional range of motion of the arm when the static stabilizers are not under tension. It is important to note that the dynamic and static stabilizers, while all separate entities, form a complex network around the glenohumeral joint (Rockwood & Matsen, 2017). For example, the long head of biceps originates from the superior labrum, while the rotator cuff tendons have attachments along the joint capsule. For the purposes of this work, relevant dynamic stabilizers of the shoulder include the rotator cuff muscles, the long head of biceps, and the deltoid (Figure 1-7).

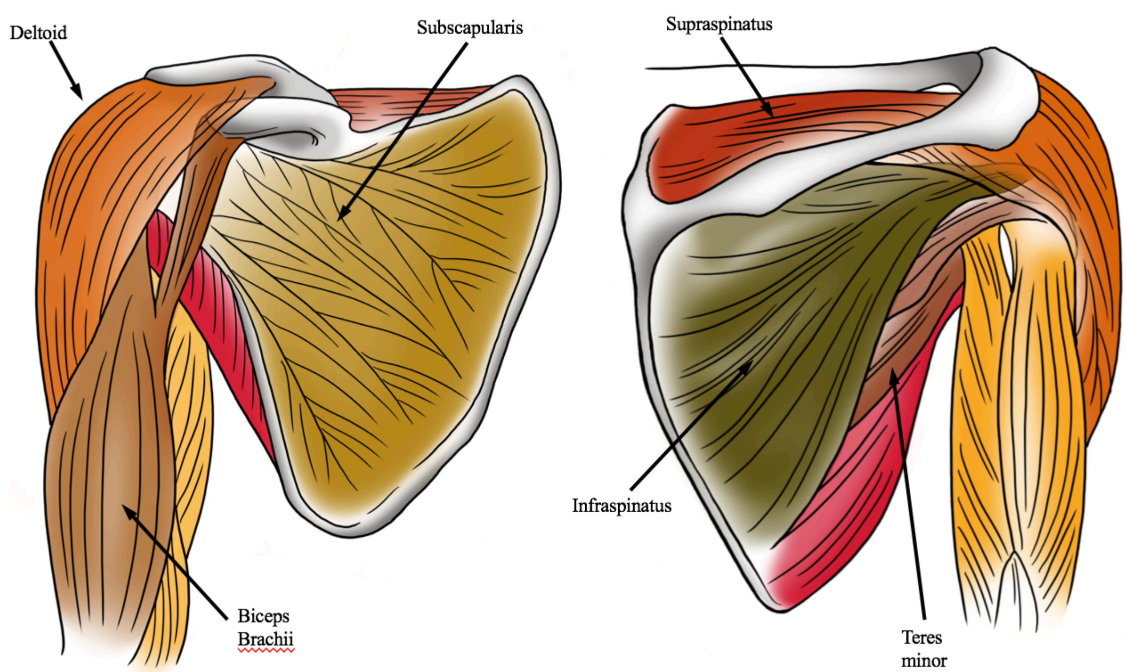

Figure 1-7: Dynamic Stabilizers of the Shoulder

Illustration depicting anterior (left) and posterior (right) views of the scapula with relevant dynamic soft tissue stabilizers of the shoulder.

1.1.4.1 Rotator Cuff Muscles

The rotator cuff is a structure that surrounds the shoulder and is made up of four distinct muscles; supraspinatus, infraspinatus, subscapularis, and teres minor. The supraspinatus is the most superior muscle, originating in the supraspinous fossa and inserting into the superior aspect of the greater tuberosity. It is innervated by the suprascapular nerve and its mechanism of action is that of shoulder abduction. The infraspinatus and teres minor muscles both originate on the posterior surface of the scapula, inferior to the scapular spine. Both insert onto the posterior aspect of the greater tuberosity. The infraspinatus is innervated by the suprascapular nerve, while teres minor is innervated by the axillary nerve. Both muscles act to externally rotate the shoulder. Finally, the subscapularis muscle originates from the subscapularis fossa on the anterior surface of the scapula and inserts onto the lesser tuberosity. It is innervated by both the upper and lower subscapular nerves and acts to internally rotate the shoulder.

When the rotator cuff muscles contract, a compressive force is applied across the joint, effectively stabilizing the joint. Described by Lippitt et al, this is a concept known as the concavity-compression effect (Lippitt et al, 1993). The superior cuff, particularly supraspinatus and upper infraspinatus, also acts as a mechanical constraint to superior head migration (Mura et al., 2003). With a large rotator cuff tear the superior structural support is lost, leading to superior humeral head migration and abnormal glenohumeral wear, a concept first described by Neer in 1983 (Neer, Craig & Fukuda, 1983).

Finally, because of the antagonistic properties of the rotator cuff muscles, they are able to act as a force couple across the joint. This allows for either simultaneous activation of both agonist and antagonist muscles or coordinated activation of an agonist with inhibition of an antagonist. With force coupling of the rotator cuff, coordinated muscle activation and appropriate transfer of forces across the joint can occur (Abboud & Soslowsky, 2002).

1.1.4.2 Long Head of Biceps Brachii

The biceps brachii is a muscle responsible for elbow flexion and forearm supination. It is innervated by the musculocutaneous nerve. It consists of two heads, the long head and the short head. The short head originates from the coracoid process and joins with the long head to insert on the bicipital tuberosity of the radius. The long head of biceps originates from the supraglenoid tubercle of the scapula at the superior labrum. It has an intra-articular course before running distally between the greater and lesser tuberosities in the bicipital groove.

As with the rotator cuff, it has been demonstrated that the long head of biceps provides compressive forces across the glenohumeral joint. It has been implicated in reducing humeral head translation in all directions in cadaveric biomechanical studies. However, there still remains some controversy in these results as there is no consensus on the physiologic load required to provide glenohumeral stability in cadaveric models (Elser et al., 2011).

1.1.4.3 Deltoid

The deltoid is a large, broad muscle overlying the shoulder and is separated from the rotator cuff muscles by the subacromial and subdeltoid bursae. Historically, the deltoid muscle has been divided into three anatomical segments; anterior, middle, and posterior. Functionally, these segments all contribute differently to range of motion around the shoulder. The anterior and middle deltoid play a large role in forward elevation in the scapular plane, while middle deltoid largely contributes to abduction and posterior deltoid to extension of the shoulder (Ackland, Pak, Richardson & Pandy, 2008). The deltoid has a common insertion into the deltoid tuberosity of the humerus. It is innervated by the axillary nerve.

While the functional role of deltoid remains undisputed, anatomists have long debated the morphologic structure of the deltoid muscle. Dating back to the early 1900s, the deltoid had been described as being made up of seven functional segments. Wickham and Brown further validated this with electromyogram (EMG) and functional studies confirming seven functional segments of deltoid (Brown, Wickham, McAndrew & Huang, 2007; Wickham & Brown, 1998).

More recently, Sakoma et al. utilized cadaveric models to investigate the actual morphology of the individual intramuscular tendons and found that deltoid was divided into seven anatomical segments. Specifically, the anterior deltoid extended from the clavicle to the anterior third of the lateral acromion and was made up of three distinct intramuscular tendons. The middle deltoid originated from the middle-third of the lateral acromion and was made up of one distinct tendon. The posterior deltoid originated from the posterior-third of the lateral acromion and scapular spine and was made up of three distinct intramuscular tendons (Sakoma et al., 2011). These seven segments corresponded with the three functional segments of deltoid (Figure 1-8).

While its role in dynamic stability of the shoulder is less recognized, the deltoid has been shown to generate compressive and shear forces across the shoulder joint. The middle and posterior heads provide the most stability through compressive force. This has an implicated role in anterior shoulder instability (Lee & An, 2002).

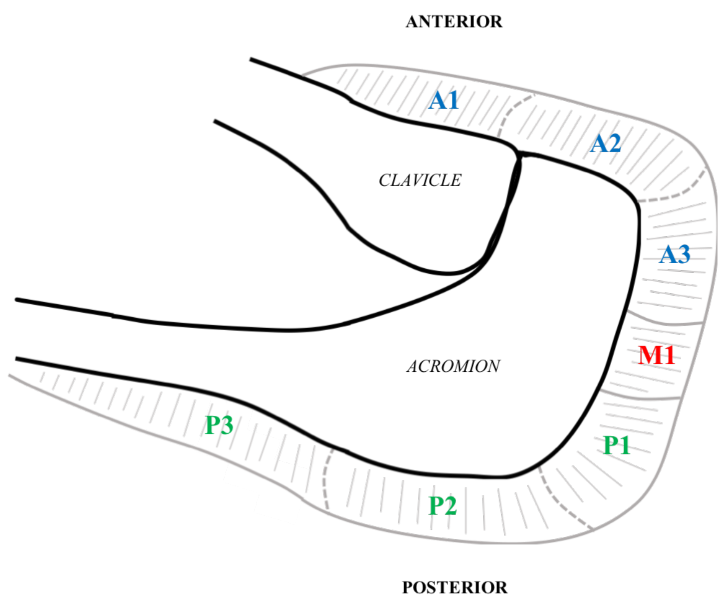

Figure 1-8: Anatomical Segments of the Deltoid Muscle Origin

Illustration depicting the seven anatomical segments of the deltoid muscle as it originates from the clavicle, acromion and scapular spine. (A1, A2, A3 = anterior intramuscular tendons, M1 = middle tendon, P1, P2, P3 = posterior intramuscular tendons)

1.2 Rotator Cuff Tear Arthropathy

1.2.1 Overview

Rotator cuff tear arthropathy was first described by Neer in 1983 when he began to recognize an abnormal pattern of glenohumeral wear following massive rotator cuff tears (Neer, Craig & Fukuda, 1983). These patients all had three essential findings in common: rotator cuff insufficiency associated with degenerative changes of the glenohumeral joint and superior migration of the humeral head (Jensen, Williams, Russell & Rockwood, 1999). Despite decades of research, there still exists controversy on the underlying etiology of this process. An early school of thought was that of a crystal-induced arthropathy, in which an inflammatory process resulted in severe degeneration of the rotator cuff, termed “Milwaukee shoulder syndrome” (McCarty et al., 1981). Neer et al. hypothesized a more commonly accepted concept that a massive rotator cuff tear leads to progression of arthropathy through both mechanical and nutritional factors (Neer, Craig & Fukuda, 1983). Figures 1-9 and 1-10 depict early and advanced radiographic findings of rotator cuff arthropathy.

Figure 1-9: Rotator Cuff Tear Arthropathy (early)

Anteroposterior (AP) radiograph of the right shoulder demonstrating early stage rotator cuff tear arthropathy with superior humeral head migration.

Figure 1-10: Rotator Cuff Tear Arthropathy (advanced)

Anteroposterior (AP) radiograph of the right shoulder demonstrating advanced rotator cuff tear arthropathy.

1.2.2 Clinical Manifestations

Rotator cuff tear arthropathy usually presents in the elderly population with symptoms of pain, weakness, and decreased range of motion of the shoulder. Physical examination findings may vary from pseudoparalysis to full shoulder range of motion if the deltoid is able to compensate. Diagnosis can be made clinically, radiographically, or with advanced imaging such as ultrasound (US), computed tomography (CT), or magnetic resonance imaging (MRI). Classic radiographic findings of rotator cuff tear arthropathy include superior migration of the humeral head causing abnormal glenohumeral and acromial wear (Nam et al., 2012).

1.2.3 Treatment Options

Treatment options for rotator cuff tear arthropathy depend on the patient, the severity of their presentation, and the effect on their quality of life. Treatment options include conservative measures such as activity modifications, oral analgesics, physiotherapy, and intra-articular injections. Surgical treatment algorithms exist, taking into consideration age, pseudoparalysis and presence of glenohumeral arthritis. In these cases, the rotator cuff tears are deemed unrepairable, and so surgical options typically include either hemiarthroplasty or reverse total shoulder arthroplasty (Nam et al., 2012).

1.3 Reverse Total Shoulder Arthroplasty

1.3.1 Overview

The conception of reverse total shoulder arthroplasty (RTSA) dates back to the 1970s when Neer realized the shortcomings of the standard total shoulder implant in the setting of patients with rotator cuff deficiency. The idea was to reverse the anatomy of the native glenohumeral joint by placing the “ball” on the glenoid side and the “socket’ on the humerus. His original designs involved a highly constrained implant with a stemmed neck on the glenoid component, lateralizing the center of rotation of the shoulder. This design had inherent faults, resulting in poor outcomes associated with continued pain, poor range of motion, and glenoid component loosening (Berliner, Regalado-Magdos, Ma & Feeley 2015; Boileau, Watkinson, Hatzidakis & Balg, 2005; Boileau, Watkinson, Hatzidakis & Hovorka, 2006; Flatow & Harrison, 2011; Gerber & Nyffeler, 2009).

It was in 1985 that Paul Grammont revolutionized the design of the reverse shoulder implant, from which implants are still based off of today (Figure 1-11). His key changes included medializing and distalizing the center of rotation in relation to the glenoid surface, which increased the moment arm of the deltoid, giving it a mechanical advantage (Ackland, Roshan-Zamir, Richardson & Pandy, 2010; Walker et al., 2016b). In contrast to the native glenohumeral joint, this center of rotation was fixed through range of motion, which minimized shear forces and maximized compressive forces at the bone-implant interface. He also created a large glenosphere which articulated with a small humeral cup, giving the implant a semiconstrained design and allowing for a large arc of motion (Berliner, Regalado-Magdos, Ma & Feeley 2015; Boileau, Watkinson, Hatzidakis & Balg, 2005; Boileau, Watkinson, Hatzidakis & Hovorka, 2006; Flatow & Harrison, 2011; Gerber & Nyffeler, 2009).

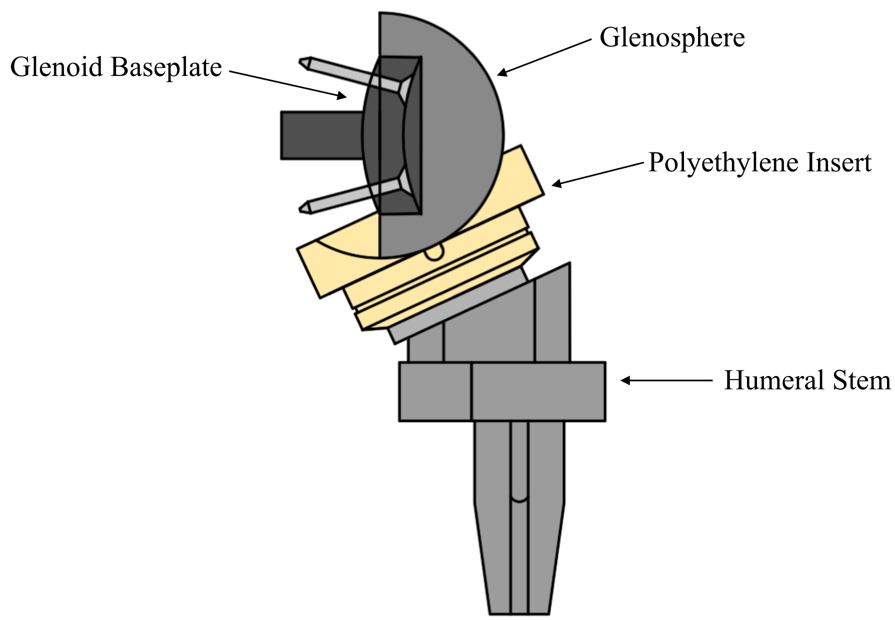

Figure 1-11: Reverse Total Shoulder Arthroplasty

Illustration depicting the components of a reverse total shoulder arthroplasty implant

1.3.2 Importance of Deltoid

The deltoid is arguably the most important structure required for a successful RTSA implant. As discussed, the medialized and distalized center of rotation in the reverse implant increases the deltoid's mechanical advantage. The deltoid moment arm has been reported to increase as much as 42% following RTSA (Kontaxis & Johnson, 2009). The shift in center of rotation of the glenohumeral joint also allows for improved deltoid efficiency by increasing recruitment of deltoid muscle fibers. Increased recruitment of both anterior and posterior deltoid fibers has been reported after RTSA, with all three portions of deltoid becoming even stronger abductors (Ackland, Roshan-Zamir, Richardson & Pandy, 2010; Walker et al., 2016b). Figure 1-12 depicts the change in deltoid biomechanics following RTSA implantation.

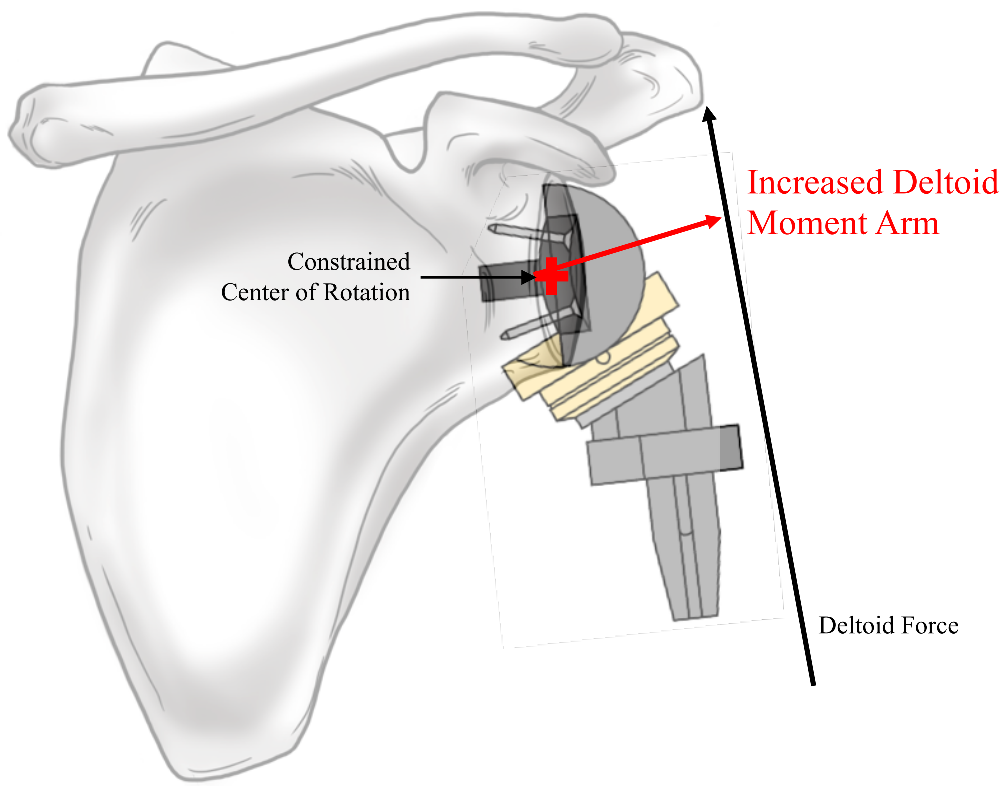

Figure 1-12: Deltoid Biomechanics Following RTSA Implantation
Illustration depicting the increased deltoid moment arm following RTSA implantation.

There is also a reported decrease in deltoid force required to generate abduction and flexion following RTSA. Henninger et al. reported a 30% decrease in abduction force following RTSA (Henninger et al., 2012b). Ackland et al. reported a 10.7% body weight (BW) decrease of middle deltoid and 2.3% BW decrease of posterior deltoid force during abduction, and a 3.1%BW decrease of middle deltoid and 6.0%BW decrease of anterior deltoid force during flexion (Ackland, Roshan-Zamir, Richardson & Pandy, 2011). These changes in deltoid action in the setting of a rotator cuff deficient shoulder do cause changes in the direction of force through the shoulder with a resultant increase in superior shear through the baseplate (Ackland, Roshan-Zamir, Richardson & Pandy, 2011; Berliner, Regalado-Magdos, Ma & Feeley 2015; Kontaxis & Johnson, 2009; Terrier, Reist, Merlini & Farron, 2008).

1.3.3 Indications

Reverse total shoulder arthroplasty has been well validated as a successful treatment option for patients with symptomatic rotator cuff tear arthropathy, relieving symptoms and restoring function (Drake, O'Connor & Edwards, 2010; Ek, Neukom, Cantanzaro & Gerber, 2013; Nolan, Ankerson & Wiater, 2011). Leung et al. demonstrated improved outcomes at 2-year follow-up with pain relief and function following RTSA as compared to hemiarthroplasty in the treatment of rotator cuff tear arthropathy (Leung, Horodyski, Struk & Wright, 2012). While RTSA has been historically indicated in elderly patients, Ek et al. reported significant functional improvement at 10-year follow-up in patients under the age of 65 treated with RTSA for irreparable rotator cuff tears (Ek, Neukom, Cantanzaro & Gerber, 2013). RTSA can also improve function in patients who have failed previous rotator cuff repair and who continue to have symptoms, however their results are inferior to primary RTSA (Boileau et al., 2009).

RTSA usage is continuously growing, accounting for one third of all shoulder arthroplasty procedures in North America in 2011. With this comes a growing list of operative indications. A report with data from 2011 indicated that 59% of all RTSA implants were for osteoarthritis, 21% for rotator cuff tear, and 10% for proximal humerus fracture. RTSA was also more likely to be performed in elderly patients than total shoulder arthroplasty (TSA) or hemiarthroplasty (Schairer et al., 2015a).

In the setting of acute proximal humerus fractures, RTSA has become increasingly utilized. An advantage of RTSA over hemiarthroplasty is that it has known success in elderly patients with rotator cuff insufficiency, and additionally does not need to rely on healing of the tuberosities. Reports suggest improved functional outcomes of RTSA versus hemiarthroplasty, however RTSA is associated with a higher complication rate but a lower revision rate (Ferrel, Trinh & Fischer, 2015; Gallinet et al., 2018; Schairer et al, 2015b; Sebastiá-Forcada, Cebrián-Gómez, Lizaur-Utrilla & Gil-Guillén, 2014). Reports have also demonstrated positive outcomes of RTSA in the setting of proximal humerus fracture malunion (Willis et al., 2012).

RTSA is also indicated in the setting of failed hemiarthroplasty or failed total shoulder arthroplasty. If there is any uncertainty of satisfactory rotator cuff function in these patients, RTSA may be considered. RTSA has been shown to have positive outcomes in treating pain and function in the revision setting, however this procedure is known to be associated with higher complication rates (Flury et al., 2011; Levy, Frankle, Mighell & Pupello, 2007; Levy, Virani, Pupello & Frankle, 2007; Walker et al., 2012).

1.3.4 Outcomes

While the indications for surgery vary, so do the functional, radiographic, and patient-reported outcomes. As discussed, RTSA has been well studied as an effective treatment option for the appropriate indication in the appropriate patient. Wall et al. followed RTSA patients post-operatively for a mean of 39.9 months and found an increase in the average Constant score from 23 points to 60 points post-operatively, with 93% of patients being satisfied or very satisfied with their results (Wall, 2007). In 2009, Young et al. reported that at a mean follow-up of 38 months, 89% of patients reported good or excellent outcomes following RTSA. They reported a mean American Shoulder and Elbow Surgeon (ASES) Score of 70.1, with patients achieving a mean active anterior elevation of 122° and a mean external rotation of 14.7° (Young et al., 2009).

Frankle et al. followed patients for an average of 33.3 months and found significant improvements in all of their outcome measures. The mean total ASES score improved from 34.3 to 68.2 post-operatively, with the mean function score improving from 16.1 to

29.4 and the mean pain score improving from 18.2 to 38.7. In terms of range of motion, forward flexion improved from 55° to 105.1°, and abduction increased from 41.4° to 101.8° (Frankle et al., 2006). More recently, Baumgarten et al. demonstrated that RTSA significantly improved patient's activity levels postoperatively, as well as their quality of life (Baumgarten, Chang, Dannenbring & Foley, 2018). While the longevity and survivorship of these implants continues to be studied, early five and ten-year follow-up results suggest high survival rate and promising long-term clinical results. Using revision as an end point, two recent studies reported a 10-year overall prosthesis survival rate of 91% and 93 % (Bacle, Nové-Josserand, Garaud & Walch, 2017; Cuff et al., 2017)

1.3.5 Complications

As RTSA becomes a more widely utilized surgical procedure, complications continue to be identified even in the most experienced of hands. RTSA has been reported to have an overall complication rate of 15%, while that of revision RTSA approaches 40%. Furthermore, RTSA has been reported to have a higher overall complication rate than total shoulder arthroplasty (Barco et al., 2016). Confusion lies in the exact definition and reporting of complications, making the literature difficult to navigate. The most commonly reported and studied complications following RTSA include infection, neurologic injury, intra-operative fracture, periprosthetic fracture, scapular notching, component loosening, and acromial fracture (Ascione et al., 2018; Barco et al., 2016; Cheung et al., 2011; Gerber & Nyffeler, 2009; Nam et al., 2012). For the purposes of this work, the focus will be placed on acromial fractures following RTSA.

1.3.5.1 Acromial Fractures

1.3.5.1.1 Overview

Acromial fractures following RTSA are a poorly understood, underdiagnosed entity, with a reported incidence ranging as high as 10% (Crosby, Hamilton & Twiss, 2011; Cuff et al., 2017; Frankle et al., 2005; Hamid, Connor, Fleischli & D'Alessandro, 2011; Hattrup, 2010; Levy, Anderson & Samson, 2013; Mayne, Bell, Wright & Coghlan, 2016; Walch et al., 2009). This value is likely understated as these fractures are a challenge to identify and diagnose. They are thought to arise through an insufficiency fracture mechanism, in which excessive stress at the deltoid attachment causes microtrauma that exceeds the ability of the body to repair the damaged bone (Gerber & Nyffeler, 2009; Hamid, Connor, Fleischli & D'Alessandro, 2011; Mayne, Bell, Wright & Coghlan, 2016; Walch et al., 2009; Wong, Langohr, Athwal & Johnson, 2016). Wong et al. used a finite element model to demonstrate that even with an RTSA configuration that caused maximal stress through the acromion, it did not approach the threshold of traumatic fracture of cortical bone (Wong, Langohr, Athwal & Johnson, 2016).

Patients with acromial fractures following RTSA may present with symptoms on a spectrum, from being asymptomatic to having complete loss of function and range of motion. Acromial fractures most often occur within the first three to ten months following surgery (Hamid, Connor, Fleischli & D'Alessandro, 2011; Teusink, Otto, Cottrell & Frankle, 2014). Presenting symptoms include pain, no improvement in motion with physiotherapy, and loss of range of motion (Cheung et al., 2011; Hamid, Connor, Fleischli & D'Alessandro, 2011; Mayne, Bell, Wright & Coghlan, 2016).

1.3.5.1.2 Etiology

Considerations for the etiology of an insufficiency fracture include both patient and technical factors. Otto et al. reported that osteoporosis significantly increased the risk of post-operative acromial fractures following RTSA (Otto et al., 2013). While wear to the acromion before surgery was thought to be a risk factor, such as in rotator cuff arthropathy when superior humeral head migration leads to acetabulization of the acromion, Walch et al. reported that this had no significant bearing on post-operative outcomes (Walch et al., 2009).

Technical factors that have been discussed include lengthening of the arm causing increased deltoid tension, as well as the position and length of the glenoid baseplate screws. Crosby et al. reported that the superior metaglene screw in the Delta III implant acted as a stress riser and recommended that this not be used routinely (Crosby, Hamilton & Twiss, 2011). Mayne et al. recommended the use of a short posterior screw (<20 mm) and a superior screw measuring less than 24 mm (Mayne, Bell, Wright & Coghlan, 2016). While the concept of arm lengthening and deltoid tension causing increased risk of fracture has been described, no evidence-based recommendations have been made (Dubrow et al., 2014; Lädermann, Edwards & Walch, 2014).

1.3.5.1.3 Classification

Crosby et al. and Levy et al. have both proposed classification systems for acromial fractures following RTSA. Crosby et al. retrospectively reviewed 400 patients treated with RTSA and identified 22 who had an identified acromial fracture. They recognized three discrete fracture patterns and defined these in relation to the acromioclavicular (AC) joint. Type I fractures were avulsion fractures of the anterior acromion, type II fractures occurred posterior to the AC joint, and type III fractures occurred along the scapular spine (Crosby, Hamilton & Twiss, 2011). Unfortunately, no functional data was included in this report and the reproducibility of this classification system was later validated by Otto et al. with only moderate reliability (Otto et al., 2013).

Levy et al. later proposed a new classification system based on the anatomic origin of the deltoid (Figure 1-13). Type I fractures were the most lateral, extending along the tip of the acromion and involving a portion of both the anterior and middle deltoid. Type II fractures involved the entire middle deltoid origin while type III fractures involved the posterior deltoid origin along the scapular spine (Levy, Anderson & Samson, 2013). Additionally, Wahlquist et al. described "acromial base fractures" as a similar pattern to type III fractures, occurring at the connection of the scapular spine and the acromion (Wahlquist, Hunt & Braman, 2011). Levy et al. acknowledged that these fractures were very difficult to identify, with even radiographs being unreliable. They recommended computed tomography (CT) scans to better delineate these fractures if there was any uncertainty in diagnosis. They were able to validate their classification system with excellent interobserver reliability (Levy, Anderson & Samson, 2013). They reported that type II fractures were the most common, followed by type III. This was consistent with results published by Wong et al. in a finite element analysis which demonstrated that the location of maximal acromial stress following RTSA was in the region of Levy type II fractures (Wong, Langohr, Athwal & Johnson, 2016).

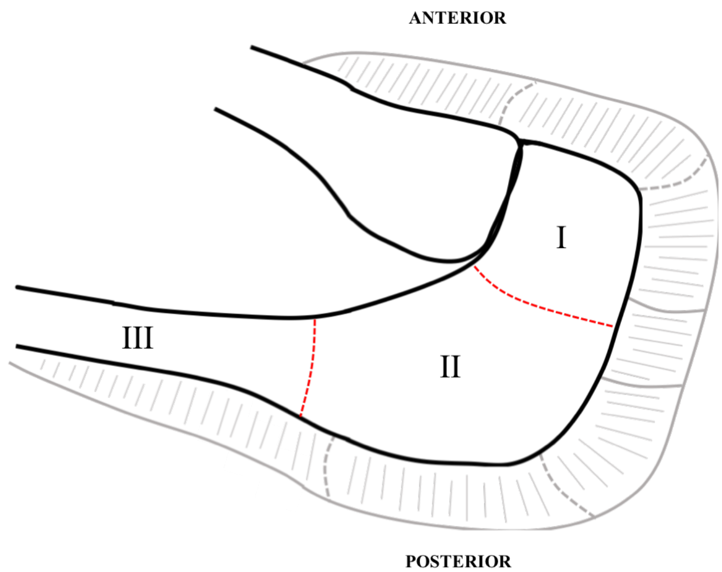

Figure 1-13: Levy Classification of Acromial Fractures
Illustration depicting the Levy classification of acromial fractures.

1.3.5.1.4 Treatment Outcomes

Treatment of acromial insufficiency fractures ranges from observation and non-operative treatment to open reduction internal fixation (ORIF). This largely depends on patient characteristics, symptoms, bone quality, fracture pattern, and surgeon preference and experience (Hattrup, 2010). While many case reports have been described, these fractures continue to be underdiagnosed and unrecognized and as such, no large-scale studies exist with evidence-based treatment recommendations. A survey by the American Shoulder and Elbow Surgery (ASES) members found that 61.5% had encountered post-operative acromial fractures in their practice, and 75% treated them non-operatively (Hamid, Connor, Fleischli & D'Alessandro, 2011).

In a retrospective case-control study by Teusink et al., 25 patients with acromial fractures following RTSA were treated non-operatively and followed for a minimum period of 2 years. They found that these patients had inferior clinical outcomes following fracture, but that overall, they had improved function as compared to pre-operatively. These patients did not gain as much forward elevation as compared to control patients, with a mean gain of 26° and 76° respectively (Teusink, Otto, Cottrell & Frankle, 2014). In another study, authors reported a 50% reduction in expected pain improvement and active elevation, and a 60% decrease in outcome scores as compared to the control group (Hattrup, 2010).

Acromial base fractures, or type III fractures, are thought to act differently than their type I and type II counterparts. It is speculated that acromial base fractures cause a larger portion of deltoid to be defunctioned, resulting in poor functional capacity. Furthermore, deltoid pull causes distraction at the fracture site and an increased risk of non-union. Wahlquist et al. reported on five patients with acromial base fractures following RTSA. Two were treated operatively with ORIF, while three were treated non-operatively. Non-operative treatment included an abduction pillow sling for 3 months with no active or passive range of motion, and a bone stimulator. Patients had improvement in pain and function after both treatment options, but because of the small sample size, no significant treatment recommendations could be made (Wahlquist, Hunt & Braman, 2011).

Rouleau et al. performed a review of the literature and identified 30 cases of patients with fractures of the acromial base or scapular spine following RTSA. Seven were treated with ORIF while 21 were treated non-operatively. Amongst those treated non-operatively, fourteen had non-union (67%) and four had malunion (19%). Amongst those with ORIF, one patient had persistent non-union, two required revision ORIF, and one patient required removal of hardware (Rouleau & Gaudelli, 2013).

Hamid et al. retrospectively reviewed 162 patients who underwent RTSA, of which they identified eight with acromial fractures. All were treated non-operatively, and six of the eight (75%) went on to fracture non-union. Hamid et al. also commented on fracture location having a role in clinical outcomes (Hamid, Connor, Fleischli & D'Alessandro, 2011). As discussed, fractures located more medially are associated with increased deltoid disruption and dysfunction, and with a high rate of non-union they may have significant loss of function. Some have advocated for non-operative treatment of lateral acromial fractures and consideration for operative intervention of medial acromial fractures, but again the evidence is not adequate.

1.3.6 RTSA Surgical and Implant Considerations

As discussed, the RTSA design drastically alters the biomechanics of the shoulder. In order to optimize range of motion and function, as well as decrease complications such as scapular notching, modifications can be made to both surgical technique and implant configuration.

As the reverse implant design has continued to evolve, so has the surgical technique. Scapular notching has become an increasingly recognized complication of the Grammont-style RTSA, in which impingement of the humeral component on the inferior scapular neck during adduction causes bone erosion (Nicholson, Strauss & Sherman, 2011). While the impact of this phenomenon continues to be under debate, techniques have been developed to minimize impingement. Numerous studies have validated the technique of placing the glenosphere baseplate flush with the inferior edge of the glenoid, improving range of motion and reducing impingement (Gutiérrez et al., 2008a; Nyffeler, Werner & Gerber, 2005; Simovitch et al., 2007). Gutiérrez et al. also recommended placement of the glenosphere baseplate with 15° of inferior tilt to minimize mechanical failure (Gutiérrez et al., 2007a). Another surgical technique to decrease notching included placement of structural bone graft beneath the glenosphere baseplate, known as bony increased-offset reverse shoulder arthroplasty (BIO-RSA). This has been shown to decrease scapular notching while maintaining range of motion and function (Athwal et al., 2015; Boileau, Moineau, Roussanne & O’Shea, 2011).

Surgical techniques to reduce the risk of acromial fracture following RTSA are largely unknown. As previously discussed, glenoid baseplate screw placement may have a role in acting as a stress riser, and care should be taken intra-operatively while these are being placed. While large-scale studies do not exist, some argue that the anterosuperior approach reduces the risk of acromial fractures as compared to the deltopectoral approach (Molé et al., 2011).

Optimal implant configuration continues to be a source of discussion. Some parameters are set when the implant is manufactured, while others can be chosen at time of implantation. Modifications to these parameters are known to play a role in determining range of motion, impingement, and stability (Roche et al., 2009). Some modifiable implant parameters include glenoid lateralization, glenosphere diameter, cup constraint, polyethylene thickness, neck-shaft angle, and humeral lateralization. For the purpose of this work, a focus will be placed on glenoid lateralization, humeral lateralization, and neck-shaft angle.

1.3.6.1 Glenoid Lateralization

The concept of lateralizing the glenoid equates to lateralizing the center of rotation (COR). While this goes against Grammont's initial design of medializing the COR, it has been shown to have implications in regards to range of motion, deltoid abduction force, and joint stability.

There exists two main methods to lateralize the glenoid component. The first is through metallic lateralization of the glenoid baseplate itself. Gutiérrez has advocated that lateralizing the COR allows for improved range of motion and reduced impingement (Gutiérrez et al., 2007a; Gutiérrez et al., 2008b; Gutiérrez et al., 2007b). Using a Sawbones model, Gutiérrez et al. demonstrated that lateralizing the COR (+0, +5 and +10 mm) resulted in the greatest improvement in abduction ROM as compared to other variables tested (Gutiérrez et al., 2008b). This hypothesis has since been demonstrated with computational models, cadaveric biomechanical studies, and retrospective and prospective reviews (Berhouet, Garaud & Favard, 2014; Jobin et al., 2012; Li et al., 2013; Valenti et al., 2011; Virani et al., 2013). Others have found that lateralization in fact did not greatly affect ROM. In a cadaveric biomechanical study, Henninger et al. demonstrated that a lateralized COR had no effect on adduction or external rotation, which contradicted the previous literature likely due to inherent differences of the types of studies. Henninger et al. did find that higher offset increased the force required to dislocate the joint, meaning the construct was more stable. The authors also demonstrated that lateralizing the COR caused an increase in deltoid abduction force and moment arm, which could have implications for acromial stress fractures and glenoid component loosening (Henninger et al., 2012a). This concept has been demonstrated by several computational, finite element analyses, and biomechanical studies, which confirmed that lateralization of the COR caused an increase in joint-reactive forces and deltoid force required for ROM (Costantini, Choi, Kontaxis & Gulotta, 2015; Giles, Langohr, Johnson & Athwal, 2015; Hettrich, Permeswaran, Goetz & Anderson, 2015; Hoenecke, Flores-Hernandez & D'Lima, 2014; Liou et al., 2017). Hettrich et al. demonstrated that for every 1 mm of lateralization of the COR, an additional 2.6% of deltoid force was required (Hettrich, Permeswaran, Goetz & Anderson, 2015).

The second method for lateralizing the COR, as previously discussed, is through bone grafting beneath the glenosphere baseplate. This technique, known as bony increased-offset reverse shoulder arthroplasty (BIO-RSA), has been described by Boileau et al. as having an advantage over metallic glenoid lateralization as it maintains the COR at the bone-prosthetic interface, which allows for decreased torque and shear through the implant (Boileau, Moineau, Roussanne & O'Shea, 2011). Again, as discussed, this was primarily used to decrease scapular notching and improve ROM. Many studies, including a randomized controlled trial by Greiner et al. in 2015, found that there was no statistically significant improvement in ROM or other outcome scores as compared to a standard RSA (Athwal et al., 2015; Collin et al., 2018; Greiner et al., 2015; Lädermann et al., 2018).

From the perspective of acromial stress fractures, Wong et al. demonstrated using a computational model that lateralization of the glenosphere caused an increase in acromial stress. They found that lateralizing the COR from 0 to 5 mm and 0 to 10 mm caused an increase of acromial stress by 7.7% and 17.2% respectively. They concluded that glenoid lateralization had a larger effect on acromial stress than inferiorization of the glenoid component (Wong, Langohr, Athwal & Johnson, 2016). Figure 1-14 demonstrates increased glenoid lateralization of a custom modular RTSA implant.

1.3.6.2 Humeral Lateralization

Modifications to humeral implant design include use of a straight versus a curved stem, use of an inlay versus an onlay humeral tray, inclination of the neck (neck-shaft angle), and medialized versus lateralized offset. Lädermann et al. investigated the effect of these modifications on range of motion following RTSA using a computational model. Specific to humeral lateralization, the authors found that by lateralizing the humeral tray, there was a very small influence on improving the mechanical advantage of the deltoid in abduction, with an even smaller effect on flexion and external rotation (Lädermann et al., 2015).

The type of humeral stem used in RTSA has been implicated as having a role in arm lengthening following surgery. They key behind arm lengthening involves adequate tensioning of the deltoid after implantation. If the deltoid isn't under enough tension, this may cause instability and reduced mechanical advantage of the deltoid. If the deltoid is under too much tension, this may cause neurologic injury, fixed abduction of the arm, or acromial fracture (Lädermann et al., 2009). While several studies have proposed techniques for assessing appropriate deltoid tension intra-operatively, as well as techniques for measuring amount of arm lengthening, few are validated (Lädermann, Edwards & Walch, 2014). Of note, Dubrow et al. performed a retrospective review on patients who underwent RTSA and found no significant difference in arm lengthening between those who sustained acromial fractures and those who did not (Dubrow et al., 2014).

Several studies have demonstrated a correlation between humeral offset and changes in deltoid moment arm (Berhouet et al., 2015; Walker et al., 2016a). Berhouet et al. performed a computational study which concluded that lateralization of the humeral component allowed for maximum abduction, forward flexion, and external rotation (Berhouet et al., 2015). Giles et al. used a cadaveric model to demonstrate that increasing humeral lateralization lead to a decrease in deltoid force required for active abduction (Giles, Langohr, Johnson & Athwal, 2015). Conversely, Tashjian et al. found that increased humeral offset lead to an increased deltoid abduction force and reduced passive rotation in the Reverse Shoulder Prosthesis manufactured by DJO Surgical (Tashjian, Burks, Zhang & Henninger, 2015).

In regards to acromial stress, Wong et al. used a finite element model to demonstrate that lateralization of the humeral component caused an increase in acromial stress. They found that lateralizing the humeral shaft from -5 to 0 mm and 0 to 5 mm increased acromial stress by 1.4% and 1.7% respectively. They also concluded that having a more medial humeral shaft allowed for a slight increase in deltoid mechanical advantage (Wong, Langohr, Athwal & Johnson, 2016). Figure 1-15 demonstrates increased humeral lateralization of a custom modular RTSA implant.

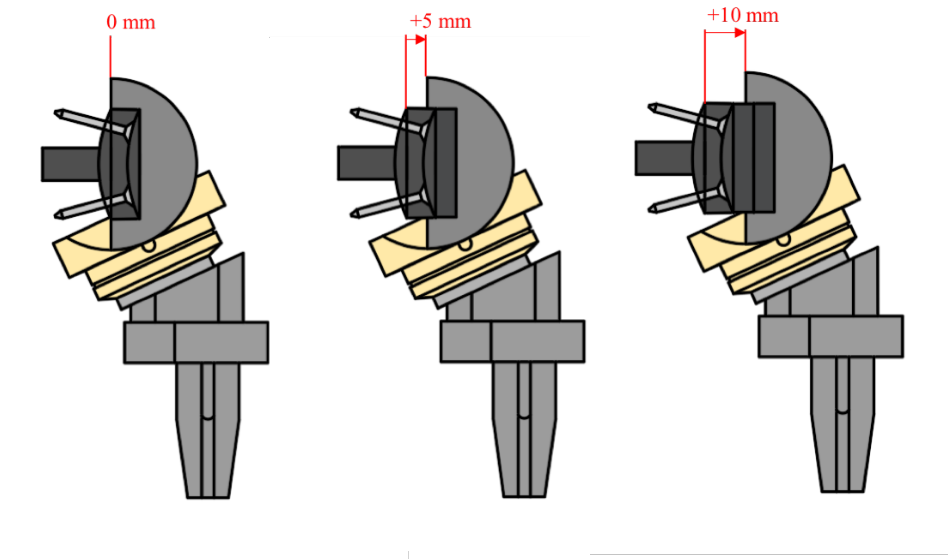

Figure 1-14: Glenoid Lateralization

Illustration depicting increased glenoid lateralization using a custom modular implant.

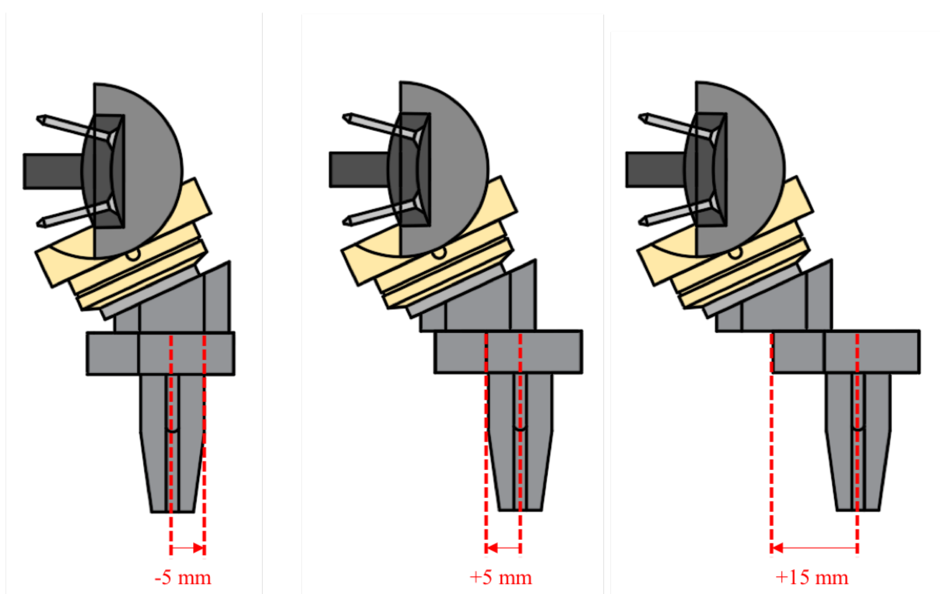

Figure 1-15: Humeral Lateralization

Illustration depicting increased humeral lateralization using a custom modular implant.

1.3.6.3 Neck-shaft Angle

Historically, the Grammont-style prosthesis was designed with a non-anatomic neck-shaft angle of 155°. The idea of the valgus neck was to add length to the humerus and therefore increase deltoid tension, allowing it to compensate for the deficient rotator cuff (Boileau, Watkinson, Hatzidakis & Balg, 2005). This design later changed as it was noted that a more valgus neck was associated with increased inferior scapular impingement and adduction deficit. This was demonstrated by Gutiérrez et al. with a Sawbones model, and later by several computational studies (de Wilde, Poncet, Middernacht & Ekelund, 2010; Gutiérrez et al., 2008a; Gutiérrez et al., 2008b; Lädermann et al., 2015; Virani et al., 2013; Werner, Chaoui & Walch, 2017). de Wilde used a two-dimensional computer model to demonstrate that a reduction in NSA from 155° to 145° allowed for a gain of 10° of impingement-free adduction (de Wilde, Poncet, Middernacht & Ekelund, 2010). Werner et al. used a three-dimensional RTSA model to demonstrate that a lower NSA allowed for improved adduction, but decreased abduction (Werner, Chaoui & Walch, 2017). Finally, Langohr et al. used finite element analysis and found that a decrease in NSA, while increasing ROM, caused an increase in maximum articular contact stress across the implant (Langohr et al., 2016). Figure 1-16 demonstrates variations in NSA of a RTSA implant. No studies have examined the role of neck-shaft angle directly on acromial strain following RTSA.

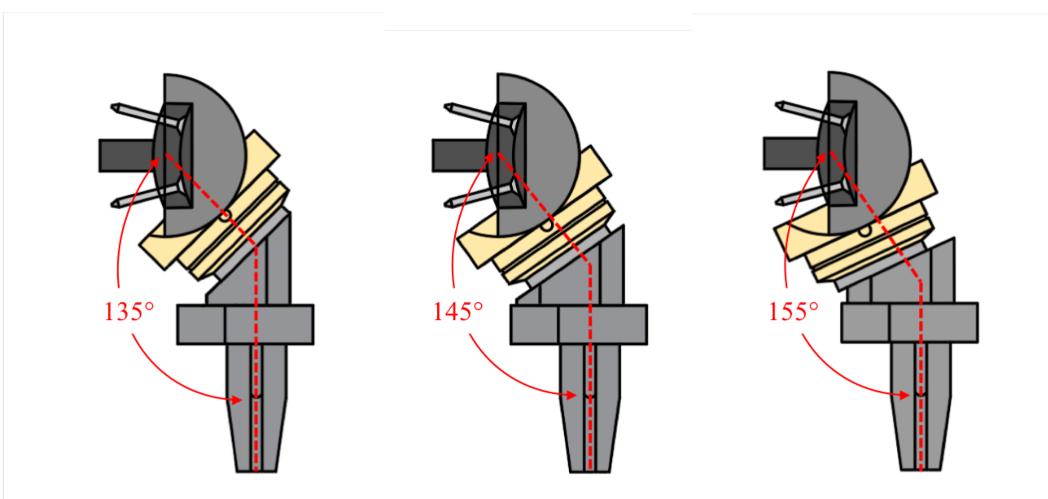

Figure 1-16: Neck-shaft Angle

Illustration depicting increasing neck-shaft using a custom modular RTSA implant.

1.4 Thesis Rationale

Reverse total shoulder arthroplasty (RTSA) is becoming an increasingly utilized surgical procedure in the aging population. This, associated with ongoing developments to increase longevity of the implant, means an associated increase in complications and adverse outcomes. Acromial stress fractures following RTSA continue to be a challenge to diagnose and are associated with inferior clinical outcomes. Unfortunately, while the existing literature focuses on etiology, classification and treatment, very little focus is placed on strategies to prevent or minimize the risk of acromial stress fractures. To date, there are no cadaveric biomechanical studies investigating the role of implant configuration on acromial insufficiency fractures.

The purpose of this thesis is to evaluate the role of RTSA implant configuration on acromial strain using a cadaveric, biomechanical model. This thesis encompasses three main studies. The first study focuses on the role of both glenoid and humeral lateralization on acromial strain following RTSA implantation. The second study examines the role of neck-shaft angle on acromial strain following RTSA implantation. Finally, the third study assesses the role of the coracoacromial (CA) ligament following RTSA implantation. These studies will yield important, relevant information regarding the optimal implant minimal strain configuration to decrease the risk of acromial stress fractures following RTSA.

1.5 Thesis Objectives

The objectives of this thesis were to examine the role of modifiable implant parameters on acromial strain following reverse total shoulder arthroplasty, as well as the role of the coracoacromial ligament.

The primary objectives of this thesis are:

1. To evaluate the role of glenoid lateralization on acromial strain following reverse total shoulder arthroplasty implantation (Chapter 2).

2. To evaluate the role of humeral lateralization on acromial strain following reverse total shoulder arthroplasty implantation (Chapter 2).

3. To evaluate the role of neck-shaft angle on acromial strain following reverse total shoulder arthroplasty implantation (Chapter 3).

4. To evaluate the role of the coracoacromial ligament following reverse total shoulder arthroplasty implantation (Chapter 4).

1.6 Thesis Hypothesis

The hypotheses of this thesis based on the objectives are:

1. Increasing glenoid lateralization will correlate with an increase in acromial strain following reverse total shoulder arthroplasty implantation (Chapter 2).

2. Increasing humeral lateralization will correlate with an increase in acromial strain following reverse total shoulder arthroplasty implantation (Chapter 2).

3. Changes in neck-shaft angle will have no significant influence on acromial strain following reverse total shoulder arthroplasty implantation (Chapter 3).

4. Disruption of the coracoacromial ligament will not have any significant effect on acromial strain and shoulder biomechanics following reverse total shoulder arthroplasty implantation (Chapter 4).

5. The acromial strain will be highest in the region of Levy type II fractures.

1.7 Thesis Overview

This thesis examines the biomechanics of RTSA in a cadaveric specimen, focusing on acromial strain. The first chapter is an overview of the relevant anatomy and pathology as well as a literature review of RTSA and acromial insufficiency fractures. Chapter 2 is focused on the biomechanics of both glenoid and humeral lateralization, and their role on acromial strain. Chapter 3 focuses solely on the role of neck-shaft angle on acromial strain. Chapter 4 examines the role of the coracoacromial ligament following reverse total shoulder arthroplasty. Finally, Chapter 5 will provide a discussion of the findings, summary of the thesis, and potential future areas of work.

1.8 References

Abboud, J. A., & Soslowsky, L. J. (2002). Interplay of the Static and Dynamic Restraints in Glenohumeral Instability: *Clinical Orthopaedics and Related Research*, *400*, 48–57.

Ackland, D. C., Pak, P., Richardson, M., & Pandy, M. G. (2008). Moment arms of the muscles crossing the anatomical shoulder. *Journal of Anatomy*, *213*, 383–390.

Ackland, D. C., Roshan-Zamir, S., Richardson, M., & Pandy, M. G. (2010). Moment Arms of the Shoulder Musculature After Reverse Total Shoulder Arthroplasty: *The Journal of Bone and Joint Surgery-American Volume*, *92*, 1221–1230.

Ackland, D. C., Roshan-Zamir, S., Richardson, M., & Pandy, M. G. (2011). Muscle and joint-contact loading at the glenohumeral joint after reverse total shoulder arthroplasty. *Journal of Orthopaedic Research*, *29*, 1850–1858.

Ascione, F., Domos, P., Guarrella, V., Chelli, M., Boileau, P., & Walch, G. (2018). Long-term humeral complications after Grammont-style reverse shoulder arthroplasty. *Journal of Shoulder and Elbow Surgery*, *27*, 1065–1071.

Athwal, G. S., MacDermid, J. C., Reddy, K. M., Marsh, J. P., Faber, K. J., & Drosdowech, D. (2015). Does bony increased-offset reverse shoulder arthroplasty decrease scapular notching? *Journal of Shoulder and Elbow Surgery*, *24*, 468–473.

Bacle, G., Nové-Josserand, L., Garaud, P., & Walch, G. (2017). Long-Term Outcomes of Reverse Total Shoulder Arthroplasty: A Follow-up of a Previous Study. *The Journal of Bone and Joint Surgery*, *99*, 454–461.

Balke, M., Schmidt, C., Dedy, N., Banerjee, M., Bouillon, B., & Liem, D. (2013). Correlation of acromial morphology with impingement syndrome and rotator cuff tears. *Acta Orthopaedica*, *84*, 178–183.

Barco, R., Savvidou, O. D., Sperling, J. W., Sanchez-Sotelo, J., & Cofield, R. H. (2016). Complications in reverse shoulder arthroplasty. *EFORT Open Reviews*, *1*, 72–80.

Baumgarten, K. M., Chang, P. S., Dannenbring, T. M., & Foley, E. K. (2018). Does total shoulder arthroplasty improve patients' activity levels? *Journal of Shoulder and Elbow Surgery*. doi:10.1016/j.jse.2018.03.028

Berhouet, J., Garaud, P., & Favard, L. (2014). Evaluation of the role of glenosphere design and humeral component retroversion in avoiding scapular notching during reverse shoulder arthroplasty. *Journal of Shoulder and Elbow Surgery*, *23*, 151–158.

Berhouet, J., Kontaxis, A., Gulotta, L. V., Craig, E., Warren, R., Dines, J., & Dines, D. (2015). Effects of the humeral tray component positioning for onlay reverse shoulder arthroplasty design: a biomechanical analysis. *Journal of Shoulder and Elbow Surgery*, *24*, 569–577.

Berliner, J. L., Regalado-Magdos, A., Ma, C. B., & Feeley, B. T. (2015). Biomechanics of reverse total shoulder arthroplasty. *Journal of Shoulder and Elbow Surgery*, *24*, 150–160.

Boileau, P., Gonzalez, J.-F., Chuinard, C., Bicknell, R., & Walch, G. (2009). Reverse total shoulder arthroplasty after failed rotator cuff surgery. *Journal of Shoulder and Elbow Surgery*, *18*, 600–606.

Boileau, P., Moineau, G., Roussanne, Y., & O'Shea, K. (2011). Bony Increased-offset Reversed Shoulder Arthroplasty: Minimizing Scapular Impingement While Maximizing Glenoid Fixation. *Clinical Orthopaedics and Related Research®*, *469*, 2558–2567.

Boileau, P., Watkinson, D., Hatzidakis, A. M., & Hovorka, I. (2006). Neer Award 2005: The Grammont reverse shoulder prosthesis: Results in cuff tear arthritis, fracture sequelae, and revision arthroplasty. *Journal of Shoulder and Elbow Surgery*, *15*, 527–540.

Boileau, P., Watkinson, D. J., Hatzidakis, A. M., & Balg, F. (2005). Grammont reverse prosthesis: Design, rationale, and biomechanics. *Journal of Shoulder and Elbow Surgery*, *14*, S147–S161.

Brown, J. M. M., Wickham, J. B., McAndrew, D. J., & Huang, X.-F. (2007). Muscles within muscles: Coordination of 19 muscle segments within three shoulder muscles during isometric motor tasks. *Journal of Electromyography and Kinesiology*, *17*, 57–73.

Cheung, E., Willis, M., Walker, M., Clark, R., & Frankle, M. A. (2011). Complications in Reverse Total Shoulder Arthroplasty: *Journal of the American Academy of Orthopaedic Surgeons*, *19*, 439–449.

Clark, J. M., & Harryman, D. T. (1992). Tendon, Ligaments, and Capsule of the Rotator Cuff. Gross and microscopic anatomy. *The Journal of Bone and Joint Surgery, 74,* 713–725.

Collin, P., Liu, X., Denard, P. J., Gain, S., Nowak, A., & Lädermann, A. (2018). Standard versus bony increased-offset reverse shoulder arthroplasty: a retrospective comparative cohort study. *Journal of Shoulder and Elbow Surgery*, *27*, 59–64.

Costantini, O., Choi, D. S., Kontaxis, A., & Gulotta, L. V. (2015). The effects of progressive lateralization of the joint center of rotation of reverse total shoulder implants. *Journal of Shoulder and Elbow Surgery*, *24*, 1120–1128.

Crosby, L. A., Hamilton, A., & Twiss, T. (2011). Scapula Fractures After Reverse Total Shoulder Arthroplasty: Classification and Treatment. *Clinical Orthopaedics and Related Research®*, *469*, 2544–2549.

Cuff, D. J., Pupello, D. R., Santoni, B. G., Clark, R. E., & Frankle, M. A. (2017). Reverse Shoulder Arthroplasty for the Treatment of Rotator Cuff Deficiency: A Concise Follow-up, at a Minimum of 10 Years, of Previous Reports*. *The Journal of Bone and Joint Surgery*, *99*, 1895–1899.

de Wilde, L. F., Poncet, D., Middernacht, B., & Ekelund, A. (2010). Prosthetic overhang is the most effective way to prevent scapular conflict in a reverse total shoulder prosthesis. *Acta Orthopaedica*, *81*, 719–726.

Drake, G. N., O’Connor, D. P., & Edwards, T. B. (2010). Indications for Reverse Total Shoulder Arthroplasty in Rotator Cuff Disease. *Clinical Orthopaedics and Related Research®*, *468*, 1526–1533.

Dubrow, S., Streit, J. J., Muh, S., Shishani, Y., & Gobezie, R. (2014). Acromial Stress Fractures: Correlation With Acromioclavicular Osteoarthritis and Acromiohumeral Distance. *Orthopedics*, *37*, e1074–e1079.

Ek, E. T. H., Neukom, L., Catanzaro, S., & Gerber, C. (2013). Reverse total shoulder arthroplasty for massive irreparable rotator cuff tears in patients younger than 65 years old: results after five to fifteen years. *Journal of Shoulder and Elbow Surgery*, *22*, 1199–1208.

Elser, F., Braun, S., Dewing, C. B., Giphart, J. E., & Millett, P. J. (2011). Anatomy, Function, Injuries, and Treatment of the Long Head of the Biceps Brachii Tendon. *Arthroscopy: The Journal of Arthroscopic & Related Surgery*, *27*, 581–592.

Ferrel, J. R., Trinh, T. Q., & Fischer, R. A. (2015). Reverse Total Shoulder Arthroplasty Versus Hemiarthroplasty for Proximal Humeral Fractures: A Systematic Review. *Journal of Orthopedic Trauma*, *29*, 60–68.

Flatow, E. L., & Harrison, A. K. (2011). A History of Reverse Total Shoulder Arthroplasty. *Clinical Orthopaedics and Related Research®*, *469*, 2432–2439.

Flury, M. P., Frey, P., Goldhahn, J., Schwyzer, H.-K., & Simmen, B. R. (2011). Reverse shoulder arthroplasty as a salvage procedure for failed conventional shoulder replacement due to cuff failure—midterm results. *International Orthopaedics*, *35*, 53–60.

Frankle, M., Levy, J. C., Pupello, D., Siegal, S., Saleem, A., Mighell, M., & Vasey, M. (2006). The Reverse Shoulder Prosthesis for Glenohumeral Arthritis Associated with Severe Rotator Cuff Deficiency: A Minimum Two-Year Follow-up Study of Sixty Patients Surgical Technique. *JBJS Essential Surgical Techniques*, *os-88*, 178–190.

Frankle, M., Siegal, S., Pupello, D., Saleem, A., Mighell, M., & Vasey, M. (2005). The Reverse Shoulder Prosthesis for Glenohumeral Arthritis Associated with Severe Rotator Cuff Deficiency: A Minimum Two-Year Follow-up Study of Sixty Patients. *The Journal of Bone and Joint Surgery, 87,* 1697–1705.

Gallinet, D., Ohl, X., Decroocq, L., Dib, C., Valenti, P., & Boileau, P. (2018). Is reverse total shoulder arthroplasty more effective than hemiarthroplasty for treating displaced proximal humerus fractures in older adults? A Systematic Review and Meta-Analysis. *Orthopaedics & Traumatology: Surgery & Research*. doi:10.1016/j.otsr.2018.04.025

Gerber, C., & Nyffeler, R. W. (2009). Reverse Total Shoulder Arthroplasty. *Journal of the American Academy of Orthopaedic Surgeons*, *17*, 284–295.

Giles, J. W., Langohr, G. D. G., Johnson, J. A., & Athwal, G. S. (2015). Implant Design Variations in Reverse Total Shoulder Arthroplasty Influence the Required Deltoid Force and Resultant Joint Load. *Clinical Orthopaedics and Related Research®*, *473*, 3615–3626.

Greiner, S., Schmidt, C., Herrmann, S., Pauly, S., & Perka, C. (2015). Clinical performance of lateralized versus non-lateralized reverse shoulder arthroplasty: a prospective randomized study. *Journal of Shoulder and Elbow Surgery*, *24*, 1397–1404.

Gutiérrez, S., Comiskey, C. A., Luo, Z.-P., Pupello, D. R., & Frankle, M. A. (2008a). Range of Impingement-Free Abduction and Adduction Deficit After Reverse Shoulder Arthroplasty: Hierarchy of Surgical and Implant-Design-Related Factors. *The Journal of Bone and Joint Surgery-American Volume*, *90*, 2606–2615.

Gutiérrez, S., Greiwe, R. M., Frankle, M. A., Siegal, S., & Lee, W. E. (2007a). Biomechanical comparison of component position and hardware failure in the reverse shoulder prosthesis. *Journal of Shoulder and Elbow Surgery*, *16*, S9–S12.

Gutiérrez, S., Levy, J. C., Frankle, M. A., Cuff, D., Keller, T. S., Pupello, D. R., & Lee, W. E. (2008b). Evaluation of abduction range of motion and avoidance of inferior scapular impingement in a reverse shoulder model. *Journal of Shoulder and Elbow Surgery*, *17*, 608–615.

Gutiérrez, S., Levy, J. C., Lee, W. E., Keller, T. S., & Maitland, M. E. (2007b). Center of Rotation Affects Abduction Range of Motion of Reverse Shoulder Arthroplasty. *Clinical Orthopaedics and Related Research*, *458*, 78 – 82.

Hamid, N., Connor, P. M., Fleischli, J. F., & D'Alessandro, D. F. (2011). Acromial Fracture After Reverse Shoulder Arthroplasty. *American Journal of Orthopedics, 40,* e125–129.

Hattrup, S. J. (2010). The Influence of Postoperative Acromial and Scapular Spine Fractures on the Results of Reverse Shoulder Arthroplasty. *Orthopedics*. doi:10.3928/01477447-20100329-04

Henninger, H. B., Barg, A., Anderson, A. E., Bachus, K. N., Burks, R. T., & Tashjian, R. Z. (2012a). Effect of lateral offset center of rotation in reverse total shoulder arthroplasty: a biomechanical study. *Journal of Shoulder and Elbow Surgery*, *21*, 1128–1135.

Henninger, H. B., Barg, A., Anderson, A. E., Bachus, K. N., Tashjian, R. Z., & Burks, R. T. (2012b). Effect of deltoid tension and humeral version in reverse total shoulder arthroplasty: a biomechanical study. *Journal of Shoulder and Elbow Surgery*, *21*, 483–490.

Hettrich, C. M., Permeswaran, V. N., Goetz, J. E., & Anderson, D. D. (2015). Mechanical tradeoffs associated with glenosphere lateralization in reverse shoulder arthroplasty. *Journal of Shoulder and Elbow Surgery*, *24*, 1774–1781.

Hoenecke, H. R., Flores-Hernandez, C., & D'Lima, D. D. (2014). Reverse total shoulder arthroplasty component center of rotation affects muscle function. *Journal of Shoulder and Elbow Surgery*, *23*, 1128–1135.

Hurov, J. (2009). Anatomy and Mechanics of the Shoulder: Review of Current Concepts. *Journal of Hand Therapy*, *22*, 328–343.

Inman, V. T., Saunders, J. B., & Abbott, L. C. (1996). Observations of the Function of the Shoulder Joint. 1944. *Clinical Orthopaedics and Related Research, 330*, 3–12.

Jensen, K. L., Williams, G. R., Russell, I. J., & Rockwood, C. A. (1999). Current Concepts Review - Rotator Cuff Tear Arthropathy. *The Journal of Bone & Joint Surgery*, *81*, 1312–24.

Jeong, J., Bryan, J., & Iannotti, J. P. (2009). Effect of a Variable Prosthetic Neck-Shaft Angle and the Surgical Technique on Replication of Normal Humeral Anatomy: *The Journal of Bone and Joint Surgery-American Volume*, *91*, 1932–1941.

Jobin, C. M., Brown, G. D., Bahu, M. J., Gardner, T. R., Bigliani, L. U., Levine, W. N., & Ahmad, C. S. (2012). Reverse total shoulder arthroplasty for cuff tear arthropathy: the clinical effect of deltoid lengthening and center of rotation medialization. *Journal of Shoulder and Elbow Surgery*, *21*, 1269–1277.

Kontaxis, A., & Johnson, G. R. (2009). The biomechanics of reverse anatomy shoulder replacement – A modelling study. *Clinical Biomechanics*, *24*, 254–260.

Lädermann, A., Denard, P. J., Boileau, P., Farron, A., Deransart, P., Terrier, A., Ston, J., & Walch, G. (2015). Effect of humeral stem design on humeral position and range of motion in reverse shoulder arthroplasty. *International Orthopaedics*, *39*, 2205–2213.

Lädermann, A., Denard, P. J., Boileau, P., Farron, A., Deransart, P., & Walch, G. (2018). What is the best glenoid configuration in onlay reverse shoulder arthroplasty? *International Orthopaedics*, *42*, 1339–1346.

Lädermann, A., Edwards, T. B., & Walch, G. (2014). Arm lengthening after reverse shoulder arthroplasty: a review. *International Orthopaedics*, *38*, 991–1000.

Lädermann, A., Williams, M. D., Melis, B., Hoffmeyer, P., & Walch, G. (2009). Objective evaluation of lengthening in reverse shoulder arthroplasty. *Journal of Shoulder and Elbow Surgery*, *18*, 588–595.

Langohr, G. D. G., Willing, R., Medley, J. B., Athwal, G. S., & Johnson, J. A. (2016). Contact mechanics of reverse total shoulder arthroplasty during abduction: the effect of neck-shaft angle, humeral cup depth, and glenosphere diameter. *Journal of Shoulder and Elbow Surgery*, *25*, 589–597.

Lee, S.-B., & An, K.-N. (2002). Dynamic Glenohumeral Stability Provided by Three Heads of the Deltoid Muscle: *Clinical Orthopaedics and Related Research*, *400*, 40–47.

Lee, T. Q., Black, A. D., Tibone, J. E., & McMahon, P. J. (2001). Release of the coracoacromial ligament can lead to glenohumeral laxity: A biomechanical study. *Journal of Shoulder and Elbow Surgery*, *10*, 68–72.

Leung, B., Horodyski, M., Struk, A. M., & Wright, T. W. (2012). Functional outcome of hemiarthroplasty compared with reverse total shoulder arthroplasty in the treatment of rotator cuff tear arthropathy. *Journal of Shoulder and Elbow Surgery*, *21*, 319–323.

Levy, J. C., Anderson, C., & Samson, A. (2013). Classification of Postoperative Acromial Fractures Following Reverse Shoulder Arthroplasty: *The Journal of Bone and Joint Surgery-American Volume*, *95*, e104-1–7.

Levy, J. C., Frankle, M., Mighell, M., & Pupello, D. (2007). The Use of the Reverse Shoulder Prosthesis for the Treatment of Failed Hemiarthroplasty for Proximal Humeral Fracture. *The Journal of Bone and Joint Surgery, 89,* 292–300.

Levy, J. C., Virani, N., Pupello, D., & Frankle, M. (2007). Use of the reverse shoulder prosthesis for the treatment of failed hemiarthroplasty in patients with glenohumeral arthritis and rotator cuff deficiency. *The Journal of Bone and Joint Surgery*, *89*, 189–195.

Li, X., Knutson, Z., Choi, D., Lobatto, D., Lipman, J., Craig, E. V., Warren, R. F., & Gulotta, L. V. (2013). Effects of glenosphere positioning on impingement-free internal and external rotation after reverse total shoulder arthroplasty. *Journal of Shoulder and Elbow Surgery*, *22*, 807–813.

Liou, W., Yang, Y., Petersen-Fitts, G. R., Lombardo, D. J., Stine, S., & Sabesan, V. J. (2017). Effect of lateralized design on muscle and joint reaction forces for reverse shoulder arthroplasty. *Journal of Shoulder and Elbow Surgery*, *26*, 564–572.

Lippitt, S. B., Vanderhooft, J. E., Harris, S. L., Sidles, J. A., Harryman, D. T., & Matsen, F. A. (1993). Glenohumeral stability from concavity-compression: A quantitative analysis. *Journal of Shoulder and Elbow Surgery*, *2*, 27–35.

Mayne, I. P., Bell, S. N., Wright, W., & Coghlan, J. A. (2016). Acromial and scapular spine fractures after reverse total shoulder arthroplasty. *Shoulder & Elbow*, *8*, 90–100.

McCarty, D. J., Halverson, P. B., Carrera, G.F., Brewer, B. J., & Kozin, F. (1981). "Milwaukee Shoulder" – Association of Microspheroids Containing Hydroxyapatite

Crystals, Activecollagenase, and Neutral Protease with Rotator Cuff Defects. I. Clinical Aspects. *Arthritis and Rheumatology, 24,* 464–473.

Molé, D., Wein, F., Dézaly, C., Valenti, P., & Sirveaux, F. (2011). Surgical Technique: The Anterosuperior Approach for Reverse Shoulder Arthroplasty. *Clinical Orthopaedics and Related Research®*, *469*, 2461–2468.

Mura, N., O'Driscoll, S. W., Zobitz, M. E., Heers, G., Jenkyn, T. R., Chou, S. M., Halder, A. M., An, K. N. (2003). The effect of infraspinatus disruption on glenohumeral torque and superior migration of the humeral head: A biomechanical study. *Journal of Shoulder and Elbow Surgery*, *12*, 179–184.

Nam, D., Maak, T. G., Raphael, B. S., Kepler, C. K., Cross, M. B., & Warren, R. F. (2012). Rotator Cuff Tear Arthropathy: Evaluation, Diagnosis, and Treatment: AAOS Exhibit Selection. *The Journal of Bone and Joint Surgery, 94*, e34-1–11.

Neer, C. S., Craig, E. V., Fukuda, H. (1983). Cuff-tear arthropathy. *The Journal of Bone and Joint Surgery, 65,* 1232–1244.

Nicholson, G. P., Strauss, E. J., & Sherman, S. L. (2011). Scapular Notching: Recognition and Strategies to Minimize Clinical Impact. *Clinical Orthopaedics and Related Research®*, *469*, 2521–2530.

Nolan, B. M., Ankerson, E., & Wiater, J. M. (2011). Reverse Total Shoulder Arthroplasty Improves Function in Cuff Tear Arthropathy. *Clinical Orthopaedics and Related Research®*, *469*, 2476–2482.

Nyffeler, R. W., Werner, C. M. L., & Gerber, C. (2005). Biomechanical relevance of glenoid component positioning in the reverse Delta III total shoulder prosthesis. *Journal of Shoulder and Elbow Surgery*, *14*, 524–528.

Otto, R. J., Virani, N. A., Levy, J. C., Nigro, P. T., Cuff, D. J., & Frankle, M. A. (2013). Scapular fractures after reverse shoulder arthroplasty: evaluation of risk factors and the reliability of a proposed classification. *Journal of Shoulder and Elbow Surgery*, *22*, 1514–1521.

Roche, C., Flurin, P.-H., Wright, T., Crosby, L. A., Mauldin, M., & Zuckerman, J. D. (2009). An evaluation of the relationships between reverse shoulder design parameters and range of motion, impingement, and stability. *Journal of Shoulder and Elbow Surgery*, *18*, 734–741.

Rockwood, C. A., Matsen, F. A. (2017). Rockwood and Matsen's The Shoulder, Fifth Edition. Philadelphia: Saunders Elsevier.

Rothenberg, A., Gasbarro, G., Chlebeck, J., & Lin, A. (2017). The Coracoacromial Ligament: Anatomy, Function, and Clinical Significance. *Orthopaedic Journal of Sports Medicine*, *5*, 232596711770339.

Rouleau, D. M., & Gaudelli, C. (2013). Successful Treatment of Fractures of the Base of the Acromion after Reverse Shoulder Arthroplasty: Case Report and Review of the Literature. *International Journal of Shoulder Surgery, 7,* 149–152.

Sakoma, Y., Sano, H., Shinozaki, N., Itoigawa, Y., Yamamoto, N., Ozaki, T., & Itoi, E. (2011). Anatomical and functional segments of the deltoid muscle: Anatomical and functional segments of deltoid. *Journal of Anatomy*, *218*, 185–190.

Schairer, W. W., Nwachukwu, B. U., Lyman, S., Craig, E. V., & Gulotta, L. V. (2015a). National utilization of reverse total shoulder arthroplasty in the United States. *Journal of Shoulder and Elbow Surgery*, *24*, 91–97.

Schairer, W. W., Nwachukwu, B. U., Lyman, S., Craig, E. V., & Gulotta, L. V. (2015b). Reverse shoulder arthroplasty versus hemiarthroplasty for treatment of proximal humerus fractures. *Journal of Shoulder and Elbow Surgery*, *24*, 1560–1566.

Sebastiá-Forcada, E., Cebrián-Gómez, R., Lizaur-Utrilla, A., & Gil-Guillén, V. (2014). Reverse shoulder arthroplasty versus hemiarthroplasty for acute proximal humeral fractures. A blinded, randomized, controlled, prospective study. *Journal of Shoulder and Elbow Surgery*, *23*, 1419–1426.

Simovitch, R. W., Zumstein, M. A., Lohri, E., Helmy, N., & Gerber, C. (2007.). Predictors of Scapular Notching in Patients Managed with the Delta III Reverse Total Shoulder Replacement. *The Journal of Bone and Joint Surgery*, *89,* 588–600.

Swarm, D. L., Mahar, A. T., Weichel, D. W., & Pedowitz, R. A. (2007). Shoulder Anatomy and Biomechanics. In R. A. Pedowitz & D. H. Johnson (Eds.), *Practical Orthopaedic Sports Medicine & Arthroscopy* (145–156). Pennsylvania, PA: Lippincott Williams & Wilkins.

Tashjian, R. Z., Burks, R. T., Zhang, Y., & Henninger, H. B. (2015). Reverse total shoulder arthroplasty: a biomechanical evaluation of humeral and glenosphere hardware configuration. *Journal of Shoulder and Elbow Surgery*, *24*, e68–e77.

Terrier, A., Reist, A., Merlini, F., & Farron, A. (2008). Simulated joint and muscle forces in reversed and anatomic shoulder prostheses. *The Journal of Bone and Joint Surgery. British Volume*, *90-B*, 751–756.

Terry, G. C., & Chopp, T. M. (2000). Functional Anatomy of the Shoulder. *Journal of Athletic Training*, *35*, 248–255.

Teusink, M. J., Otto, R. J., Cottrell, B. J., & Frankle, M. A. (2014). What is the effect of postoperative scapular fracture on outcomes of reverse shoulder arthroplasty? *Journal of Shoulder and Elbow Surgery*, *23*, 782–790.

Valenti, P., Sauzières, P., Katz, D., Kalouche, I., & Kilinc, A. S. (2011). Do Less Medialized Reverse Shoulder Prostheses Increase Motion and Reduce Notching? *Clinical Orthopaedics and Related Research®*, *469*, 2550–2557.

Virani, N. A., Cabezas, A., Gutiérrez, S., Santoni, B. G., Otto, R., & Frankle, M. (2013). Reverse shoulder arthroplasty components and surgical techniques that restore glenohumeral motion. *Journal of Shoulder and Elbow Surgery*, *22*, 179–187.

Wahlquist, T. C., Hunt, A. F., & Braman, J. P. (2011). Acromial base fractures after reverse total shoulder arthroplasty: report of five cases. *Journal of Shoulder and Elbow Surgery*, *20*, 1178–1183.

Walch, G., Mottier, F., Wall, B., Boileau, P., Molé, D., & Favard, L. (2009). Acromial insufficiency in reverse shoulder arthroplasties. *Journal of Shoulder and Elbow Surgery*, *18*, 495–502.

Walker, D. R., Kinney, A. L., Wright, T. W., & Banks, S. A. (2016a). How sensitive is the deltoid moment arm to humeral offset changes with reverse total shoulder arthroplasty? *Journal of Shoulder and Elbow Surgery*, *25*, 998–1004.

Walker, D. R., Struk, A. M., Matsuki, K., Wright, T. W., & Banks, S. A. (2016b). How do deltoid muscle moment arms change after reverse total shoulder arthroplasty? *Journal of Shoulder and Elbow Surgery*, *25*, 581–588.

Walker, M., Willis, M. P., Brooks, J. P., Pupello, D., Mulieri, P. J., & Frankle, M. A. (2012). The use of the reverse shoulder arthroplasty for treatment of failed total shoulder arthroplasty. *Journal of Shoulder and Elbow Surgery*, *21*, 514–522.

Wall, B. (2007). Reverse Total Shoulder Arthroplasty: A Review of Results According to Etiology. *The Journal of Bone and Joint Surgery (American)*, *89*, 1476–1485.

Wellmann, M., Petersen, W., Zantop, T., Schanz, S., Raschke, M. J., & Hurschler, C. (2008). Effect of Coracoacromial Ligament Resection on Glenohumeral Stability Under Active Muscle Loading in an In Vitro Model. *Arthroscopy: The Journal of Arthroscopic & Related Surgery*, *24*, 1258–1264.

Werner, B. S., Chaoui, J., & Walch, G. (2017). The influence of humeral neck shaft angle and glenoid lateralization on range of motion in reverse shoulder arthroplasty. *Journal of Shoulder and Elbow Surgery*, *26*, 1726–1731.

Wickham, J. B., & Brown, J. M. M. (1998). Muscles within muscles: the neuromotor control of intra-muscular segments. *European Journal of Applied Physiology*, *78*, 219–225.

Willis, M., Min, W., Brooks, J. P., Mulieri, P., Walker, M., Pupello, D., & Frankle, M. (2012). Proximal humeral malunion treated with reverse shoulder arthroplasty. *Journal of Shoulder and Elbow Surgery*, *21*, 507–513.

Wong, M. T., Langohr, G. D. G., Athwal, G. S., & Johnson, J. A. (2016). Implant positioning in reverse shoulder arthroplasty has an impact on acromial stresses. *Journal of Shoulder and Elbow Surgery*, *25*, 1889–1895.

Young, S. W., Everts, N. M., Ball, C. M., Astley, T. M., & Poon, P. C. (2009). The SMR reverse shoulder prosthesis in the treatment of cuff-deficient shoulder conditions. *Journal of Shoulder and Elbow Surgery*, *18*, 622–626.

Chapter 2

2 The Role of Glenoid and Humeral Lateralization on Acromial Strain

Acromial insufficiency fractures occur in up to 10% of patients following reverse total shoulder arthroplasty (RTSA). The etiology is largely unknown, and there is a paucity of literature on factors that minimize the risk of acromial insufficiency fractures. This chapter investigates the role of both glenoid lateralization and humeral lateralization on acromial strain following RTSA, which has not been investigated by any previous biomechanical studies.

2.1 Introduction

[NB: A portion of this material was presented in Chapter 1 and is also included here in order to ensure that this chapter is in "article" format].

Reverse total shoulder arthroplasty (RTSA) is a successful surgical treatment option for symptomatic rotator cuff tear arthropathy, acute proximal humerus fractures, and revision arthroplasty (Boileau et al., 2009; Drake, O'Connor & Edwards, 2010; Ek, Neukom, Cantanzaro & Gerber, 2013; Ferrel, Trinh & Fischer, 2015; Flury et al., 2011; Gallinet et al., 2018; Leung, Horodyski, Struk & Wright, 2012; Levy, Frankle, Mighell & Pupello, 2007; Levy, Virani, Pupello & Frankle, 2007; Nolan, Ankerson & Wiater, 2011; Schairer et al, 2015b; Sebastiá-Forcada, Cebrián-Gómez, Lizaur-Utrilla & Gil-Guillén, 2014; Walker et al., 2012; Willis et al., 2012). RTSA is becoming a more widely accepted and utilized procedure across the United States (Schairer et al., 2015a). RTSA is associated with a 15% overall complication rate (Barco et al., 2016). Amongst this, acromial insufficiency fractures are reported to occur in up to 10% of patients, usually within the first 3 to 10 months following surgery (Crosby, Hamilton & Twiss, 2011; Cuff et al., 2017; Frankle et al., 2005; Hamid, Connor, Fleischli & D'Alessandro, 2011; Hattrup, 2010; Levy, Anderson & Samson, 2013; Mayne, Bell, Wright & Coghlan, 2016; Teusink, Otto, Cottrell & Frankle, 2014; Walch et al., 2009).

Acromial insufficiency fractures following RTSA are poorly understood, difficult to diagnose, and associated with inferior clinical outcomes. They are hypothesized to occur through an insufficiency fracture mechanism as opposed to an acute traumatic event (Gerber & Nyffeler, 2009; Hamid, Connor, Fleischli & D'Alessandro, 2011; Mayne, Bell, Wright & Coghlan, 2016; Walch et al., 2009; Wong, Langohr, Athwal & Johnson, 2016). Wong et al. confirmed in their finite element analysis that after RTSA implantation, the acromion never reached the threshold of traumatic fracture even with the highest stress implant configuration (Wong, Langohr, Athwal & Johnson, 2016).

The deltoid muscle is arguably the most crucial structure required for a successful RTSA reconstruction. The deltoid muscle has a broad origin along the entire scapular spine, acromion, and lateral clavicle. The biomechanics of the shoulder, including the deltoid, are completely altered in the RTSA construct. The center of rotation (COR) is medialized and distalized, causing an increase in deltoid moment arm as high as 42% (Kontaxis & Johnson, 2009). With this, the deltoid becomes more efficient, with increased recruitment of both anterior and posterior fibers and overall increased strength of abduction (Ackland, Roshan-Zamir, Richardson & Pandy, 2010; Walker et al., 2016b). These changes in deltoid mechanics cause a resultant shift in the muscle line of action and the pull of the tendon along its origin on the acromion.

Commercially available RTSA systems vary in their implant configurations. Modifiable parameters include glenoid lateralization, humeral lateralization, neck-shaft angle, glenosphere diameter, and polyethylene thickness, amongst others. The optimal RTSA implant configuration has long been debated, and with improvement in one outcome comes compromise of another. For example, lateralization of the glenoid, while reducing scapular impingement, leads to an increase in joint-reactive forces and deltoid force required for range of motion (Costantini, Choi, Kontaxis & Gulotta, 2015; Hettrich, Permeswaran, Goetz & Anderson, 2015; Hoenecke, Flores-Hernandez & D'Lima, 2014; Liou et al., 2017).

It is for this purpose that glenoid lateralization has been addressed in some investigations, from basic science studies to randomized controlled trials. Unfortunately, very little of this literature focuses on the effect of glenoid lateralization on the acromion. Wong et al. examined this in their finite element analysis, which found that incremental lateralization of the glenoid COR caused a resultant increase in acromial stress (Wong, Langohr, Athwal & Johnson, 2016).

Humeral lateralization has been studied as a subset of modifications that can be made to the humeral stem. Humeral stem type has been implicated in post-operative deltoid tension and arm lengthening (Lädermann et al., 2009). Humeral lateralization has been shown by computational models and biomechanical studies to have mixed effects on range of motion and deltoid mechanical advantage. Wong et al. reported that with lateralization of the humeral shaft, small increases in acromial stress were noted (Wong, Langohr, Athwal & Johnson, 2016).

Overall, there remains a lack of evidence regarding which RTSA implant configurations minimize strain through the acromion. Hence, the purpose of this *in-vitro* biomechanical cadaveric simulator study was to specifically investigate the role of both glenoid lateralization and humeral lateralization on acromial strain following RTSA implantation. This was evaluated with 9 different implant configurations through 4 planes of elevation (0° and 90° abduction, 0° and 90° forward flexion). A custom modular RTSA system permitted testing of 145° neck-shaft angle implants with varying glenoid lateralization (0, 5, and 10 mm) and humeral lateralization (-5, 5, and 15 mm). It is hypothesized that increasing both glenoid lateralization and humeral lateralization will correlate with an increase in acromial strain. It is hypothesized that acromial strain will be highest in the region of Levy type II fractures (Levy, Anderson & Samson, 2013). These conclusions will yield important information regarding the role of modifiable implant parameters on acromial insufficiency fractures.

2.2 Materials and Methods

2.2.1 Specimen Preparation

Eight fresh frozen right male cadaveric shoulders (8 males, mean age 73 years, range 61-88 years) were thawed for at least 24 hours prior to testing. The humerus was transected midshaft to accommodate the shoulder simulator. Overlying soft tissues were dissected and the underlying muscles were exposed, leaving the deltoid and rotator cuff muscles intact. In order to enter and visualize the glenohumeral (GH) joint, the subscapularis muscle was elevated off of the subscapular fossa of the scapula, leaving its insertion along the lesser tuberosity intact. The GH capsule was breached in order to enter the joint and released circumferentially. The labrum was resected, as well as any remaining articular cartilage on the glenoid.

In order to simulate a rotator-cuff deficient shoulder, full-thickness supraspinatus and upper infraspinatus tears were created by releasing them from their insertion on the greater tuberosity. The infraspinatus was released such that it was level with the upper edge of the subscapularis tendon so as to have a symmetric anterior and posterior force couple for testing. As shown in Figure 2-1, the anterior (subscapularis) and posterior (lower infraspinatus and teres minor) cuff were sutured with a running locking stitch using a heavy #5 non-absorbable braided suture (Ethibond, Ethicon, Johnson & Johnson, New Jersey, USA).

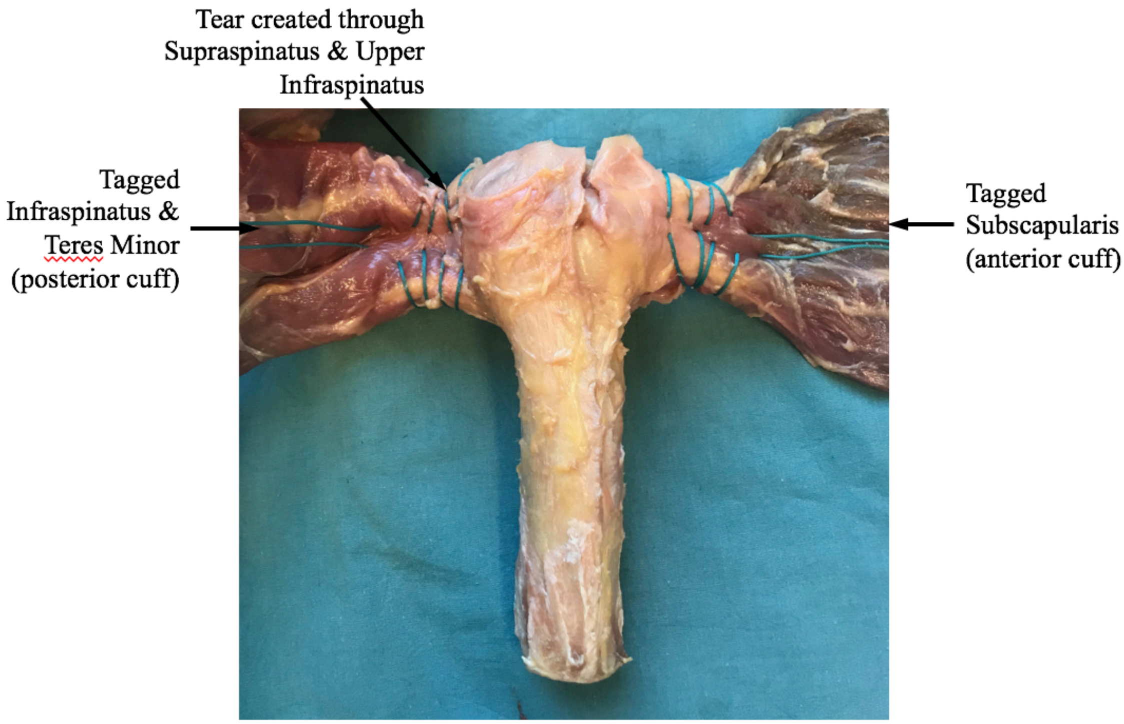

Figure 2-1: Tagged Rotator Cuff Tendons

Heavy #5 Ethibond suture used to tag the anterior and posterior rotator cuff tendons. A tear in supraspinatus and upper infraspinatus was created in order to mimic a rotator cuff-deficient shoulder.

The deltoid was then released from its distal insertion on the deltoid tuberosity of the humerus. The three heads of deltoid were then identified based on the anatomic description by Sakoma et al (Sakoma et al., 2011). The lateral edge of the acromion was divided into thirds. The anterior deltoid extended from the lateral aspect of the distl clavicle to the anterior third of the lateral acromion. The middle deltoid originated from the middle-third of the lateral acromion. The posterior deltoid originated from the posterior-third of the lateral acromion and extended along the medial aspect of the scapular spine. As shown in Figure 2-2, nylon mesh was sewn at the muscle origin along the tendinous edge of each deltoid segment using #5 Ethibond suture (Ethibond, Ethicon, Johnson & Johnson, New Jersey, USA). Another #5 Ethibond suture was then sutured through the Nylon mesh in order to attach it to the pneumatic actuators of the shoulder simulator.

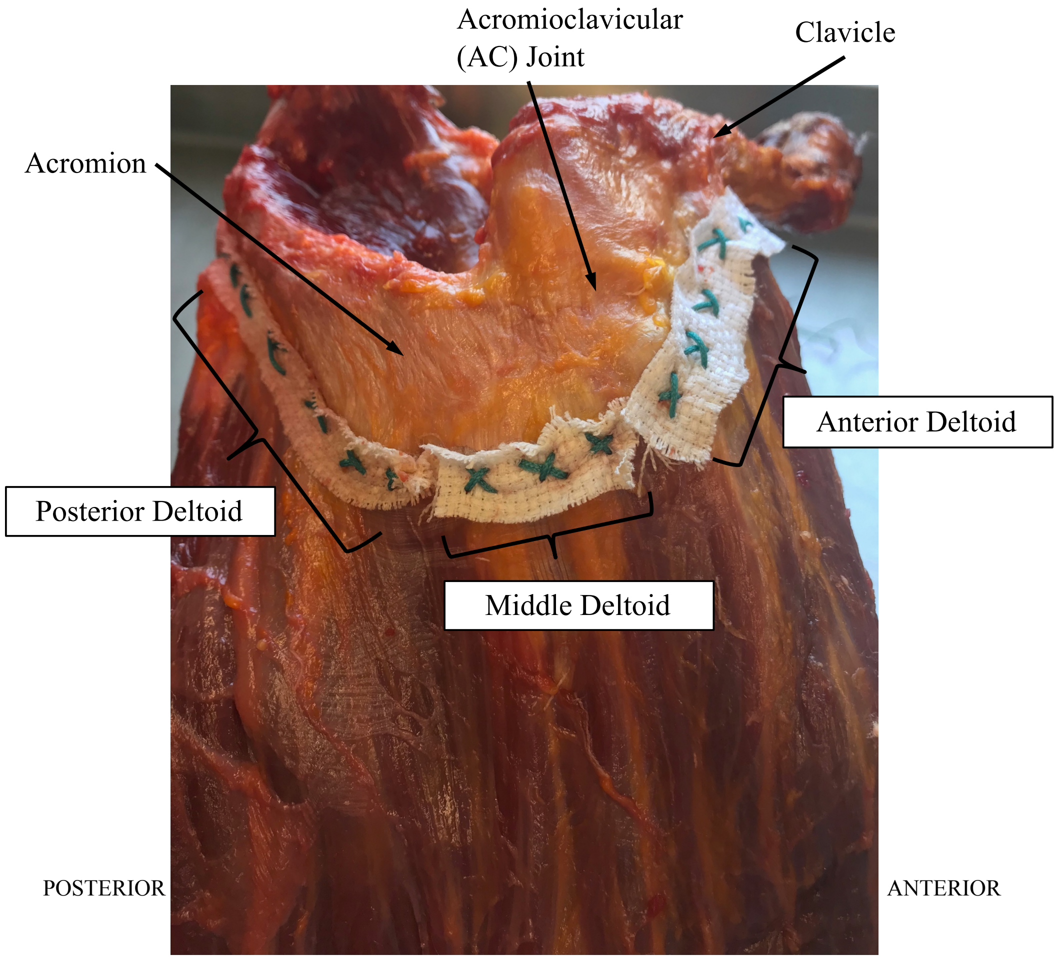

Figure 2-2: Tagged Heads of Deltoid Origin

Nylon mesh and heavy #5 Ethibond suture used to tag three heads of deltoid at the tendinous origin along the lateral clavicle, acromion and scapular spine.

The humerus and glenoid were then prepared for RTSA implantation. A sagittal saw was used to resect the humeral head circumferentially at the level of the articular margin (anatomical neck). The proximal humerus was first reamed using a power reamer, followed by reaming of the humeral shaft. The glenoid was reamed with a power reamer so as to remove all cartilage and accommodate placement of a vertically oriented baseplate.

The custom RTSA system was then implanted using a modified technique from the Wright Medical – Tornier Aequalis surgical technique manual (Wright Medical Technologies, Memphis, Tennessee). The humeral component was cemented in anatomic version relative to the transepicondylar axis, with humeral distalization dictated by aligning the inferior edge of the humeral cup with the superior aspect of the greater tuberosity. A humeral rod was cemented into the distal humeral shaft to allow for attachment to the shoulder simulator. The glenoid baseplate was then secured by drilling screws into the glenoid and placed in neutral orientation, with the inferior edge of the baseplate lining up with the inferior-most rim of the native glenoid.

The surface of the acromion was prepared for strain gauge placement. All soft tissue, muscle, and periosteum were dissected off the superior edge of the acromion and scapular spine, leaving the deltoid insertion intact along its edge. The bone was then cleaned and degreased with ethanol, and sandpaper was used to smooth the bone surface for strain gauge (SG) placement. Once the acromion was adequately prepared, adhesive glue was then used to place four strain gauges along the acromion and scapular spine (Strain gauge model # KFH-06-120-C1-11L3M3R, OMEGA Engineering, Quebec, Canada). The strain gauges were left to set for 30 minutes after the adhesive was applied.

For reproducibility between specimens, four specific landmarks were used for strain gauge placement (Figure 2-3, Figure 2-4):

1. Strain gauge 1 was placed midway between the anterior and posterior edge of the acromioclavicular (AC) joint, and midway between the medial and lateral edge of the acromial tip. The strain gauge was positioned in line with the anterior acromion, with the gauge leads exiting posteriorly.
2. Strain gauge 2 was placed halfway between the leading edge of SG 3 and the lateral edge of the acromion. The strain gauge was positioned in line with the scapular spine, with the gauge leads exiting medially.
3. Strain gauge 3 was placed directly above the spinoglenoid notch. The strain gauge was positioned in line with the scapular spine, with the gauge leads exiting medially.
4. Strain gauge 4 was placed 2 cm medial to the first strain gauge, measured from the leading edge (lateral edge) of both gauges. The strain gauge was positioned in line with the scapular spine, with the gauge leads exiting medially.

Strain gauge leads were then connected through a data acquisition unit (National Instruments, Model # NI USB-9237) to a central computer for data collection.

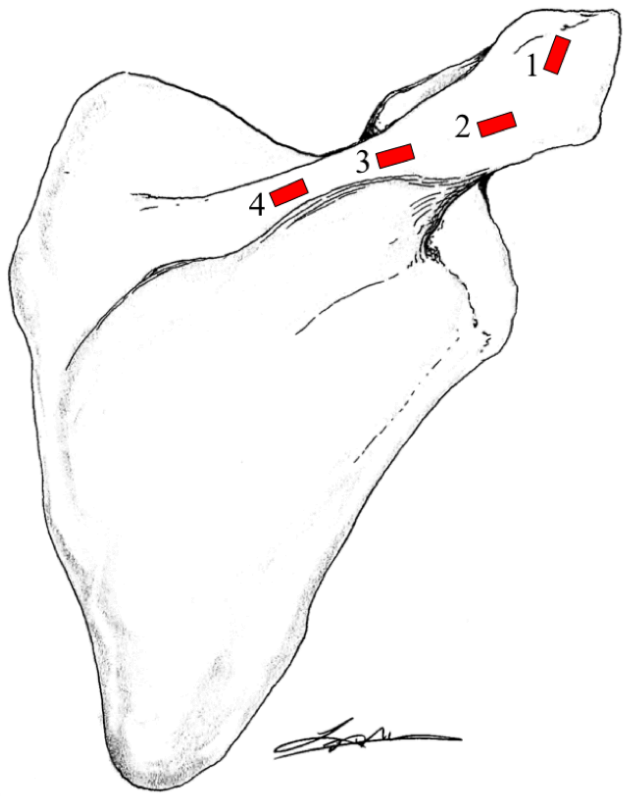

Figure 2-3: Illustration depicting the anatomic location of the strain gauges on a right scapula

(B)

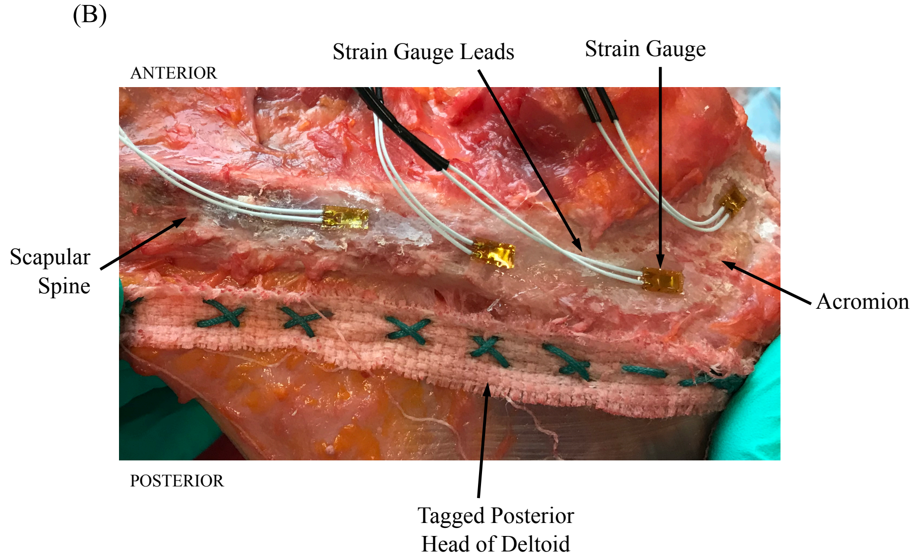

Figure 2-4: Strain gauge placement as seen on the right scapular spine and acromion of a study specimen

2.2.2 Shoulder Simulator

The scapulae were mounted onto the shoulder simulator using a scapular clamp and bolts drilled into the lateral scapular body (Figure 2-5). The distal humeral rod made contact with the simulator such that all load first passed through a load cell which was mounted to an abduction arc. This permitted freedom of motion of the humerus in all three directions of translation, as well as axial rotation, while constraining plane of elevation angles. The scapula was oriented so that the glenoid was vertical and the glenoid COR was in line with the abduction arc COR. The tagged rotator cuff muscles and three heads of deltoid were attached to cables and routed along their physiologic lines of action to computer-controlled pneumatic actuators. The clavicle was affixed to the simulator in its anatomic position.

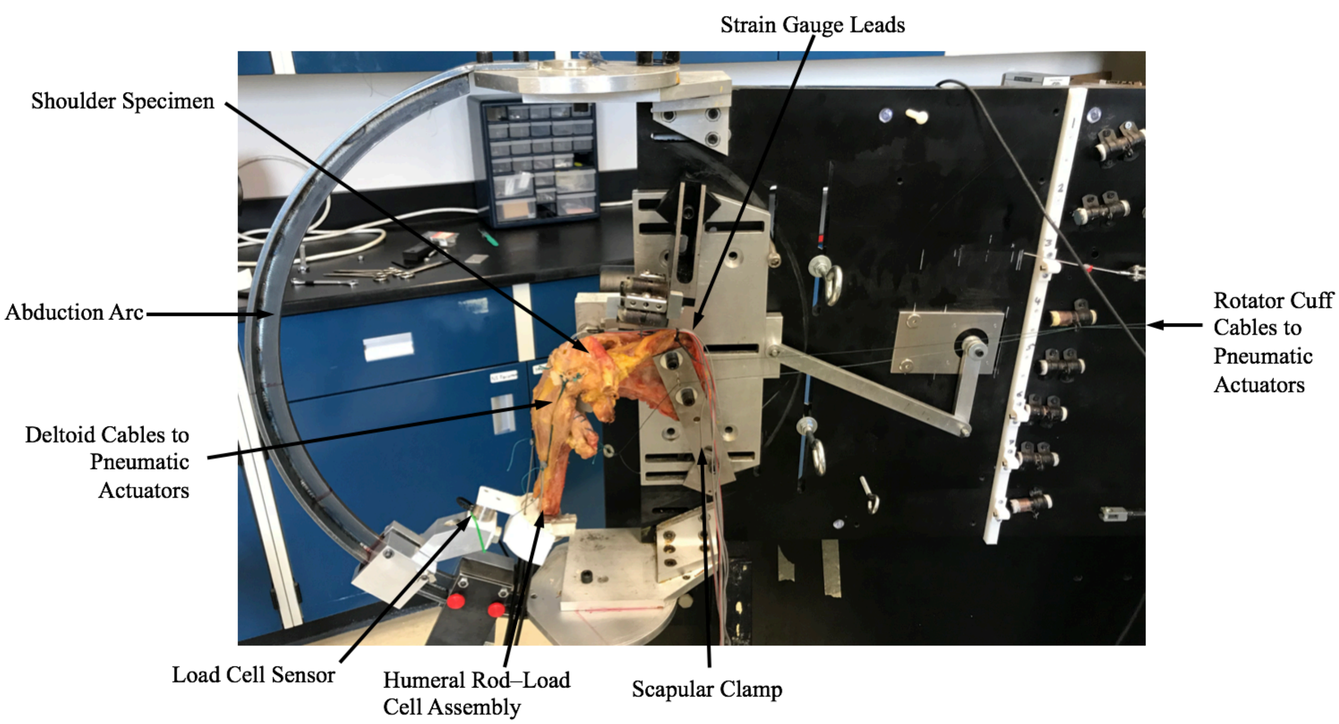

Figure 2-5: Shoulder Simulator Setup

A specimen is seen mounted to the shoulder simulator using a scapular clamp. The humeral rod makes contact with the load cell sensor located on the abduction arc. Cables from tagged tendons (deltoid, rotator cuff) are seen running to pneumatic actuators (out of view).

Computer-controlled pneumatic actuators were used to apply loads to each muscle tendon unit. Deltoid muscle loading ratios were calculated based on data from a biomechanical study reporting on muscle load contribution after RTSA implantation (Ackland, Roshan-Zamir, Richardson & Pandy, 2011). Based on these calculations, deltoid muscle loading ratios for shoulder abduction motion (15% anterior deltoid, 70% middle deltoid, 15% posterior deltoid) and flexion motion (40% anterior deltoid, 50% middle deltoid, 10% posterior deltoid) were used to guide the force applied by the simulator. The anterior and posterior cuff had a cumulative load of 10 N applied to preserve tension around the implant.

2.2.3 Testing Protocol

After mounting the specimen, the distance from the COR of the glenosphere to the distal humerus where it contacted the load cell was measured. This represented the moment arm length that permitted the conversion of abduction force measured at the load cell to an abduction moment.

Using a custom modular RTSA system, implant configurations were evaluated in a randomized order (Giles, Langohr, Johnson & Athwal, 2015; Langohr, Giles, Athwal & Johnson, 2015). With a set neck-shaft angle of 145°, nine implant configurations were evaluated based on two parameters at three levels: (1) glenosphere lateralization 0, 5, 10 mm; and (2) humeral lateralization -5, 5, 15 mm (Figure 1-14, Figure 1-15). All other parameters were held constant, with a glenosphere and humeral cup size of 42 mm and glenosphere inferiorization of 0 mm.

For each configuration, static range of motion was simulated in two planes of elevation at two angles: 0° and 90° abduction in the scapular plane (scaption), and 0° and 90° forward flexion. Elevation in both planes was measured at 60° of glenohumeral elevation, which corresponds to 90° of humerothoracic elevation. An increasing deltoid force was applied by the simulator until a target abduction moment of 1.5 N·m, as measured by the load cell, was achieved. Once a steady state was reached, the deltoid force was held constant, and ten seconds of strain gauge data was captured. This cycle was repeated three times for each plane of elevation to improve accuracy.

2.2.4 Outcome Variables

The main outcome variable of this study was acromial strain, as measured by the 4 strain gauges placed along the acromion and scapular spine. For each implant configuration, acromial strain was recorded in four planes of elevation, and each cycle was repeated three times for accuracy. Strain, which is defined as a change in length of a material over the original length, has no units and is reported as a ratio or a percentage. For the purpose of this study, strain values were analyzed in microstrain units (µStrain, strain x 10^6).

As a secondary outcome, total deltoid force was recorded across all three heads of the deltoid. This represented the force required for the muscle to abduct or forward flex the arm to reach a target moment of 1.5 N·m, as measured by the load cell. Again, deltoid force was measured for all implant configurations, in four planes of elevation, and repeated three times for accuracy. This outcome variable was measured to assess the efficiency of the deltoid across all implant configurations.

2.2.5 Statistical Analysis

Two three-way (glenoid lateralization, plane of elevation, angle of elevation; humeral lateralization, plane of elevation, angle of elevation) repeated measures analysis of variance (RM-ANOVA) were used for statistical analysis (SPSS Version 25.0; SPSS Inc, Chicago, IL, USA). Pairwise comparisons and analyses of interactions were performed to assess for significance. Statistical significance was defined as $p < 0.05$. A sample size of eight specimens was chosen based on previous similar biomechanical cadaver studies (Ackland, Roshan-Zamir, Richardson & Pandy, 2011; Chan et al., 2017; Schwartz et al., 2013). All statistically significant differences detected in the outcome variables were found to have a power greater than 0.8.

2.3 Results

2.3.1 Acromial Strain

Acromial strain was measured by 4 strain gauges placed along the acromion and scapular spine. Figure 2-6 shows the measured acromial strain of each SG and each plane of elevation for an implant with 145° NSA, 5 mm glenoid lateralization and 5 mm humeral lateralization. In abduction, SG 2 had a significantly higher strain measurement than SG 1 (p=0.007, p=0.005), SG 3 (p=0.036, p=0.049), and SG 4 (p=0.001, p=0.046). In 0° forward flexion, SG 2 had a significantly higher strain measurement than SG 1 (p=0.044) and SG 3 (p=0.042). In 90° forward flexion, SG 2 had a significantly higher strain measurement than SG 1 (p=0.021). Overall, significantly higher strain values were measured in forward flexion than in abduction (p=0.001).

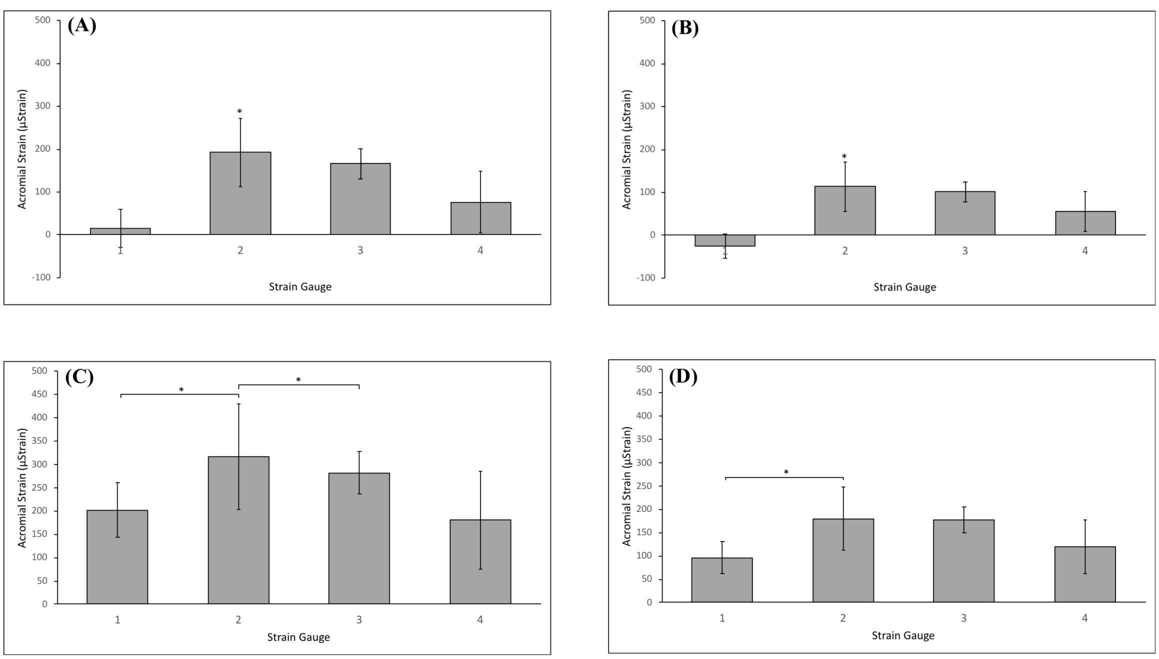

Figure 2-6: Averaged Acromial Strain for All Strain Gauges

Mean (+/- 1 SD) acromial strain measured by all 4 strain gauges at (A) 0° abduction, (B) 90° abduction, (C) 0° forward flexion, and (D) 90° forward flexion for an implant with 145° NSA, 5 mm glenoid lateralization, and 5 mm humeral lateralization. Significance (p<0.05) denoted with a ''.*

2.3.1.1 The Effect of Glenoid Lateralization on Acromial Strain

Figure 2-7 shows the results of glenoid lateralization on acromial strain for each strain gauge at each plane of elevation.

For SG 1, lateralization of the glenosphere from 0 to 10 mm in 0° forward flexion increased acromial strain by 28.7% ($p = 0.009$). At 90° forward flexion, acromial strain increased by 14.9% as glenoid lateralization increased from 5 to 10 mm ($p = 0.038$). There was no significant change in strain measured at SG 1 with glenoid lateralization when the arm was in abduction.

For SG 2, there was an opposite trend as lateralization of the glenosphere from 0 to 10 mm in 0° forward flexion decreased acromial strain by 20.2% ($p = 0.007$). At 90° forward flexion, acromial strain decreased by 39% as glenoid lateralization increased from 5 to 10 mm ($p = 0.01$). There was no significant change in strain measured at SG 2 with glenoid lateralization when the arm was in abduction.

For SG 3, lateralization of the glenosphere from 0 to 10 mm in 0° forward flexion increased acromial strain by 15.1% ($p = 0.002$). Conversely, at 90° forward flexion, acromial strain decreased by 18.7% as glenoid lateralization increased from 5 to 10 mm ($p = 0.004$). There was no significant change in strain measured at SG 3 with glenoid lateralization when the arm was in abduction.

For SG 4, a significant increase in strain was seen with the arm in 0° forward flexion as lateralization of the glenosphere from 0 to 10 mm increased acromial strain by 12.3% ($p = 0.026$). At 90° forward flexion, acromial strain decreased by 21.1% as glenoid lateralization increased from 5 to 10 mm ($p = 0.008$). At 0° abduction, a significant decrease in strain was measured as glenoid lateralization increased from 0 to 10 mm ($p = 0.05$). There was no significant effect on strain with glenoid lateralization when the arm was in 90° abduction.

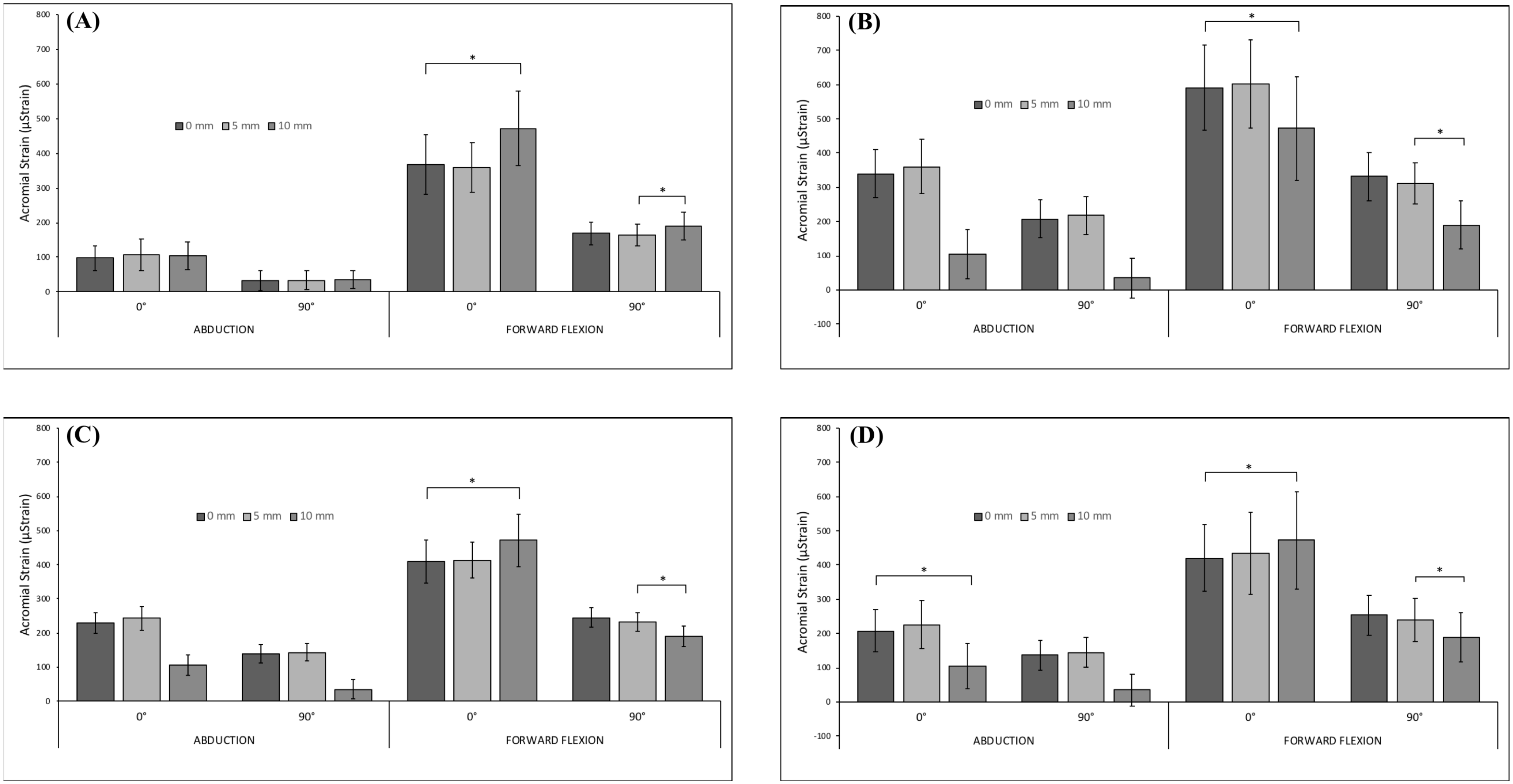

Figure 2-7: The Effect of Glenoid Lateralization on Acromial Strain

Mean (+/- 1 SD) acromial strain measured by (A) strain gauge 1, (B) strain gauge 2, (C) strain gauge 3, and (D) strain gauge 4 for increasing glenosphere lateralization (0, 5, and 10 mm) during all 4 planes of elevation. Significance (p<0.05) denoted with a ''.*

2.3.1.2 The Effect of Humeral Lateralization on Acromial Strain

Figure 2-8 shows the results of humeral lateralization on acromial strain for each strain gauge at each plane of elevation.

For SG 1, lateralization of the humeral component did not cause any significant change in acromial strain in either abduction or forward flexion.

For SG 2, a trend was seen towards decreased acromial strain with increasing humeral lateralization. With the arm in 0° abduction, acromial strain decreased by 20.4% and 69.8% as the humerus was lateralized from -5 to 5 mm ($p = 0.013$) and 5 to 15 mm ($p=0.026$), with an overall 76% decrease ($p=0.015$) from -5 to 15mm. Similarly, at 90° abduction, acromial strain decreased by 7.9% and 84.7% as the humerus was lateralized from -5 to 5 mm ($p = 0.025$) and 5 to 15 mm ($p=0.003$), with an overall 85.9% decrease from -5 to 15 mm ($p=0.002$). There was a trend towards decreasing acromial strain at 0° forward flexion, but this did not reach statistical significance. At 90° forward flexion, an 8.7% decrease in acromial strain was measured as the humerus was lateralized from -5 to 5 mm ($p=0.046$).

For SG 3, a similar trend was observed with a significant decrease in acromial strain with increasing humeral lateralization at both 0° and 90° abduction ($p=0.006$, $p<0.001$). Statistical significance was not reached at 0° forward flexion, however there was a significant decrease in acromial strain at 90° forward flexion as humeral lateralization increased from -5 to 15 mm ($p=0.032$).

For SG 4, again a similar trend was observed with a significant decrease in acromial strain with increasing humeral lateralization at both 0° and 90° abduction ($p=0.04$, $p=0.009$). Statistical significance was not reached at 0° and 90° forward flexion.

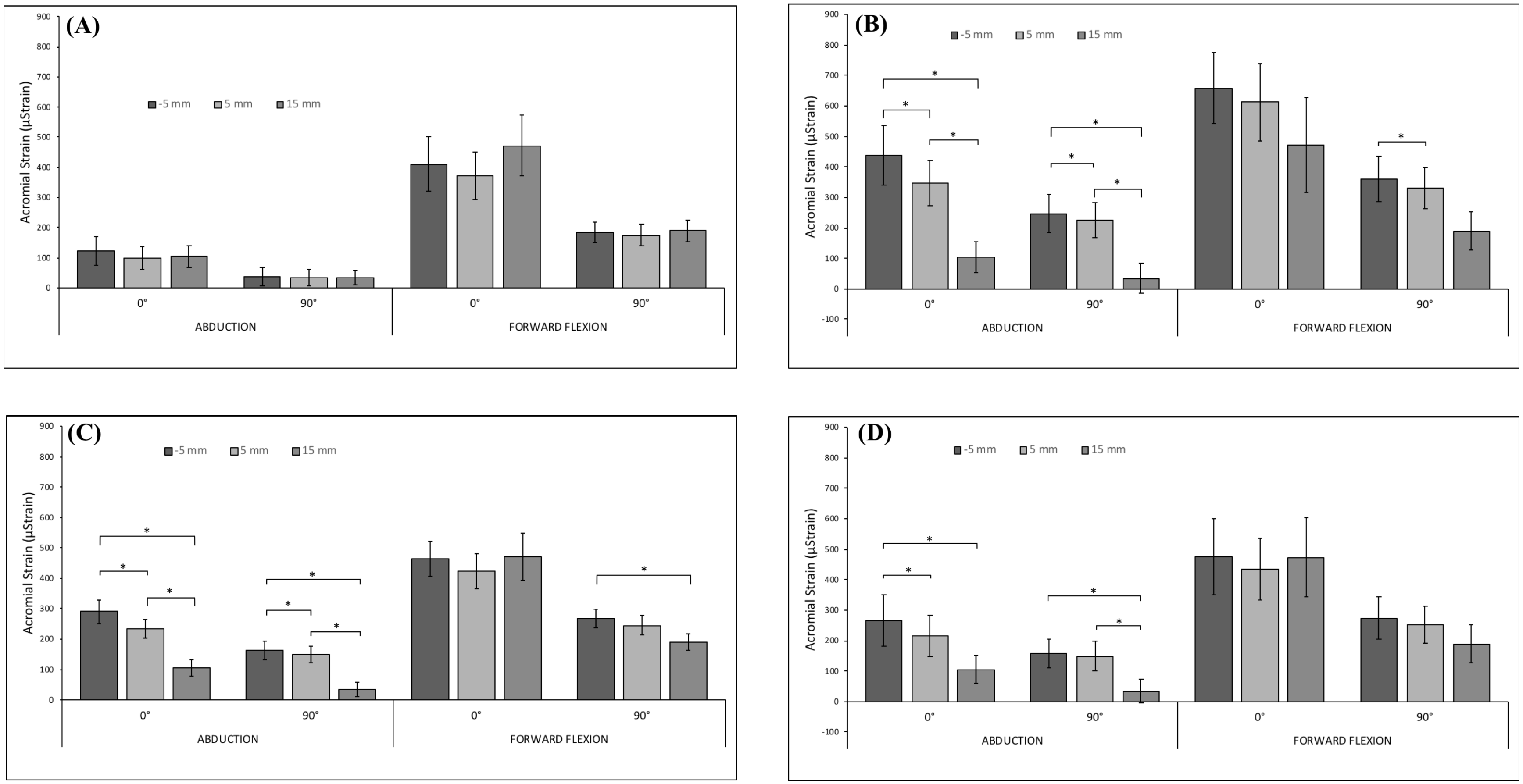

Figure 2-8: The Effect of Humeral Lateralization on Acromial Strain

Mean (+/- 1 SD) acromial strain measured by (A) strain gauge 1, (B) strain gauge 2, (C) strain gauge 3, and (D) strain gauge 4 for increasing humeral lateralization (-5, 5, and 15 mm) during all 4 planes of elevation. Significance (p<0.05) denoted with a ''.*

2.3.2 Total Deltoid Force

For all implant configurations, a higher total deltoid force was required to achieve forward flexion than abduction (p=0.012).

2.3.2.1 The Effect of Glenoid Lateralization on Total Deltoid Force

Figure 2-9 shows the results of glenoid lateralization on total deltoid force. Total deltoid force was found to significantly decrease with increasing glenoid lateralization at both 0° and 90° abduction (p=0.023, p=0.008). Though no statistically significant, there was a trend towards increased total deltoid force with increased glenoid lateralization at 0° forward flexion.

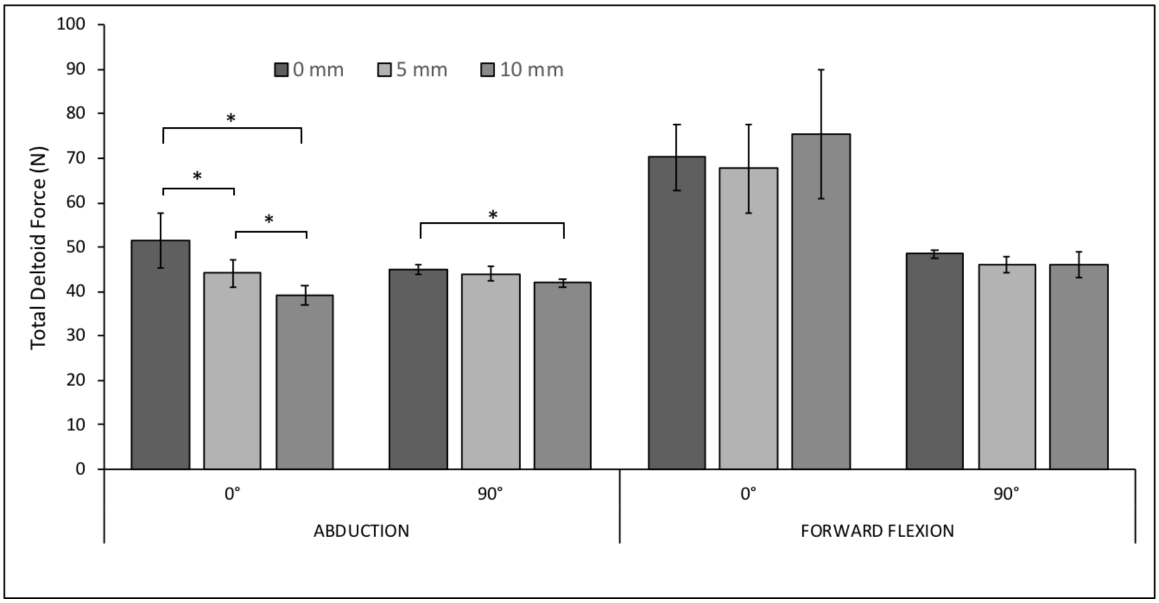

Figure 2-9: The Effect of Glenoid Lateralization on Total Deltoid Force

Mean (+/- 1 SD) total deltoid force measured for increasing glenoid lateralization (0, 5, and 10 mm) during all 4 planes of elevation. Significance (p<0.05) denoted with a ''.*

2.3.2.2 The Effect of Humeral Lateralization on Total Deltoid Force

Figure 2-10 demonstrates the effect of humeral laterization on total deltoid force. There was no significant effect of humeral lateralization on total deltoid force with the arm in abduction. At 0° forward flexion, total deltoid force significantly increased as humeral lateralization increased from -5 to 15 mm (p=0.005). At forward flexion of 90°, total deltoid force increased as humeral lateralization increased from 5 to 15 mm (p=0.011).

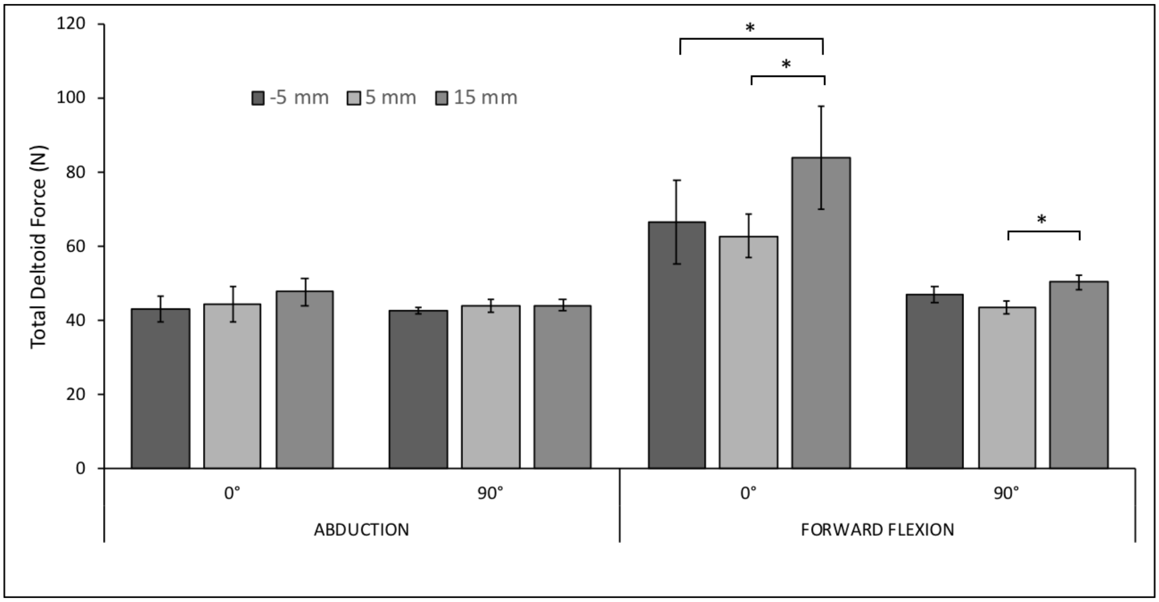

Figure 2-10: The Effect of Humeral Lateralization on Total Deltoid Force

Mean (+/- 1 SD) total deltoid force measured for increasing humeral lateralization (-5, 5, and 15 mm) during all 4 planes of elevation. Significance (p<0.05) denoted with a ''.*

2.4 Discussion

The primary objective of this study was to assess the role of implant configuration on acromial strain following RTSA implantation. Specifically, this study focused on glenoid lateralization (0, 5, and 10 mm) and humeral lateralization (-5, 5, and 15 mm) while keeping all other parameters constant. Strain was measured by 4 strain gauges through 4 planes of elevation (0° and 90° abduction, 0° and 90° forward flexion). To review, strain is defined as a change in length of a material over its original length. In order to positively correlate deltoid force and acromial strain, one must assume that with increased deltoid force, there is a relative deformation of the acromion which results in a change in strain.

In this study, it was found that acromial strain was significantly higher in the region of SG 2. This SG was positioned in the area of Levy type II acromial fractures, which is reported to be the most common pattern of acromial fracture (Levy, Anderson & Samson, 2013). Furthermore, in order to comment on the physiologic failure of cortical bone, deltoid load can be used as a metric for physiologic load. With the arm at 90° abduction, deltoid load should approach 1 body weight in a physiologic model. Based on the deltoid loads achieved in this study, and an average body weight of 60-80 kg (600-800 N), the loads in this study are about 10-fold less than physiologic. Assuming that this is a linear system, strain values can therefore be amplified by a factor of 10 in order to compare to the physiologic failure of cortical bone. With the arm at 90° abduction, the highest measured value for acromial strain can be converted to stress using Young's modulus for cortical bone, yielding a maximal acromial stress of 10.73 MPa in this study. Increasing this by 10-fold, a maximal stress of 107.3 MPa would be reached in a physiologic model. Interestingly, this is very close to approaching the traumatic fracture yield of cortical bone reported in the literature of 120-130 MPa (Cezaryirliouglu, Bahniuk, Davy & Heiple, 1985; Rho, Ashman & Turner, 1993). Of note, the highest values for acromial stress in this study were reached with the arm in forward flexion, with values as high as 28.67 MPa. If the same assumptions for a physiologic model are made with the arm in forward flexion, this would equate to stress values that exceed the traumatic fracture yield of cortical bone.

This study also found that acromial strain was measured to be significantly higher in forward flexion than in abduction. This is supported by the finding that total deltoid force was also measured to be higher in forward flexion than in abduction. There exists strong evidence that the direction of force of the deltoid in the setting of a rotator cuff-deficient shoulder is converted from compressive force to superior shear (Ackland, Roshan-Zamir, Richardson & Pandy, 2011; Berliner, Regalado-Magdos, Ma & Feeley 2015; Kontaxis & Johnson, 2009; Terrier, Reist, Merlini & Farron, 2008). Ackland et al. further validated this by showing that superior shear across a RTSA implant is greater in flexion than in abduction (Ackland, Roshan-Zamir, Richardson & Pandy, 2010). The findings of this study support the existing literature and suggest that forward flexion should be avoided under excessive load in the post-operative healing phase.

2.4.1 Glenoid Lateralization

Based on the results of this study, a few overarching patterns were observed. With the arm in abduction, there was no significant change in acromial strain as the glenosphere was lateralized. At 0° forward flexion, there was a general trend towards increased strain with increased glenoid lateralization. At 90° forward flexion, there was a general trend towards decreased strain with increased glenoid lateralization, specifically from 5 to 10 mm.

Total deltoid force was also measured as a secondary outcome. Overall, it was found that as the glenoid was lateralized, a decrease in total deltoid force was required for both 0° and 90° abduction. While not statistically significant, a trend was seen towards increased total deltoid force as the glenoid was lateralized with the arm at 0° forward flexion.

Specifically looking at the data with the arm at 0° forward flexion, the results of this study support the literature. Overall, with increased glenoid lateralization, there was both an increase in acromial strain and, although not statistically significant, a trend towards increased total deltoid force. A host of biomechanical studies exist which have focused on the effect of lateralizing the glenosphere. Overall, the concept is that as the COR is lateralized, deltoid moment arm decreases, resulting in a less efficient deltoid muscle that requires more force to perform range of motion and increased joint-reactive forces

(Costantini, Choi, Kontaxis & Gulotta, 2015; Giles, Langohr, Johnson & Athwal, 2015; Hettrich, Permeswaran, Goetz & Anderson, 2015; Hoenecke, Flores-Hernandez & D'Lima, 2014; Liou et al., 2017). Wong et al. have been the only to specifically focus on acromial stress, finding that lateralization of the COR from 0 to 5 mm and 0 to 10 mm caused an increase of acromial stress by 7.7% and 17.2% respectively (Wong, Langohr, Athwal & Johnson, 2016). However, this computational model simulated only an abduction arc of motion from 0° to 120° and did not investigate forward flexion.

2.4.2 Humeral Lateralization

Humeral lateralization was also associated with several overarching patterns. An overall trend towards decreased acromial strain with increased humeral lateralization was seen. SG 1, located at the tip of the acromion, did not measure any significant change in acromial strain. The remaining 3 strain gauges found that in abduction, acromial strain decreased as the humerus was lateralized. Total deltoid force did not significantly change in abduction but did increase in forward flexion with increasing humeral lateralization.

With regards to abduction, acromial strain decreased as the humerus was lateralized. Giles et al. demonstrated in a cadaveric model that increasing humeral lateralization decreased deltoid force required for active abduction (Giles, Langohr, Johnson & Athwal, 2015). While total deltoid force required for abduction in this study did not reach statistical significance, this existing literature does lend itself to the finding of decreased acromial strain with increased humeral lateralization in abduction. This does, however, contradict the findings by Wong et al. In their computational study, they found that humeral lateralization from -5 to 0 mm and 0 to 5 mm increased acromial stress by 1.4% and 1.7% respectively (Wong, Langohr, Athwal & Johnson, 2016). As per this present study, they did not increase humeral lateralization as far as 15 mm, and this model was only simulated in abduction.

2.4.3 Strengths and Limitations

This is the first cadaveric biomechanical study to examine the role of glenoid and humeral component lateralization on acromial strain following RTSA implantation. Using a custom designed prosthesis system, multiple permutations of implant configurations were able to be tested. As this was a modular system, it allowed for all configurations to be tested in each specimen. The shoulder simulator used in this study allowed for computer-controlled range of motion in both forward flexion and abduction. Few studies have focused on both planes of elevation in such a biomechanical model.

Biomechanical studies using cadaveric models have inherent limitations. Despite an attempt to best replicate *in-vivo* mechanics and physiology, a computer-controlled simulator cannot account for dynamic muscle changes, soft tissue adaptation, and proprioception. In dissecting the specimens, much of the surrounding soft tissues were removed, including the distal deltoid insertion, which may have played a role in soft tissue tensioning post-implantation. Similarly, while a rotator cuff tear was simulated in this study, it does not truly replicate the *in-vivo* degenerative, torn rotator cuff. While the shoulder simulator was able to accommodate elevation in both forward flexion and abduction, this still limits the true multiaxial nature of the joint. Additionally, the scapula was mounted to the simulator in a fixed position, thus preventing true scapulohumeral rhythm during humeral elevation. To account for this, 60° of glenohumeral elevation was used to simulate 90° of humerothoracic elevation based on a 2:1 ratio described by Inman et al. (Inman, Saunders & Abbott, 1996).

2.5 Conclusions

This study provides further insight into the role of glenoid and humeral component lateralization on acromial strain following RTSA implantation. Specifically, an overall trend was found that increasing glenoid lateralization causes an increase in acromial strain in 0° forward flexion, while increasing humeral lateralization caused a decrease in acromial strain in abduction. Total deltoid force was found to generally correlate with acromial strain, although not always with statistical significance.

The findings in this study have clinical importance in the future research and design of RTSA implants. From an implant design perspective, glenoid lateralization has been used to eliminate scapular notching and impingement while conversely causing decreased deltoid efficiency and increased joint-reactive forces (Berhouet, Garaud & Favard, 2014; Costantini, Choi, Kontaxis & Gulotta, 2015; Giles, Langohr, Johnson & Athwal, 2015; Gutiérrez et al., 2007a; Gutiérrez et al., 2008; Gutiérrez et al., 2007b; Hettrich, Permeswaran, Goetz & Anderson, 2015; Hoenecke, Flores-Hernandez & D'Lima, 2014; Jobin et al., 2012; Li et al., 2013; Liou et al., 2017; Valenti et al., 2011; Virani et al., 2013). Humeral lateralization has been reported to increase deltoid moment arm, decrease joint-reactive forces, improve rotator cuff torque, and restore the normal shoulder contour (Berhouet et al., 2015; Chan et al., 2017; Giles, Langohr, Johnson & Athwal, 2015; Walker et al., 2016a).

This study found that both acromial strain and total deltoid force were highest in forward flexion as opposed to abduction. This suggests that post-operative rehabilitation should avoid excessive loading of the arm in this plane of elevation. This study has also given further evidence into the pattern and etiology of acromial fractures. The highest strain values were measured in the region of Levy type II acromial fractures, which supports the existing literature. Interestingly, when compared to a physiologic model, stress values approached the traumatic fracture yield of cortical bone, which contests the theory of an insufficiency mechanism of acromial fractures.

2.6 References

Ackland, D. C., Roshan-Zamir, S., Richardson, M., & Pandy, M. G. (2010). Moment Arms of the Shoulder Musculature After Reverse Total Shoulder Arthroplasty: *The Journal of Bone and Joint Surgery-American Volume*, *92*, 1221–1230.

Ackland, D. C., Roshan-Zamir, S., Richardson, M., & Pandy, M. G. (2011). Muscle and joint-contact loading at the glenohumeral joint after reverse total shoulder arthroplasty. *Journal of Orthopaedic Research*, *29*, 1850–1858.

Barco, R., Savvidou, O. D., Sperling, J. W., Sanchez-Sotelo, J., & Cofield, R. H. (2016). Complications in reverse shoulder arthroplasty. *EFORT Open Reviews*, *1*, 72–80.

Berhouet, J., Garaud, P., & Favard, L. (2014). Evaluation of the role of glenosphere design and humeral component retroversion in avoiding scapular notching during reverse shoulder arthroplasty. *Journal of Shoulder and Elbow Surgery*, *23*, 151–158.

Berhouet, J., Kontaxis, A., Gulotta, L. V., Craig, E., Warren, R., Dines, J., & Dines, D. (2015). Effects of the humeral tray component positioning for onlay reverse shoulder arthroplasty design: a biomechanical analysis. *Journal of Shoulder and Elbow Surgery*, *24*, 569–577.

Berliner, J. L., Regalado-Magdos, A., Ma, C. B., & Feeley, B. T. (2015). Biomechanics of reverse total shoulder arthroplasty. *Journal of Shoulder and Elbow Surgery*, *24*, 150–160.

Boileau, P., Gonzalez, J.-F., Chuinard, C., Bicknell, R., & Walch, G. (2009). Reverse total shoulder arthroplasty after failed rotator cuff surgery. *Journal of Shoulder and Elbow Surgery*, *18*, 600–606.

Cezaryirliouglu, H., Bahniuk, E., Davy, D. T., & Heiple, K. G. (1985). Anisotropic yield behavior of bone under combined axial force and torque. *Journal of Biomechanics, 18*, 61-69.

Chan, K., Langohr, G. D. G., Mahaffy, M., Johnson, J. A., & Athwal, G. S. (2017). Does Humeral Component Lateralization in Reverse Shoulder Arthroplasty Affect Rotator Cuff Torque? Evaluation in a Cadaver Model. *Clinical Orthopaedics and Related Research®*, *475*, 2564–2571.

Costantini, O., Choi, D. S., Kontaxis, A., & Gulotta, L. V. (2015). The effects of progressive lateralization of the joint center of rotation of reverse total shoulder implants. *Journal of Shoulder and Elbow Surgery*, *24*, 1120–1128.

Crosby, L. A., Hamilton, A., & Twiss, T. (2011). Scapula Fractures After Reverse Total Shoulder Arthroplasty: Classification and Treatment. *Clinical Orthopaedics and Related Research®*, *469*, 2544–2549.

Cuff, D. J., Pupello, D. R., Santoni, B. G., Clark, R. E., & Frankle, M. A. (2017). Reverse Shoulder Arthroplasty for the Treatment of Rotator Cuff Deficiency: A Concise Follow-up, at a Minimum of 10 Years, of Previous Reports*. *The Journal of Bone and Joint Surgery*, *99*, 1895–1899.

Drake, G. N., O'Connor, D. P., & Edwards, T. B. (2010). Indications for Reverse Total Shoulder Arthroplasty in Rotator Cuff Disease. *Clinical Orthopaedics and Related Research®*, *468*, 1526–1533.

Ek, E. T. H., Neukom, L., Catanzaro, S., & Gerber, C. (2013). Reverse total shoulder arthroplasty for massive irreparable rotator cuff tears in patients younger than 65 years old: results after five to fifteen years. *Journal of Shoulder and Elbow Surgery*, *22*, 1199–1208.

Ferrel, J. R., Trinh, T. Q., & Fischer, R. A. (2015). Reverse Total Shoulder Arthroplasty Versus Hemiarthroplasty for Proximal Humeral Fractures: A Systematic Review. *Journal of Orthopedic Trauma*, *29*, 60–68.

Flury, M. P., Frey, P., Goldhahn, J., Schwyzer, H.-K., & Simmen, B. R. (2011). Reverse shoulder arthroplasty as a salvage procedure for failed conventional shoulder replacement due to cuff failure—midterm results. *International Orthopaedics*, *35*, 53–60.

Frankle, M., Levy, J. C., Pupello, D., Siegal, S., Saleem, A., Mighell, M., & Vasey, M. (2006). The Reverse Shoulder Prosthesis for Glenohumeral Arthritis Associated with Severe Rotator Cuff Deficiency: A Minimum Two-Year Follow-up Study of Sixty Patients Surgical Technique. *JBJS Essential Surgical Techniques*, *os-88*, 178–190.

Gallinet, D., Ohl, X., Decroocq, L., Dib, C., Valenti, P., & Boileau, P. (2018). Is reverse total shoulder arthroplasty more effective than hemiarthroplasty for treating displaced proximal humerus fractures in older adults? A Systematic Review and Meta-Analysis. *Orthopaedics & Traumatology: Surgery & Research*. doi:10.1016/j.otsr.2018.04.025

Gerber, C., & Nyffeler, R. W. (2009). Reverse Total Shoulder Arthroplasty. *Journal of the American Academy of Orthopaedic Surgeons*, *17*, 284–295.

Giles, J. W., Langohr, G. D. G., Johnson, J. A., & Athwal, G. S. (2015). Implant Design Variations in Reverse Total Shoulder Arthroplasty Influence the Required Deltoid Force and Resultant Joint Load. *Clinical Orthopaedics and Related Research®*, *473*, 3615–3626.

Gutiérrez, S., Greiwe, R. M., Frankle, M. A., Siegal, S., & Lee, W. E. (2007a). Biomechanical comparison of component position and hardware failure in the reverse shoulder prosthesis. *Journal of Shoulder and Elbow Surgery*, *16*, S9–S12.

Gutiérrez, S., Levy, J. C., Frankle, M. A., Cuff, D., Keller, T. S., Pupello, D. R., & Lee, W. E. (2008). Evaluation of abduction range of motion and avoidance of inferior scapular impingement in a reverse shoulder model. *Journal of Shoulder and Elbow Surgery*, *17*, 608–615.

Gutiérrez, S., Levy, J. C., Lee, W. E., Keller, T. S., & Maitland, M. E. (2007b). Center of Rotation Affects Abduction Range of Motion of Reverse Shoulder Arthroplasty. *Clinical Orthopaedics and Related Research*, *458*, 78 – 82.

Hamid, N., Connor, P. M., Fleischli, J. F., & D'Alessandro, D. F. (2011). Acromial Fracture After Reverse Shoulder Arthroplasty. *American Journal of Orthopedics, 40,* e125–129.

Hattrup, S. J. (2010). The Influence of Postoperative Acromial and Scapular Spine Fractures on the Results of Reverse Shoulder Arthroplasty. *Orthopedics*. doi:10.3928/01477447-20100329-04

Hettrich, C. M., Permeswaran, V. N., Goetz, J. E., & Anderson, D. D. (2015). Mechanical tradeoffs associated with glenosphere lateralization in reverse shoulder arthroplasty. *Journal of Shoulder and Elbow Surgery*, *24*, 1774–1781.

Hoenecke, H. R., Flores-Hernandez, C., & D'Lima, D. D. (2014). Reverse total shoulder arthroplasty component center of rotation affects muscle function. *Journal of Shoulder and Elbow Surgery*, *23*, 1128–1135.

Inman, V. T., Saunders, J. B., & Abbott, L. C. (1996). Observations of the Function of the Shoulder Joint. 1944. *Clinical Orthopaedics and Related Research, 330*, 3–12.

Jobin, C. M., Brown, G. D., Bahu, M. J., Gardner, T. R., Bigliani, L. U., Levine, W. N., & Ahmad, C. S. (2012). Reverse total shoulder arthroplasty for cuff tear arthropathy: the clinical effect of deltoid lengthening and center of rotation medialization. *Journal of Shoulder and Elbow Surgery*, *21*, 1269–1277.

Kontaxis, A., & Johnson, G. R. (2009). The biomechanics of reverse anatomy shoulder replacement – A modelling study. *Clinical Biomechanics*, *24*, 254–260.

Lädermann, A., Williams, M. D., Melis, B., Hoffmeyer, P., & Walch, G. (2009). Objective evaluation of lengthening in reverse shoulder arthroplasty. *Journal of Shoulder and Elbow Surgery*, *18*, 588–595.

Langohr, G. D. G., Giles, J. W., Athwal, G. S., & Johnson, J. A. (2015). The effect of glenosphere diameter in reverse shoulder arthroplasty on muscle force, joint load, and range of motion. *Journal of Shoulder and Elbow Surgery*, *24*, 972–979.

Leung, B., Horodyski, M., Struk, A. M., & Wright, T. W. (2012). Functional outcome of hemiarthroplasty compared with reverse total shoulder arthroplasty in the treatment of rotator cuff tear arthropathy. *Journal of Shoulder and Elbow Surgery*, *21*, 319–323.

Levy, J. C., Anderson, C., & Samson, A. (2013). Classification of Postoperative Acromial Fractures Following Reverse Shoulder Arthroplasty: *The Journal of Bone and Joint Surgery-American Volume*, *95*, e104-1–7.

Levy, J. C., Frankle, M., Mighell, M., & Pupello, D. (2007). The Use of the Reverse Shoulder Prosthesis for the Treatment of Failed Hemiarthroplasty for Proximal Humeral Fracture. *The Journal of Bone and Joint Surgery, 89,* 292–300.

Levy, J. C., Virani, N., Pupello, D., & Frankle, M. (2007). Use of the reverse shoulder prosthesis for the treatment of failed hemiarthroplasty in patients with glenohumeral arthritis and rotator cuff deficiency. *The Journal of Bone and Joint Surgery*, *89*, 189–195.

Li, X., Knutson, Z., Choi, D., Lobatto, D., Lipman, J., Craig, E. V., Warren, R. F., & Gulotta, L. V. (2013). Effects of glenosphere positioning on impingement-free internal and external rotation after reverse total shoulder arthroplasty. *Journal of Shoulder and Elbow Surgery*, *22*, 807–813.

Liou, W., Yang, Y., Petersen-Fitts, G. R., Lombardo, D. J., Stine, S., & Sabesan, V. J. (2017). Effect of lateralized design on muscle and joint reaction forces for reverse shoulder arthroplasty. *Journal of Shoulder and Elbow Surgery*, *26*, 564–572.

Mayne, I. P., Bell, S. N., Wright, W., & Coghlan, J. A. (2016). Acromial and scapular spine fractures after reverse total shoulder arthroplasty. *Shoulder & Elbow*, *8*, 90–100.

Nolan, B. M., Ankerson, E., & Wiater, J. M. (2011). Reverse Total Shoulder Arthroplasty Improves Function in Cuff Tear Arthropathy. *Clinical Orthopaedics and Related Research®*, *469*, 2476–2482.

Rho, J. Y., Ashman, B. A., & Turner, C. H. (1993). Young's modulus of trabecular and cortical bone material: Ultrasonic and microtensile measurements. *Journal of Biomechanics, 26,* 111-119.

Sakoma, Y., Sano, H., Shinozaki, N., Itoigawa, Y., Yamamoto, N., Ozaki, T., & Itoi, E. (2011). Anatomical and functional segments of the deltoid muscle: Anatomical and functional segments of deltoid. *Journal of Anatomy*, *218*, 185–190.

Schairer, W. W., Nwachukwu, B. U., Lyman, S., Craig, E. V., & Gulotta, L. V. (2015a). National utilization of reverse total shoulder arthroplasty in the United States. *Journal of Shoulder and Elbow Surgery*, *24*, 91–97.

Schairer, W. W., Nwachukwu, B. U., Lyman, S., Craig, E. V., & Gulotta, L. V. (2015b). Reverse shoulder arthroplasty versus hemiarthroplasty for treatment of proximal humerus fractures. *Journal of Shoulder and Elbow Surgery*, *24*, 1560–1566.

Schwartz, D. G., Kang, S. H., Lynch, T. S., Edwards, S., Nuber, G., Zhang, L.-Q., & Saltzman, M. (2013). The anterior deltoid's importance in reverse shoulder arthroplasty: a cadaveric biomechanical study. *Journal of Shoulder and Elbow Surgery*, *22*, 357–364.

Sebastiá-Forcada, E., Cebrián-Gómez, R., Lizaur-Utrilla, A., & Gil-Guillén, V. (2014). Reverse shoulder arthroplasty versus hemiarthroplasty for acute proximal humeral fractures. A blinded, randomized, controlled, prospective study. *Journal of Shoulder and Elbow Surgery*, *23*, 1419–1426.

Terrier, A., Reist, A., Merlini, F., & Farron, A. (2008). Simulated joint and muscle forces in reversed and anatomic shoulder prostheses. *The Journal of Bone and Joint Surgery. British Volume*, *90-B*, 751–756.

Teusink, M. J., Otto, R. J., Cottrell, B. J., & Frankle, M. A. (2014). What is the effect of postoperative scapular fracture on outcomes of reverse shoulder arthroplasty? *Journal of Shoulder and Elbow Surgery*, *23*, 782–790.

Valenti, P., Sauzières, P., Katz, D., Kalouche, I., & Kilinc, A. S. (2011). Do Less Medialized Reverse Shoulder Prostheses Increase Motion and Reduce Notching? *Clinical Orthopaedics and Related Research®*, *469*, 2550–2557.

Virani, N. A., Cabezas, A., Gutiérrez, S., Santoni, B. G., Otto, R., & Frankle, M. (2013). Reverse shoulder arthroplasty components and surgical techniques that restore glenohumeral motion. *Journal of Shoulder and Elbow Surgery*, *22*, 179–187.

Walch, G., Mottier, F., Wall, B., Boileau, P., Molé, D., & Favard, L. (2009). Acromial insufficiency in reverse shoulder arthroplasties. *Journal of Shoulder and Elbow Surgery*, *18*, 495–502.

Walker, D. R., Kinney, A. L., Wright, T. W., & Banks, S. A. (2016a). How sensitive is the deltoid moment arm to humeral offset changes with reverse total shoulder arthroplasty? *Journal of Shoulder and Elbow Surgery*, *25*, 998–1004.

Walker, D. R., Struk, A. M., Matsuki, K., Wright, T. W., & Banks, S. A. (2016b). How do deltoid muscle moment arms change after reverse total shoulder arthroplasty? *Journal of Shoulder and Elbow Surgery*, *25*, 581–588.

Walker, M., Willis, M. P., Brooks, J. P., Pupello, D., Mulieri, P. J., & Frankle, M. A. (2012). The use of the reverse shoulder arthroplasty for treatment of failed total shoulder arthroplasty. *Journal of Shoulder and Elbow Surgery*, *21*, 514–522.

Willis, M., Min, W., Brooks, J. P., Mulieri, P., Walker, M., Pupello, D., & Frankle, M. (2012). Proximal humeral malunion treated with reverse shoulder arthroplasty. *Journal of Shoulder and Elbow Surgery*, *21*, 507–513.

Wong, M. T., Langohr, G. D. G., Athwal, G. S., & Johnson, J. A. (2016). Implant positioning in reverse shoulder arthroplasty has an impact on acromial stresses. *Journal of Shoulder and Elbow Surgery*, *25*, 1889–1895.

Chapter 3

3 The Role of Neck-Shaft Angle on Acromial Strain

Modifiable implant parameters in reverse total shoulder arthroplasty (RTSA) have been well studied with respect to the variables of range of motion, deltoid function, and stability. A lack of knowledge exists, however, on the impact of these changes on acromial strain. This chapter will focus specifically on the role of neck-shaft angle (NSA) on acromial strain. Similar concepts to Chapter 2 will be discussed in the introduction, and similar methodology will be applied. This is the first cadaveric biomechanical study to examine the role of NSA on acromial strain following RTSA implantation.

3.1 Introduction

[NB: A portion of this material was presented in Chapters 1 and 2 and is also included here in order to ensure that this chapter is in "article" format].

Reverse total shoulder arthroplasty (RTSA) is becoming a more widely accepted surgical treatment option in the setting of severe rotator cuff tear arthropathy, acute proximal humerus fractures, and revision surgery after failed rotator cuff repair or failed arthroplasty (Boileau et al., 2009; Drake, O'Connor & Edwards, 2010; Ek, Neukom, Cantanzaro & Gerber, 2013; Ferrel, Trinh & Fischer, 2015; Flury et al., 2011; Gallinet et al., 2018; Leung, Horodyski, Struk & Wright, 2012; Levy, Frankle, Mighell & Pupello, 2007; Levy, Virani, Pupello & Frankle, 2007; Nolan, Ankerson & Wiater, 2011; Schairer et al, 2015; Sebastiá-Forcada, Cebrián-Gómez, Lizaur-Utrilla & Gil-Guillén, 2014; Walker et al., 2012; Willis et al., 2012). As more surgeons are performing this procedure, post-operative complications are becoming more evident. Acromial fractures have a reported incidence as high as 10% following RTSA, although his value is likely underestimated as these fractures are a challenge to identify and diagnose (Crosby, Hamilton & Twiss, 2011; Cuff et al., 2017; Frankle et al., 2005; Hamid, Connor, Fleischli & D'Alessandro, 2011; Hattrup, 2010; Levy, Anderson & Samson, 2013; Mayne, Bell, Wright & Coghlan, 2016; Teusink, Otto, Cottrell & Frankle, 2014; Walch et al., 2009).

The pathophysiology of acromial fractures following RTSA is thought to be through an insufficiency fracture mechanism. Osteoporosis was found to be the only risk factor that increased the chance of acromial fractures post-operatively (Otto et al., 2013). Walch et al. demonstrated that pre-operative acromial lesions caused no increased risk of post-operative fracture (Walch et al., 2009). Wong et al. validated this hypothesis in their computational study which demonstrated that the acromion never reached a threshold of traumatic fracture following RTSA, but rather sustained repetitive stress through the deltoid that likely exceeded the ability of the body to repair the damaged bone (Wong, Langohr, Athwal & Johnson, 2016).

RTSA, as the name implies, reverses the native anatomy of the glenohumeral joint. Originally conceptualized by Neer in the 1970s, Grammont later revolutionized the design to the reverse implant that is known today. His original designs involved a glenoid center of rotation (COR) that was medialized and distalized, allowing for improved deltoid mechanical advantage. The original design was also semiconstrained, with a non-anatomic NSA of 155° aimed to lengthen the arm and increase deltoid tension, again allowing for optimized deltoid function (Ackland, Roshan-Zamir, Richardson & Pandy, 2010; Boileau, Watkinson, Hatzidakis & Balg, 2005; Walker et al., 2016).

The evolution of the design later changed, as the valgus neck (155°) was noted to cause scapular notching and a deficit in adduction range of motion. Computational studies demonstrated a trade-off in range of motion, with a decrease in NSA allowing for improved adduction, but decreased abduction (de Wilde, Poncet, Middernacht & Ekelund, 2010; Werner, Chaoui & Walch, 2017). Langohr et al. demonstrated with a finite element analysis that decreasing the NSA caused a resultant increase in contact stress across the implant (Langohr et al., 2016).

Commercially available RTSA systems today offer neck-shaft angles ranging from 127.5° to 155° (Werthel et al., 2018). There remains a lack of knowledge regarding the consequence of a more varus or valgus neck and how this affects acromial strain. The purpose of this *in-vitro* biomechanical cadaveric simulator study was to investigate the role of NSA on acromial strain following RTSA implantation. This was evaluated with three different implants through four planes of elevation (0° and 90° abduction, 0° and 90° forward flexion). A custom modular RTSA system will allow for testing of implants with varying neck-shaft angles (135°, 145°, and 155°) and otherwise identical configuration parameters. It is hypothesized that changes in NSA will not have a significant effect on acromial strain following RTSA implantation. To the author's knowledge, this is the first biomechanical study to investigate the relationship between NSA and acromial strain.

3.2 Materials and Methods

3.2.1 Specimen Preparation

[NB: Cadaveric specimen preparation is similar to that described in Chapter 2].

Eight fresh frozen right male cadaveric shoulders (8 males, mean age 73 years, range 61-88 years) were thawed for at least 24 hours prior to testing. The humerus was cut midshaft, and soft tissues were dissected and removed including skin and subcutaneous tissue. The rotator cuff muscles and deltoid were identified and left intact. The subscapularis muscle was elevated off the subscapular fossa in order to enter the glenohumeral joint. The joint capsule and labrum were incised and resected circumferentially, and the glenoid articular cartilage was removed.

Full-thickness supraspinatus and upper infraspinatus tears were created in order to simulate a rotator-cuff deficient shoulder. The tear was extended so as to create a balanced force couple both anteriorly and posteriorly; to do so, infraspinatus was released to the level of the upper edge of subscapularis tendon. The anterior (subscapularis) and posterior (lower infraspinatus and teres minor) cuff were tagged with a running locking stitch using a heavy #5 non-absorbable braided suture (Ethibond, Ethicon, Johnson & Johnson, New Jersey, USA).

The deltoid muscle was then released from its distal insertion on the deltoid tuberosity, and the three heads of deltoid were identified. Based on the anatomic description by Sakoma et al. (Sakoma et al., 2011), the acromion was divided into thirds and the deltoid was tagged with nylon mesh in a similar fashion as described in Chapter 2.

Next, the specimen was prepared for RTSA implantation. The humeral head was resected at the anatomical neck using a sagittal saw, and the canal was reamed using a power reamer. The glenoid was reamed in order to place a vertically oriented baseplate. Using a modified technique from the Wright Medical – Tornier Aequalis surgical technique manual, the custom RTSA system was implanted as described in Chapter 2 (Wright Medical Technologies, Memphis, Tennessee). The components were placed in neutral orientation. The acromion was prepared for strain gauge placement. The bone was stripped of all soft tissue and periosteum. The surface was cleaned and dried with ethanol and sandpaper. Using adhesive glue, 4 strain gauges were placed along the acromion and scapular spine (Strain gauge model # KFH-06-120-C1-11L3M3R, OMEGA Engineering, Quebec, Canada). The strain gauges were left to set for 30 minutes once the adhesive was applied.

The placement of the strain gauges is described in Chapter 2. For summary, their location is reviewed below and shown in Figure 3-1:

1. Strain gauge 1 was placed midway between the anterior and posterior edge of the acromioclavicular (AC) joint, and midway between the medial and lateral edge of the acromial tip. The strain gauge was positioned in line with the anterior acromion, with the gauge leads exiting posteriorly.
2. Strain gauge 2 was placed halfway between the leading edge of SG 3 and the lateral edge of the acromion. The strain gauge was positioned in line with the scapular spine, with the gauge leads exiting medially.
3. Strain gauge 3 was placed directly above the spinoglenoid notch. The strain gauge was positioned in line with the scapular spine, with the gauge leads exiting medially.
4. Strain gauge 4 was placed 2 cm medial to the first strain gauge, measured from the leading edge (lateral edge) of both gauges. The strain gauge was positioned in line with the scapular spine, with the gauge leads exiting medially.

Strain gauge leads were then connected through a data acquisition unit (National Instruments, Model # NI USB-9237) to a central computer for data collection.

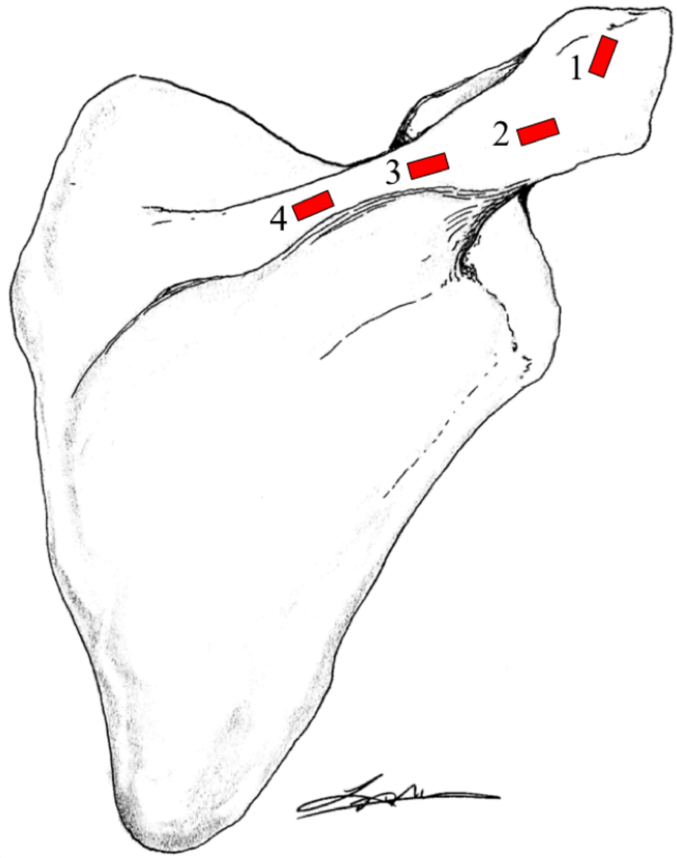

Figure 3-1: Strain Gauge Placement

Illustration depicting the anatomic location of the 4 strain gauges on a right scapula.

3.2.2 Shoulder Simulator

The shoulder simulator used in this study is the same as that described in Chapter 2. To review, a scapular clamp was drilled into the lateral scapular body in order to mount the specimens onto the shoulder simulator. The shoulder simulator consisted of a load cell that was mounted to an abduction arc. The specimen was positioned as described in Chapter 2. The same deltoid muscle loading ratios were used in this study. To review, deltoid muscle loading ratios were calculated for shoulder abduction (15% anterior deltoid, 70% middle deltoid, 15% posterior deltoid) and flexion (40% anterior deltoid, 50% middle deltoid, 10% posterior deltoid) based on previous biomechanical data (Ackland, Roshan-Zamir, Richardson & Pandy, 2011). The rotator cuff had a combined load of 10 N applied by the simulator.

3.2.3 Testing Protocol

Once the specimen was appropriately mounted, the moment arm length was measured. This was defined by the distance from the center of rotation (COR) of the glenosphere to the distal aspect of the humerus at the point that it contacted the load cell. The moment arm length allowed for conversion of the abduction force to an abduction moment, as measured by the load cell.

Using a custom modular RTSA system (Giles, Langohr, Johnson & Athwal, 2015; Langohr, Giles, Athwal & Johnson, 2015), three implant configurations were evaluated in a randomized order. These three implants all had varying NSA of 135°, 145°, and 155° (Figure 1-16). The remainder of the implant parameters remained unchanged: 5 mm glenoid laterl offset with 0 mm of inferiorization, 5 mm humeral lateralization, and 42 mm glenosphere and humeral cup size.

For each of these three configurations, static range of motion was simulated in a similar fashion as described in Chapter 2. This included 0° and 90° abduction in the scapular plane (scaption), and 0° and 90° forward flexion. Again, elevation was measured at 60° of glenohumeral elevation in both planes, which corresponds to 90° of humerothoracic elevation. Similar to Chapter 2, deltoid force was applied by computer-controlled pneumatic actuators until a target abduction moment of 1.5 N·m was reached as measured by the load cell. Ten seconds of data was captured once deltoid force reached a steady state. This cycle was repeated three times for each plane of elevation.

3.2.4 Outcome Variables

This study targeted the same outcome variables as those described in Chapter 2. The principal outcome variable was acromial strain. This was measured by 4 strain gauges placed along the acromion and scapular spine. Strain values were analyzed in microstrain units (μStrain, strain x 10^6). Total deltoid force was also recorded as a secondary outcome. This represents the efficiency of the deltoid in its ability to abduct or forward flex the arm in order to reach a target moment of 1.5 N·m, as measured by the load cell. Both of these outcome variables were measured for all three implant configurations, in four planes of elevation, and repeated three times at each level for accuracy.

3.2.5 Statistical Analysis

Statistical analysis was similar to that described in Chapter 2. A three-way (NSA, plane of elevation, angle of elevation) repeated measures analysis of variance (RM-ANOVA) was used for statistical analysis (SPSS Version 25.0; SPSS Inc, Chicago, IL, USA). Pairwise comparisons and analyses of interactions were performed to assess for significance. Statistical significance was defined as $p < 0.05$. A sample size of eight specimens had been chosen based on previous similar biomechanical cadaver studies (Ackland, Roshan-Zamir, Richardson & Pandy, 2011; Chan et al., 2017; Schwartz et al., 2013). All outcome variables that reached statistical significance were found to have a power greater than 0.8.

3.3 Results

3.3.1 Acromial Strain

3.3.1.1 The Effect of Neck-Shaft Angle on Acromial Strain

Figure 3-3 shows the results of NSA on acromial strain for each strain gauge at each plane of elevation. With a change in NSA, no statistically significant effect was measured on acromial strain ($p>0.136$). In abduction, an overall trend of decreased strain with increasing NSA was noted, however this did not reach statistical significance.

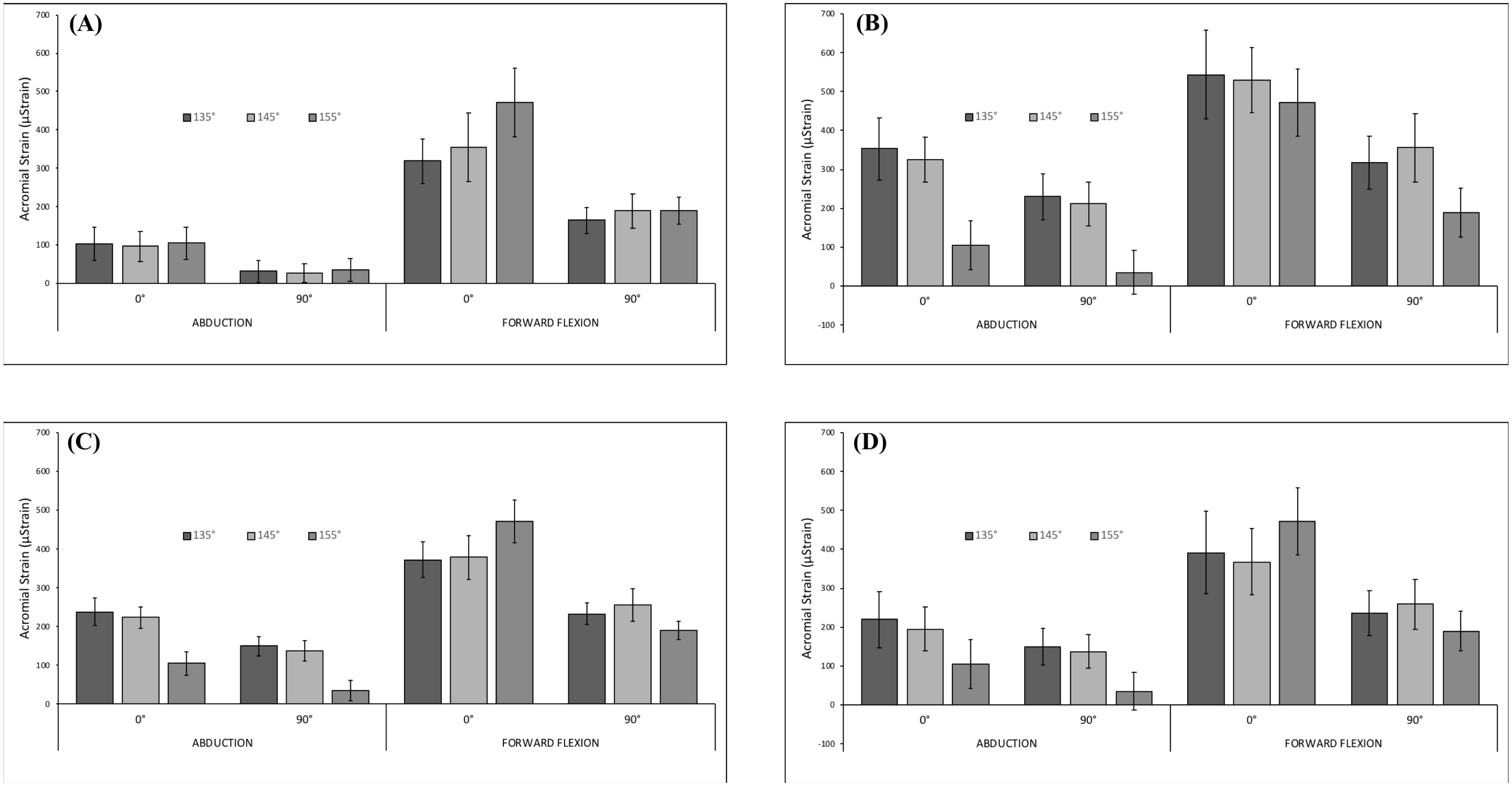

Figure 3-2: The Effect of Neck-Shaft Angle on Acromial Strain

Mean (+/- 1 SD) acromial strain measured by (A) strain gauge 1, (B) strain gauge 2, (C) strain gauge 3, and (D) strain gauge 4 for increasing neck-shaft angle (135°, 145°, 155°*) during all 4 planes of elevation.*

3.3.2 Total Deltoid Force

3.3.2.1 The Effect of Neck-Shaft Angle on Total Deltoid Force

Figure 3-4 shows the results of increasing NSA on total deltoid force. Overall, change in NSA was not shown to have a significant effect on total deltoid force (p>0.087).

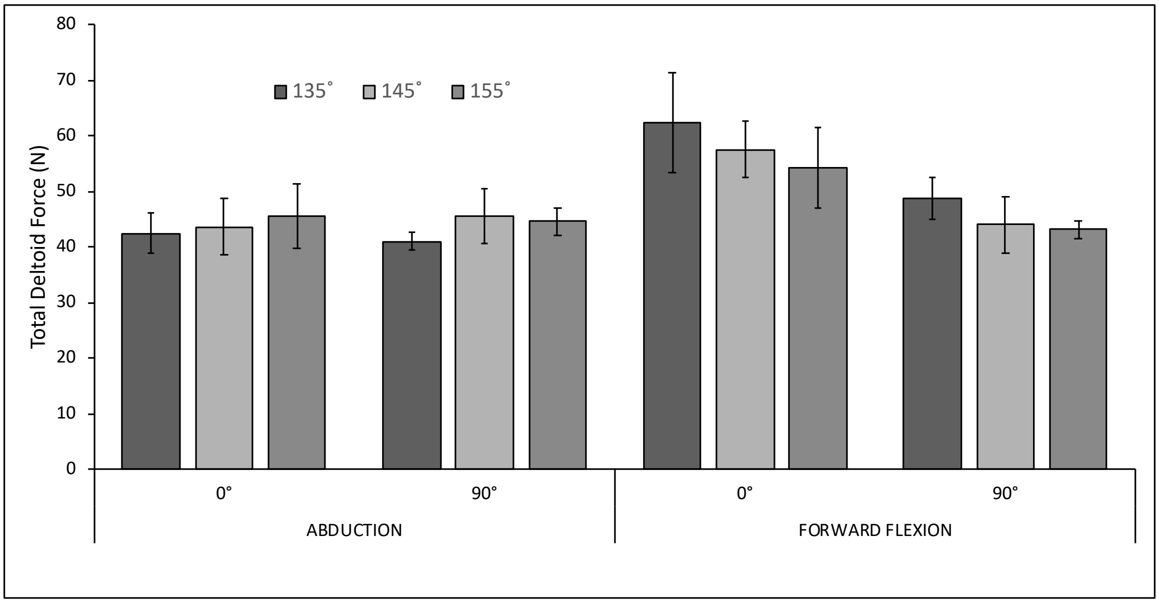

Figure 3-3: The Effect of Neck-Shaft Angle on Total Deltoid Force

Mean (+/- 1 SD) total deltoid force measured for increasing neck-shaft angle (135°, 145°, 155°) during all 4 planes of elevation.

3.4 Discussion

The primary objective of this study was to assess the role of NSA on acromial strain following RTSA implantation. This was measured using 4 strain gauges placed along the acromion and scapular spine. Through 4 planes of elevation (0° and 90° abduction, 0° and 90° forward flexion), no significant change in strain was measured as NSA was altered (135°, 145°, 155°).

Total deltoid force was measured as a secondary outcome. This included total force of all three heads of the deltoid required to achieve a target moment of 1.5 N·m, as measured by a load cell. Changing the NSA was not found to have a significant effect on total deltoid force required for abduction or forward flexion.

NSA has been thoroughly investigated for its role in range of motion and inferior scapular impingement. There exists a trade-off in range of motion, as a more varus neck allows for improved adduction by decreasing impingement, but limits abduction. This occurs as a lower humeral inclination causes a small increase in humeral offset, which may lead to impingement of the greater tuberosity on the acromion (Lädermann et al., 2015; Werner, Chaoui & Walch, 2017). Lädermann et al. demonstrated that with a decrease in humeral inclination from 155° to 135°, there was only a 2 mm increase in humeral offset (Lädermann et al., 2015). As such, the effect of this change in offset is likely negligible and supports the finding that NSA has no significant effect on acromial strain.

While not statistically significant, a trend was noted towards decreased strain with increased NSA with the arm in abduction, most notably measured by SG 2, SG 3 and SG4. A similar pattern was found in a finite element analysis by Langohr et al. who concluded that increasing the NSA lead to a decrease in maximum articular contact stress of the implant (Langohr et al., 2016). While implant contact stress and acromial strain are two separate entities, they exist within the same mechanical construct and thus may be interrelated.

Grammont's original design with a 155° valgus neck was felt to add length to the arm and thereby increase passive deltoid tension. Appropriate tensioning of the deltoid after RTSA implantation is felt to be important for avoiding complications; if deltoid is over-tensioned, it may cause undue stress on the acromion and a resultant acromial fracture, whereas if deltoid is not under adequate tension, this may cause instability of the implant (Boileau, Watkinson, Hatzidakis & Balg, 2005; Lädermann et al., 2009). In this study, the deltoid was released from its distal insertion on the humerus in order to mount it to the shoulder simulator. As such, the concept of NSA affecting deltoid tension was unable to be evaluated in this study.

3.4.1 Strengths and Limitations

This is the first cadaveric biomechanical study to examine the role of NSA on acromial strain following RTSA implantation. While many studies have examined RTSA implant parameters in a cadaveric model, none have focused specifically on acromial strain. Furthermore, few studies have examined both abduction and forward flexion in such a biomechanical model. This study utilized a custom designed prosthesis system which allowed for multiple implant configurations to be tested with only minor technical adjustments. This study also used a shoulder simulator apparatus which allowed for computer-controlled active shoulder motion and real-time feedback.

Cadaveric studies have inherent limitations. An attempt is always made to best replicate *in-vivo* mechanics and loading. Computer-controlled simulation cannot account for proprioception and dynamically changing muscle control. The specimens were dissected so that only the deltoid and rotator cuff muscles spanned the glenohumeral joint. The deltoid was also released from its distal insertion on the humerus, thereby eliminating the contribution of deltoid muscle tensioning. The present study did not account for scapulohumeral rhythm during humeral elevation, as the scapula was clamped to the shoulder simulator in a static state. However, based on a 2:1 scapulohumeral rhythm, 60° of glenohumeral elevation was used to simulate 90° of humerothoracic elevation (Inman, Saunders & Abbott, 1996). While a rotator cuff tear was simulated in this study with balanced anterior and posterior tendons, this does not necessarily recreate the *dynamic in-vivo* forces of patients with rotator cuff disease. Finally, despite static testing in 4 planes of elevation, this does not capture the true multiaxial and continuous nature of the glenohumeral joint.

3.5 Conclusions

This study provides further insight into the role of RTSA implant configurations. Specifically, this study has found that with all other parameters held constant, a change in NSA does not have a significant effect on acromial strain or total deltoid force required for abduction or forward flexion. This finding has importance in the future design and manufacturing of implants.

3.6 References

Ackland, D. C., Roshan-Zamir, S., Richardson, M., & Pandy, M. G. (2010). Moment Arms of the Shoulder Musculature After Reverse Total Shoulder Arthroplasty: *The Journal of Bone and Joint Surgery-American Volume*, *92*, 1221–1230.

Ackland, D. C., Roshan-Zamir, S., Richardson, M., & Pandy, M. G. (2011). Muscle and joint-contact loading at the glenohumeral joint after reverse total shoulder arthroplasty. *Journal of Orthopaedic Research*, *29*, 1850–1858.

Berliner, J. L., Regalado-Magdos, A., Ma, C. B., & Feeley, B. T. (2015). Biomechanics of reverse total shoulder arthroplasty. *Journal of Shoulder and Elbow Surgery*, *24*, 150–160.

Boileau, P., Gonzalez, J.-F., Chuinard, C., Bicknell, R., & Walch, G. (2009). Reverse total shoulder arthroplasty after failed rotator cuff surgery. *Journal of Shoulder and Elbow Surgery*, *18*, 600–606.

Boileau, P., Watkinson, D. J., Hatzidakis, A. M., & Balg, F. (2005). Grammont reverse prosthesis: Design, rationale, and biomechanics. *Journal of Shoulder and Elbow Surgery*, *14*, S147–S161.

Cezaryirliouglu, H., Bahniuk, E., Davy, D. T., & Heiple, K. G. (1985). Anisotropic yield behavior of bone under combined axial force and torque. *Journal of Biomechanics, 18*, 61-69.

Chan, K., Langohr, G. D. G., Mahaffy, M., Johnson, J. A., & Athwal, G. S. (2017). Does Humeral Component Lateralization in Reverse Shoulder Arthroplasty Affect Rotator

Cuff Torque? Evaluation in a Cadaver Model. *Clinical Orthopaedics and Related Research®*, *475*, 2564–2571.

Crosby, L. A., Hamilton, A., & Twiss, T. (2011). Scapula Fractures After Reverse Total Shoulder Arthroplasty: Classification and Treatment. *Clinical Orthopaedics and Related Research®*, *469*, 2544–2549.

Cuff, D. J., Pupello, D. R., Santoni, B. G., Clark, R. E., & Frankle, M. A. (2017). Reverse Shoulder Arthroplasty for the Treatment of Rotator Cuff Deficiency: A Concise Follow-up, at a Minimum of 10 Years, of Previous Reports*. *The Journal of Bone and Joint Surgery*, *99*, 1895–1899.

de Wilde, L. F., Poncet, D., Middernacht, B., & Ekelund, A. (2010). Prosthetic overhang is the most effective way to prevent scapular conflict in a reverse total shoulder prosthesis. *Acta Orthopaedica*, *81*, 719–726.

Drake, G. N., O'Connor, D. P., & Edwards, T. B. (2010). Indications for Reverse Total Shoulder Arthroplasty in Rotator Cuff Disease. *Clinical Orthopaedics and Related Research®*, *468*, 1526–1533.

Ek, E. T. H., Neukom, L., Catanzaro, S., & Gerber, C. (2013). Reverse total shoulder arthroplasty for massive irreparable rotator cuff tears in patients younger than 65 years old: results after five to fifteen years. *Journal of Shoulder and Elbow Surgery*, *22*, 1199–1208.

Ferrel, J. R., Trinh, T. Q., & Fischer, R. A. (2015). Reverse Total Shoulder Arthroplasty Versus Hemiarthroplasty for Proximal Humeral Fractures: A Systematic Review. *Journal of Orthopaedic Trauma*, *29*, 60-68.

Flury, M. P., Frey, P., Goldhahn, J., Schwyzer, H.-K., & Simmen, B. R. (2011). Reverse shoulder arthroplasty as a salvage procedure for failed conventional shoulder replacement due to cuff failure—midterm results. *International Orthopaedics*, *35*, 53–60.

Frankle, M., Levy, J. C., Pupello, D., Siegal, S., Saleem, A., Mighell, M., & Vasey, M. (2006). The Reverse Shoulder Prosthesis for Glenohumeral Arthritis Associated with Severe Rotator Cuff Deficiency: A Minimum Two-Year Follow-up Study of Sixty Patients Surgical Technique. *JBJS Essential Surgical Techniques*, *os-88*, 178–190.

Gallinet, D., Ohl, X., Decroocq, L., Dib, C., Valenti, P., & Boileau, P. (2018). Is reverse total shoulder arthroplasty more effective than hemiarthroplasty for treating displaced proximal humerus fractures in older adults? A Systematic Review and Meta-Analysis. *Orthopaedics & Traumatology: Surgery & Research*. doi:10.1016/j.otsr.2018.04.025

Giles, J. W., Langohr, G. D. G., Johnson, J. A., & Athwal, G. S. (2015). Implant Design Variations in Reverse Total Shoulder Arthroplasty Influence the Required Deltoid Force and Resultant Joint Load. *Clinical Orthopaedics and Related Research®*, *473*, 3615–3626.

Hamid, N., Connor, P. M., Fleischli, J. F., & D'Alessandro, D. F. (2011). Acromial Fracture After Reverse Shoulder Arthroplasty. *American Journal of Orthopedics, 40,* e125–129.

Hattrup, S. J. (2010). The Influence of Postoperative Acromial and Scapular Spine Fractures on the Results of Reverse Shoulder Arthroplasty. *Orthopedics*. doi:10.3928/01477447-20100329-04

Inman, V. T., Saunders, J. B., & Abbott, L. C. (1996). Observations of the Function of the Shoulder Joint. 1944. *Clinical Orthopaedics and Related Research, 330*, 3–12.

Kontaxis, A., & Johnson, G. R. (2009). The biomechanics of reverse anatomy shoulder replacement – A modelling study. *Clinical Biomechanics*, *24*, 254–260.

Lädermann, A., Denard, P. J., Boileau, P., Farron, A., Deransart, P., Terrier, A., Ston, J., & Walch, G. (2015). Effect of humeral stem design on humeral position and range of motion in reverse shoulder arthroplasty. *International Orthopaedics*, *39*, 2205–2213.

Lädermann, A., Williams, M. D., Melis, B., Hoffmeyer, P., & Walch, G. (2009). Objective evaluation of lengthening in reverse shoulder arthroplasty. *Journal of Shoulder and Elbow Surgery*, *18*, 588–595.

Langohr, G. D. G., Giles, J. W., Athwal, G. S., & Johnson, J. A. (2015). The effect of glenosphere diameter in reverse shoulder arthroplasty on muscle force, joint load, and range of motion. *Journal of Shoulder and Elbow Surgery*, *24*, 972–979.

Langohr, G. D. G., Willing, R., Medley, J. B., Athwal, G. S., & Johnson, J. A. (2016). Contact mechanics of reverse total shoulder arthroplasty during abduction: the effect of neck-shaft angle, humeral cup depth, and glenosphere diameter. *Journal of Shoulder and Elbow Surgery*, *25*, 589–597.

Leung, B., Horodyski, M., Struk, A. M., & Wright, T. W. (2012). Functional outcome of hemiarthroplasty compared with reverse total shoulder arthroplasty in the treatment of rotator cuff tear arthropathy. *Journal of Shoulder and Elbow Surgery*, *21*, 319–323.

Levy, J. C., Anderson, C., & Samson, A. (2013). Classification of Postoperative Acromial Fractures Following Reverse Shoulder Arthroplasty: *The Journal of Bone and Joint Surgery-American Volume*, *95*, e104-1–7.

Levy, J. C., Frankle, M., Mighell, M., & Pupello, D. (2007). The Use of the Reverse Shoulder Prosthesis for the Treatment of Failed Hemiarthroplasty for Proximal Humeral Fracture. *The Journal of Bone and Joint Surgery, 89,* 292–300.

Levy, J. C., Virani, N., Pupello, D., & Frankle, M. (2007). Use of the reverse shoulder prosthesis for the treatment of failed hemiarthroplasty in patients with glenohumeral arthritis and rotator cuff deficiency. *The Journal of Bone and Joint Surgery*, *89*, 189–195.

Mayne, I. P., Bell, S. N., Wright, W., & Coghlan, J. A. (2016). Acromial and scapular spine fractures after reverse total shoulder arthroplasty. *Shoulder & Elbow*, *8*, 90–100.

Nolan, B. M., Ankerson, E., & Wiater, J. M. (2011). Reverse Total Shoulder Arthroplasty Improves Function in Cuff Tear Arthropathy. *Clinical Orthopaedics and Related Research®*, *469*, 2476–2482.

Otto, R. J., Virani, N. A., Levy, J. C., Nigro, P. T., Cuff, D. J., & Frankle, M. A. (2013). Scapular fractures after reverse shoulder arthroplasty: evaluation of risk factors and the reliability of a proposed classification. *Journal of Shoulder and Elbow Surgery*, *22*, 1514–1521.

Rho, J. Y., Ashman, B. A., & Turner, C. H. (1993). Young's modulus of trabecular and cortical bone material: Ultrasonic and microtensile measurements. *Journal of Biomechanics, 26,* 111-119.

Sakoma, Y., Sano, H., Shinozaki, N., Itoigawa, Y., Yamamoto, N., Ozaki, T., & Itoi, E. (2011). Anatomical and functional segments of the deltoid muscle: Anatomical and functional segments of deltoid. *Journal of Anatomy*, *218*, 185–190.

Schairer, W. W., Nwachukwu, B. U., Lyman, S., Craig, E. V., & Gulotta, L. V. (2015). National utilization of reverse total shoulder arthroplasty in the United States. *Journal of Shoulder and Elbow Surgery*, *24*, 91–97.

Schwartz, D. G., Kang, S. H., Lynch, T. S., Edwards, S., Nuber, G., Zhang, L.-Q., & Saltzman, M. (2013). The anterior deltoid's importance in reverse shoulder arthroplasty: a cadaveric biomechanical study. *Journal of Shoulder and Elbow Surgery*, *22*, 357–364.

Sebastiá-Forcada, E., Cebrián-Gómez, R., Lizaur-Utrilla, A., & Gil-Guillén, V. (2014). Reverse shoulder arthroplasty versus hemiarthroplasty for acute proximal humeral fractures. A blinded, randomized, controlled, prospective study. *Journal of Shoulder and Elbow Surgery*, *23*, 1419–1426.

Terrier, A., Reist, A., Merlini, F., & Farron, A. (2008). Simulated joint and muscle forces in reversed and anatomic shoulder prostheses. *The Journal of Bone and Joint Surgery. British Volume*, *90-B*, 751–756.

Teusink, M. J., Otto, R. J., Cottrell, B. J., & Frankle, M. A. (2014). What is the effect of postoperative scapular fracture on outcomes of reverse shoulder arthroplasty? *Journal of Shoulder and Elbow Surgery*, *23*, 782–790.

Walch, G., Mottier, F., Wall, B., Boileau, P., Molé, D., & Favard, L. (2009). Acromial insufficiency in reverse shoulder arthroplasties. *Journal of Shoulder and Elbow Surgery*, *18*, 495–502.

Walker, D. R., Struk, A. M., Matsuki, K., Wright, T. W., & Banks, S. A. (2016). How do deltoid muscle moment arms change after reverse total shoulder arthroplasty? *Journal of Shoulder and Elbow Surgery*, *25*, 581–588.

Walker, M., Willis, M. P., Brooks, J. P., Pupello, D., Mulieri, P. J., & Frankle, M. A. (2012). The use of the reverse shoulder arthroplasty for treatment of failed total shoulder arthroplasty. *Journal of Shoulder and Elbow Surgery*, *21*, 514–522.

Werner, B. S., Chaoui, J., & Walch, G. (2017). The influence of humeral neck shaft angle and glenoid lateralization on range of motion in reverse shoulder arthroplasty. *Journal of Shoulder and Elbow Surgery*, *26*, 1726–1731.

Werthel, J-D., Walch, G., Vegehan, E., Deransart, P., Sanchez-Sotelo, J., & Valenti, P. (2018). Lateralization in Reverse Shoulder Arthroplasty: a descriptive analysis of humeral and glenoid lateralization. *Not yet in print.*

Willis, M., Min, W., Brooks, J. P., Mulieri, P., Walker, M., Pupello, D., & Frankle, M. (2012). Proximal humeral malunion treated with reverse shoulder arthroplasty. *Journal of Shoulder and Elbow Surgery*, *21*, 507–513.

Wong, M. T., Langohr, G. D. G., Athwal, G. S., & Johnson, J. A. (2016). Implant positioning in reverse shoulder arthroplasty has an impact on acromial stresses. *Journal of Shoulder and Elbow Surgery*, *25*, 1889–1895.

Chapter 4

4 The Effect of Coracoacromial Ligament State on Acromial Strain

The coracoacromial (CA) ligament is known to play an important role in joint stability and proprioception in the native shoulder. In reverse total shoulder arthroplasty (RTSA), the anatomy is reversed, and the center of rotation is constrained, altering the biomechanics of the shoulder. The role of the CA ligament after RTSA implantation is largely unknown. This chapter will examine changes in acromial strain and deltoid force after complete incision of the CA ligament following RTSA implantation. This is the first biomechanical study to examine the role of the CA ligament in the RTSA construct.

4.1 Introduction

[NB: A portion of this material was presented in Chapters 1, 2 and 3 and is also included here in order to ensure that this chapter is in "article" format].

The coracoacromial (CA) ligament is a structure that runs from the inferior anterolateral acromion to the lateral boarder of the coracoid process (Figure 4-1). Based on anatomical studies, the CA ligament is known to be intimately related to the anterior deltoid where it originates off the acromion (Hunt, Moore & Krishnan, 2000). The CA ligament, along with the coracoid process and the acromion, make up an osseoligamentous complex known as the coracoacromial arch.

As part of the coracoacromial arch, the CA ligament has been described as a static stabilizer of the shoulder. Biomechanical studies have investigated the role of the CA ligament in the native shoulder, specifically focusing on humeral head translation before and after ligament resection. These studies have found that the CA ligament is an important secondary restraint to anterior and superior migration of the humeral head (Lee, Black, Tibone & McMahon, 2001; Wellmann et al., 2008). It has been demonstrated that after the CA ligament has been resected in the native shoulder, a resultant 25-30% increase in rotator cuff force is required to maintain glenohumeral mechanics (Budoff et al., 2016).

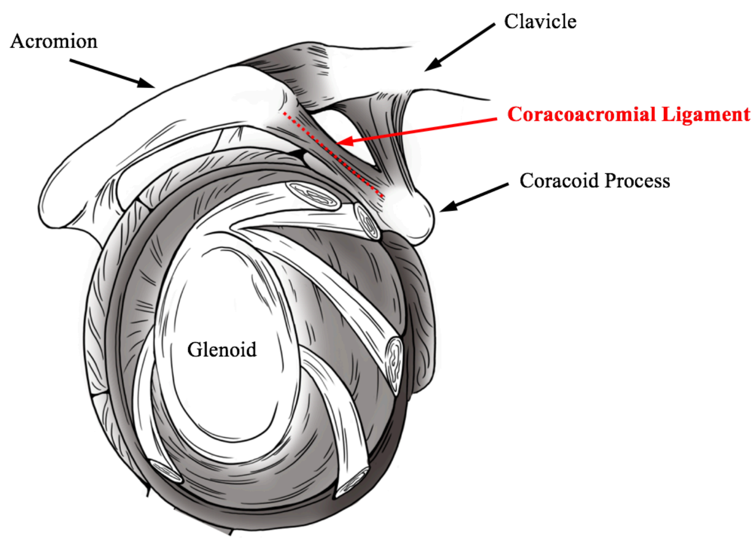

Figure 4-1: Anatomy of the Coracoacromial Ligament

Illustration depicting the anatomy of the CA ligament, running from the anterolateral acromion to the lateral coracoid process.

The CA ligament has also been described as a tension band, through which muscle forces exerted on the coracoid process are able to be transmitted to the acromion (Gallino, Battiston, Annaratone & Terragnoli, 1995). The CA ligament may also have a role in pain generation and proprioception. It is known to have a high density of mechanoreceptors. Diederichsen et al. found that with direct stimulation of the ligament, there was an involuntary loss of muscle control (Diederichsen et al., 2004). This suggests that the CA ligament may play a part in muscle coordination and proprioception.

Very few studies have focused on the role of the CA ligament in shoulder arthroplasty. A biomechanical study focusing on hemiarthroplasty after irreparable rotator cuff tear confirmed that even in this construct, the CA ligament acted as a restraint to anterosuperior dislocation (Hockman, Lucas & Roth, 2004). The authors went on to conclude that the coracoacromial arch itself may act as a superior fulcrum through which the humerus is able to produce functional range of motion.

There exists a lack of knowledge regarding the importance of the CA ligament in reverse total shoulder arthroplasty (RTSA) specifically. As previously discussed, RTSA is used successfully for many surgical indications including rotator cuff tear arthropathy, acute proximal humerus fractures, and revision arthroplasty (Boileau et al., 2009; Drake, O'Connor & Edwards, 2010; Ek, Neukom, Cantanzaro & Gerber, 2013; Ferrel, Trinh & Fischer, 2015; Flury et al., 2011; Gallinet et al., 2018; Leung, Horodyski, Struk & Wright, 2012; Levy, Frankle, Mighell & Pupello, 2007; Levy, Virani, Pupello & Frankle, 2007; Nolan, Ankerson & Wiater, 2011; Schairer et al, 2015; Sebastiá-Forcada, Cebrián-Gómez, Lizaur-Utrilla & Gil-Guillén, 2014; Walker et al., 2012; Willis et al., 2012). The RTSA construct itself dates back to the 1970s when Neer conceptualized the idea of reversing the "ball" and "socket" of the native glenohumeral joint in order to compensate for the rotator cuff-deficient shoulder. Paul Grammont later revised this design in 1985, with important modifications that are still used today. This design included a center of rotation (COR) that was medialized and distalized, which allowed the deltoid improved mechanical advantage. Additionally, the COR in this construct was fixed through range of motion, in contrast to the native glenohumeral joint. This allowed for maximal compressive forces at the joint while minimizing shear forces across the implant (Berliner, Regalado-Magdos, Ma & Feeley, 2015; Boileau, Watkinson, Hatzidakis & Balg, 2005; Boileau, Watkinson, Hatzidakis & Hovorka, 2006; Flatow & Harrison, 2011; Gerber & Nyffeler, 2009).

When considering the surgical approach to the shoulder for RTSA implantation, two main techniques have been described. Perhaps more commonly used is the deltopectoral approach, which utilizes the interval between anterior deltoid and pectoralis major to enter the joint and gain adequate exposure to the glenoid without compromising the deltoid muscle. It also allows for an extended incision in complex or revision cases (Nové-Josserand & Clavert, 2018). Conversely, less commonly used is the anterosuperior approach for RTSA which has been described as a "simpler" approach, with good glenoid exposure, less trauma to subscapularis, and a lower reported rate of post-operative glenohumeral instability (Molé et al., 2011). This technique utilizes a transdeltoid approach, in which deltoid is split between the anterior and middle heads, and the anterior deltoid is released off of the acromion along with the CA ligament. An important drawback of this approach includes compromise to the anterior deltoid (Molé et al., 2011; Nové-Josserand & Clavert, 2018). While several studies have compared the complications and outcomes of these two approaches, none have commented on the importance of the CA ligament.

The purpose of this *in-vitro* biomechanical cadaveric study was to further investigate and elucidate the role of the CA ligament in the RTSA construct with a focus on acromial loading. This was evaluated by measuring acromial strain and deltoid force before and after performing a full incision of the CA ligament. The custom modular RTSA system previously described was used, with implant parameters set at 145° neck-shaft angle, 5 mm glenoid lateral offset, and 5 mm humeral lateralization. Given the constrained design of the reverse implant, it was hypothesized that complete incision of the CA ligament would not cause any significant changes in acromial strain or deltoid force.

4.2 Materials and Methods

4.2.1 Specimen Preparation

[NB: Cadaveric specimen preparation is similar to that described in Chapters 2 and 3].

Eight fresh frozen right male cadaveric shoulders (8 males, mean age 73 years, range 61-88 years) were thawed for at least 24 hours prior to dissection. The humerus was transected midshaft in order to be mounted onto the shoulder simulator. Soft tissue dissection was carried out as is described in Chapters 2 and 3. This involved isolating the rotator cuff muscles and deltoid. Subscapularis muscle was reflected off of the subscapular fossa in order to enter the glenohumeral joint. The capsule was incised and resected circumferentially along with the glenoid labrum and articular cartilage. The coracoacromial (CA) ligament was left intact.

In order to mimic a rotator-cuff deficient shoulder, full-thickness supraspinatus and upper infraspinatus tears were created. Infraspinatus was released to the level of upper subscapularis tendon in order to create a symmetric force couple anteriorly and posteriorly. The anterior and posterior cuff were then tagged with a running locking #5 Ethibond suture (Ethibond, Ethicon, Johnson & Johnson, New Jersey, USA). The deltoid was then released distally from its insertion on the deltoid tuberosity. Based on the anatomic description by Sakoma et al. (Sakoma et al., 2011), the three heads of deltoid were identified and tagged using #5 Ethibond suture (Ethibond, Ethicon, Johnson & Johnson, New Jersey, USA) as is described in Chapters 2 and 3.

The specimen was then prepared for RTSA implantation as described in Chapters 2 and 3. The custom RTSA system was implanted using a modified technique from the Wright Medical – Tornier Aequalis surgical technique manual (Wright Medical Technologies, Memphis, Tennessee). The components were all placed in anatomic alignment.

Finally, the surface of the acromion was prepared for strain gauge placement. All soft tissues were dissected off the bone, being careful not to disrupt the tendon origin of the deltoid. Ethanol was used to clean and degrease the bone surface, followed by sandpaper. Adhesive glue was then used to apply four strain gauges along the acromion and scapular spine (Strain gauge model # KFH-06-120-C1-11L3M3R, OMEGA Engineering, Quebec, Canada). The strain gauges were left to set for 30 minutes after the adhesive was applied.

As described in Chapters 2 and 3, the strain gauges were placed in relation to specific landmarks for reproducibility (Figure 4-2):

1. Strain gauge 1 was placed midway between the anterior and posterior edge of the acromioclavicular (AC) joint, and midway between the medial and lateral edge of the acromial tip. The strain gauge was positioned in line with the anterior acromion, with the gauge leads exiting posteriorly.
2. Strain gauge 2 was placed halfway between the leading edge of SG 3 and the lateral edge of the acromion. The strain gauge was positioned in line with the scapular spine, with the gauge leads exiting medially.
3. Strain gauge 3 was placed directly above the spinoglenoid notch. The strain gauge was positioned in line with the scapular spine, with the gauge leads exiting medially.
4. Strain gauge 4 was placed 2 cm medial to the first strain gauge, measured from the leading edge (lateral edge) of both gauges. The strain gauge was positioned in line with the scapular spine, with the gauge leads exiting medially.

Strain gauge leads were then connected through a data acquisition unit (National Instruments, Model # NI USB-9237) to a central computer for data collection.

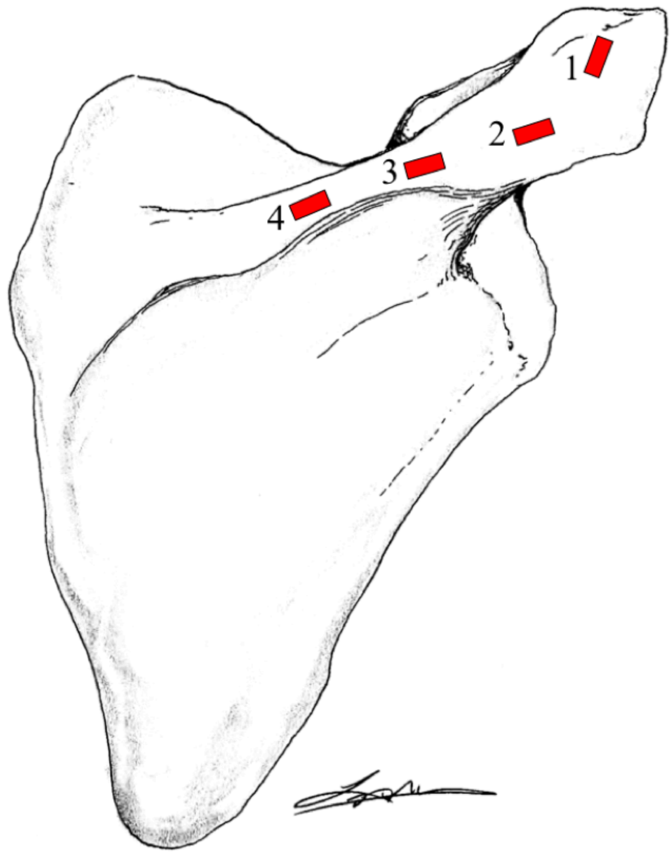

Figure 4-2: Strain Gauge Placement

Illustration depicting the anatomic location of 4 strain gauges on a right scapula.

4.2.2 Shoulder Simulator

The specimens were mounted onto the shoulder simulator using a scapular clamp that was drilled into the lateral scapular body. The shoulder simulator is described in Chapters 2 and 3. A load cell mounted onto an abduction arc allowed the humerus freedom of motion in all planes. Computer-controlled pneumatic actuators were used to apply loads to the three heads of deltoid. As per Chapters 2 and 3, deltoid muscle loading ratios were calculating from previous biomechanical data (Ackland, Roshan-Zamir, Richardson & Pandy, 2011). To review, this included deltoid muscle loading ratios for shoulder abduction (15% anterior deltoid, 70% middle deltoid, 15% posterior deltoid) and flexion (40% anterior deltoid, 50% middle deltoid, 10% posterior deltoid). The rotator cuff had a cumulative load of 10 N applied to maintain tension around the implant.

4.2.3 Testing Protocol

Once the specimen was prepared and mounted, the moment arm length was measured from the center of rotation (COR) of the glenosphere to the distal humerus where it contacted the load cell. In order to assess the role of the CA ligament, each specimen was tested in an "intact" state, followed by a "cut" state. For both shoulder states, the same implant parameters were used. Using a custom modular RTSA system (Giles, Langohr, Johnson & Athwal, 2015; Langohr, Giles, Athwal & Johnson, 2015), implant configuration included a neck-shaft angle of 145°, 5 mm glenoid lateral offset with 0 mm of inferiorization, 5 mm humeral lateralization, and 42 mm glenosphere and humeral cup size.

The specimens were first cycled through static range of motion in the "intact" state as described in Chapters 2 and 3. This included 0° and 90° abduction in the scapular plane (scaption), and 0° and 90° forward flexion. Elevation was defined as 60° of glenohumeral elevation, which corresponds to 90° of humerothoracic elevation. The simulator increased the deltoid force until it reached a target abduction moment of 1.5 N·m, as measured by the load cell. Data was then captured once a steady state was reached, and this was repeated three times for each plane of elevation.

Next, a complete release of the CA ligament was performed. To do so, the specimens were placed in 0° abduction and load was applied to the deltoid, as in the standard protocol. Once a steady state was reached, ten seconds of data were then captured during which the CA ligament was cut. The CA ligament was cut entirely off its coracoid attachment. Within this ten second window, three seconds of data was captured before and after CA ligament release. The testing protocol was then repeated in the "cut" state in the same fashion as described above.

4.2.4 Outcome Variables

The outcome variables of this study are similar to those described in Chapters 2 and 3. This includes acromial strain as a main outcome variable. This was measured by the 4 strain gauges placed along the acromion and scapular spine. Strain is defined as a change in length of a material over the original length, is reported as a ratio or a percentage. For the purpose of this study, strain values were analyzed in microstrain units (μStrain, strain x 10^6). Total deltoid force was measured as a secondary outcome in order to assess the efficiency of the deltoid across all implant configurations.

4.2.5 Statistical Analysis

A three-way (CA ligament state, plane of elevation, angle of elevation) repeated measures analysis of variance (RM-ANOVA) was used for statistical analysis (SPSS Version 25.0; SPSS Inc, Chicago, IL, USA). Pairwise comparisons and analyses of interactions were performed to assess for significance. Statistical significance was defined as $p < 0.05$. A sample size of eight specimens had been chosen based on previous similar biomechanical cadaver studies (Ackland, Roshan-Zamir, Richardson & Pandy, 2011; Chan et al., 2017; Schwartz et al., 2013). All statistically significant differences detected in the outcome variables were found to have a power greater than 0.8.

4.3 Results

4.3.1 Acromial Strain

4.3.1.1 The Effect of Coracoacromial Ligament State on Acromial Strain

Figure 4-4 shows the results of cutting the CA ligament on acromial strain for each strain gauge at each plane of elevation.

Overall, no significant change in strain was measured with release of the CA ligament ($p>0.078$). SG 3 was the only to measure a decrease in strain at 90° abduction ($p=0.032$). While not statistically significant, a trend was seen in all strain gauges towards increased acromial strain after the CA ligament was cut with the arm in 0° forward flexion. Strain gauges 1, 3 and 4 measured an increase in acromial strain that approached significance ($p=0.072$, $p=0.079$, $p=0.084$).

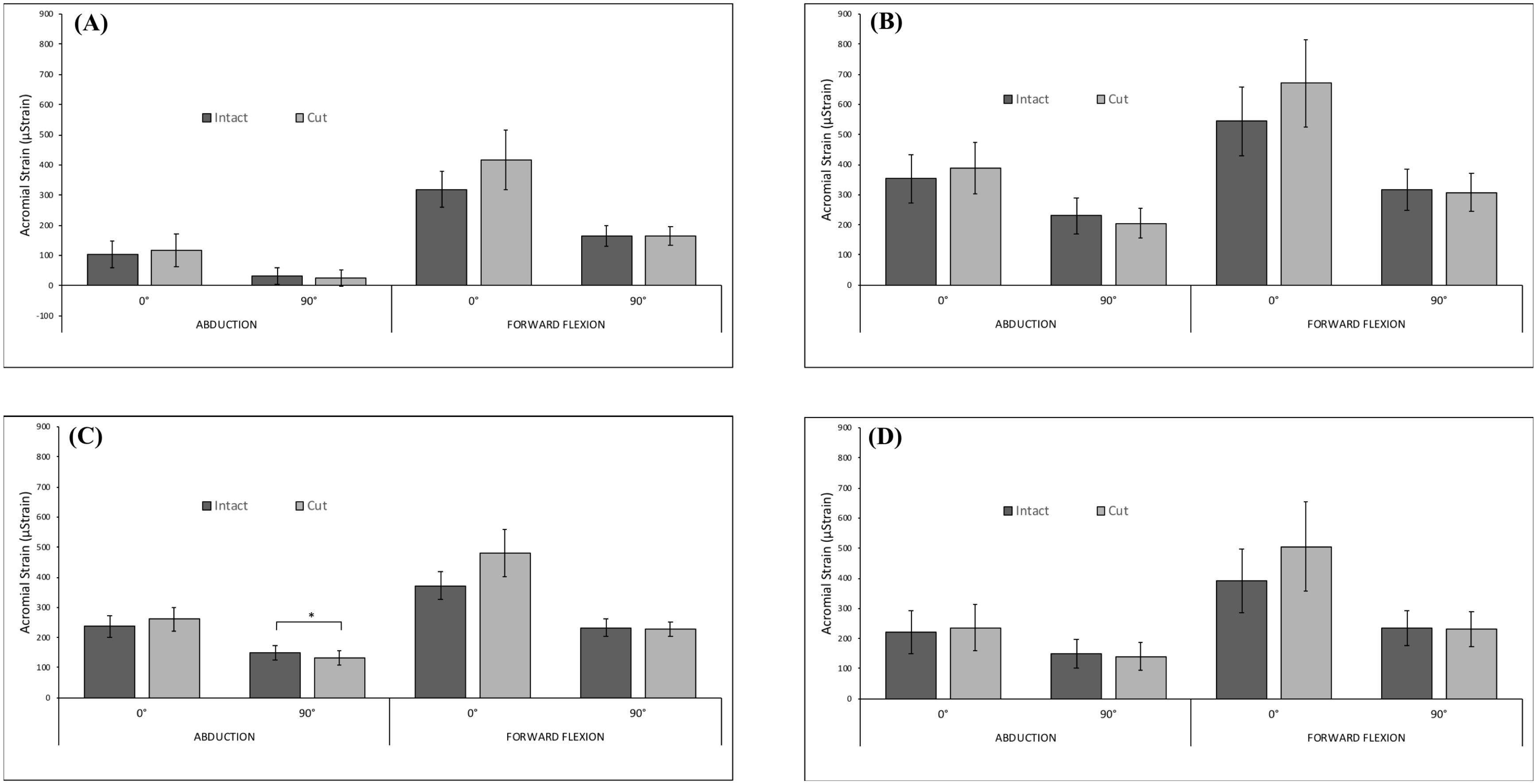

Figure 4-3: The Effect of Coracoacromial Ligament State on Acromial Strain

Mean (+/- 1 SD) acromial strain measured by (A) strain gauge 1, (B) strain gauge 2, (C) strain gauge 3, and (D) strain gauge 4 for both CA ligament states (cut vs. uncut) during all 4 planes of elevation. Significance (p<0.05) denoted with a ''.*

4.3.2 Total Deltoid Force

4.3.2.1 The Effect of Coracoacromial Ligament State on Total Deltoid Force

Figure 4-5 shows the results of cutting the CA ligament on total deltoid force. No significant effect was seen on total deltoid force once the CA ligament was cut. Similar to acromial strain, a trend was seen towards increased total deltoid force at 0° forward flexion once the CA ligament was cut.

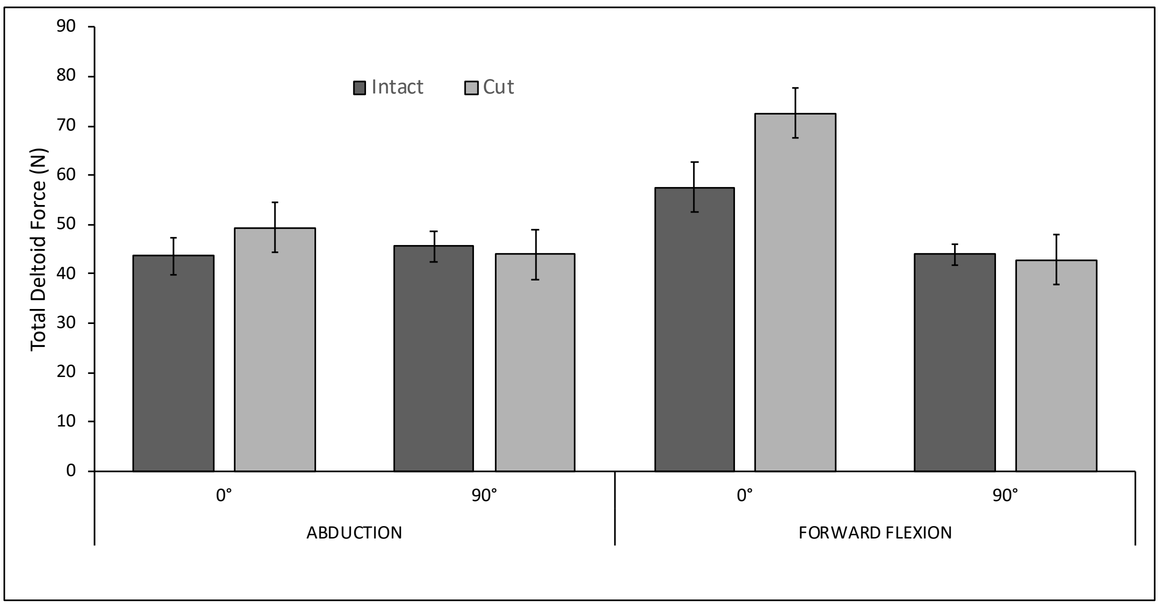

Figure 4-4: The Effect of Coracoacromial Ligament State on Total Deltoid Force

Mean (+/- 1 SD) total deltoid force measured for both CA ligament states (cut vs. uncut) during all 4 planes of elevation.

4.4 Discussion

The primary objective of this study was to assess the effect of CA ligament state on acromial strain following RTSA implantation. Strain was measured through 4 planes of elevation (0° and 90° abduction, 0° and 90° forward flexion) before and after the CA ligament was cut. All other implant parameters were held constant (145° neck-shaft angle, 5 mm glenoid lateralization, 5 mm humeral lateralization). Overall, no significant change in strain was measured after the CA ligament was cut.

There currently exists no literature that examines the role of the CA ligament in RTSA in any capacity. As such, the hypothesis of this study was based on the existing knowledge surrounding both CA ligament and RTSA biomechanics. In the native shoulder, the CA ligament is known to prevent superior and anterior migration of the humeral head, acting to stabilize the glenohumeral joint through range of motion (Budoff et al., 2016; Lee, Black, Tibone & McMahon, 2001; Wellmann et al., 2008). The RTSA construct hinges on a fixed center of rotation, which is thought to minimize shear force and maximize compressive force through the bone-implant interface and allow for a large arc of motion (Berliner, Regalado-Magdos, Ma & Feeley, 2015; Boileau, Watkinson, Hatzidakis & Balg, 2005; Boileau, Watkinson, Hatzidakis & Hovorka, 2006; Flatow & Harrison, 2011; Gerber & Nyffeler, 2009). Hence, it is hypothesized that the constrained RTSA construct does not rely on the CA ligament for stability. This supports the findings of this study.

The CA ligament is also known to be intimately related to the anterior deltoid as it originates off the acromion and has been described as a structure that distributes muscle forces exerted between the acromion and the coracoid process (Gallino, Battiston, Annaratone & Terragnoli, 1995; Hunt, Moore & Krishnan, 2000). The extent of this is unknown. In this study, SG 1 was placed at the tip of the acromion in close proximity to the attachment of the CA ligament. Again, there was no significant change in strain measured in this area after cutting of the CA ligament. There was a trend towards increased strain at 0° forward flexion which did approach significance after the CA ligament was cut. Forward flexion does employ a higher percentage of anterior deltoid muscle fibers than abduction. Without the CA ligament intact, the anterior deltoid fibers may have increased tension and thus cause an increase in strain at the acromion. Again, total deltoid force did not have a significant change with cutting of the CA ligament, but a similar trend was seen at 0° forward flexion.

4.4.1 Strengths and Limitations

This is the first cadaveric biomechanical study to examine the effect of CA ligament state on acromial strain in the setting of RTSA. No previous study has commented on the role of the CA ligament in the RTSA construct, and this is the first to specifically examine acromial strain in this setting as well. The findings of this study provide relevant and important information for surgeons performing this procedure. The shoulder simulator used in this study allowed for real-time computer-controlled active shoulder range of motion in both abduction and forward flexion, and the placement of 4 strain gauges allowed for a detailed evaluation of strain distribution across the acromion.

Any biomechanical study that utilizes cadaveric specimens has inherent limitations. From a soft tissue perspective, it is difficult to replicate the true dynamic nature of *in-vivo* mechanics and joint loading. For appropriate specimen preparation, all soft tissues were dissected around the glenohumeral joint except for deltoid and the rotator cuff. The deltoid was required to be released from its distal insertion on the deltoid tuberosity in order to mount it to the simulator. While a rotator cuff tear was simulated, it does not necessarily reflect the true pathology that is seen in patients with chronic rotator cuff tear arthropathy. While an attempt was made to best mimic *in-vivo* shoulder biomechanics, this study did not account for scapulohumeral rhythm during humeral elevation and was limited to four planes of static elevation.

Another final limitation of this study was the sample size. A trend was seen towards statistical significance however p-values remained greater than 0.05. If more specimens had been included in the study, these results may have reached statistical significance.

4.5 Conclusions

This study provides further insight into the role of the CA ligament in the RTSA construct. This finding has importance in our understanding of shoulder biomechanics following RTSA as well as the significance of soft tissue disruption during surgical approaches to the shoulder. This study has found that disruption of the CA ligament has no effect on acromial strain or total deltoid force after RTSA implantation.

4.6 References

Ackland, D. C., Roshan-Zamir, S., Richardson, M., & Pandy, M. G. (2010). Moment Arms of the Shoulder Musculature After Reverse Total Shoulder Arthroplasty: *The Journal of Bone and Joint Surgery-American Volume*, *92*, 1221–1230.

Ackland, D. C., Roshan-Zamir, S., Richardson, M., & Pandy, M. G. (2011). Muscle and joint-contact loading at the glenohumeral joint after reverse total shoulder arthroplasty. *Journal of Orthopaedic Research*, *29*, 1850–1858.

Berliner, J. L., Regalado-Magdos, A., Ma, C. B., & Feeley, B. T. (2015). Biomechanics of reverse total shoulder arthroplasty. *Journal of Shoulder and Elbow Surgery*, *24*, 150–160.

Boileau, P., Gonzalez, J.-F., Chuinard, C., Bicknell, R., & Walch, G. (2009). Reverse total shoulder arthroplasty after failed rotator cuff surgery. *Journal of Shoulder and Elbow Surgery*, *18*, 600–606.

Boileau, P., Watkinson, D. J., Hatzidakis, A. M., & Balg, F. (2005). Grammont reverse prosthesis: Design, rationale, and biomechanics. *Journal of Shoulder and Elbow Surgery*, *14*, S147–S161.

Boileau, P., Watkinson, D. J., Hatzidakis, A. M., & Hovorka, I. (2006). Neer Award 2005: The Grammont reverse shoulder prosthesis: Results in cuff tear arthritis, fracture sequelae, and revision arthroplasty. *Journal of Shoulder and Elbow Surgery*, *15*, 527–540.

Budoff, J. E., Lin, C.-L., Hong, C.-K., Chiang, F. L., & Su, W.-R. (2016). The effect of coracoacromial ligament excision and acromioplasty on the amount of rotator cuff force production necessary to restore intact glenohumeral biomechanics. *Journal of Shoulder and Elbow Surgery*, *25*, 967–972.

Cezaryirliouglu, H., Bahniuk, E., Davy, D. T., & Heiple, K. G. (1985). Anisotropic yield behavior of bone under combined axial force and torque. *Journal of Biomechanics, 18*, 61-69.

Chan, K., Langohr, G. D. G., Mahaffy, M., Johnson, J. A., & Athwal, G. S. (2017). Does Humeral Component Lateralization in Reverse Shoulder Arthroplasty Affect Rotator Cuff Torque? Evaluation in a Cadaver Model. *Clinical Orthopaedics and Related Research®*, *475*, 2564–2571.

Diederichsen, L. P., Nørregaard, J., Krogsgaard, M., Fischer-Rasmussen, T., & Dyhre-Poulsen, P. (2004). Reflexes in the shoulder muscles elicited from the human coracoacromial ligament. *Journal of Orthopaedic Research*, *22*, 976–983.

Drake, G. N., O'Connor, D. P., & Edwards, T. B. (2010). Indications for Reverse Total Shoulder Arthroplasty in Rotator Cuff Disease. *Clinical Orthopaedics and Related Research®*, *468*, 1526–1533.

Ek, E. T. H., Neukom, L., Catanzaro, S., & Gerber, C. (2013). Reverse total shoulder arthroplasty for massive irreparable rotator cuff tears in patients younger than 65 years old: results after five to fifteen years. *Journal of Shoulder and Elbow Surgery*, *22*, 1199–1208.

Ferrel, J. R., Trinh, T. Q., & Fischer, R. A. (2015). Reverse Total Shoulder Arthroplasty Versus Hemiarthroplasty for Proximal Humeral Fractures: A Systematic Review. *Journal of Orthopaedic Trauma*, *29*, 60-68.

Flatow, E. L., & Harrison, A. K. (2011). A History of Reverse Total Shoulder Arthroplasty. *Clinical Orthopaedics and Related Research®*, *469*, 2432–2439.

Flury, M. P., Frey, P., Goldhahn, J., Schwyzer, H.-K., & Simmen, B. R. (2011). Reverse shoulder arthroplasty as a salvage procedure for failed conventional shoulder replacement due to cuff failure—midterm results. *International Orthopaedics*, *35*, 53–60.

Gallinet, D., Ohl, X., Decroocq, L., Dib, C., Valenti, P., & Boileau, P. (2018). Is reverse total shoulder arthroplasty more effective than hemiarthroplasty for treating displaced proximal humerus fractures in older adults? A Systematic Review and Meta-Analysis. *Orthopaedics & Traumatology: Surgery & Research*. doi:10.1016/j.otsr.2018.04.025

Gallino, M., Battiston, B., Annaratone, G., & Terragnoli, F. (1995). Coracoacromial ligament: A comparative arthroscopic and anatomic study. *Arthroscopy: The Journal of Arthroscopic & Related Surgery*, *11*, 564–567.

Gerber, C., & Nyffeler, R. W. (2009). Reverse Total Shoulder Arthroplasty. *Journal of the American Academy of Orthopaedic Surgeons*, *17*, 284–295.

Giles, J. W., Langohr, G. D. G., Johnson, J. A., & Athwal, G. S. (2015). Implant Design Variations in Reverse Total Shoulder Arthroplasty Influence the Required Deltoid Force and Resultant Joint Load. *Clinical Orthopaedics and Related Research®*, *473*, 3615–3626.

Hockman, D. E., Lucas, G. L., & Roth, C. A. (2004). Role of the Coracoacromial Ligament as Restraint after Shoulder Hemiarthroplasty: *Clinical Orthopaedics and Related Research*, *419*, 80–82.

Hunt, J. L., Moore, R. J., & Krishnan, J. (2000). The fate of the coracoacromial ligament in arthroscopic acromioplasty: An anatomical study. *Journal of Shoulder and Elbow Surgery*, *9*, 491–494.

Langohr, G. D. G., Giles, J. W., Athwal, G. S., & Johnson, J. A. (2015). The effect of glenosphere diameter in reverse shoulder arthroplasty on muscle force, joint load, and range of motion. *Journal of Shoulder and Elbow Surgery*, *24*, 972–979.

Lee, T. Q., Black, A. D., Tibone, J. E., & McMahon, P. J. (2001). Release of the coracoacromial ligament can lead to glenohumeral laxity: A biomechanical study. *Journal of Shoulder and Elbow Surgery*, *10*, 68–72.

Leung, B., Horodyski, M., Struk, A. M., & Wright, T. W. (2012). Functional outcome of hemiarthroplasty compared with reverse total shoulder arthroplasty in the treatment of rotator cuff tear arthropathy. *Journal of Shoulder and Elbow Surgery*, *21*, 319–323.

Levy, J. C., Anderson, C., & Samson, A. (2013). Classification of Postoperative Acromial Fractures Following Reverse Shoulder Arthroplasty: *The Journal of Bone and Joint Surgery-American Volume*, *95*, e104-1–7.

Levy, J. C., Frankle, M., Mighell, M., & Pupello, D. (2007). The Use of the Reverse Shoulder Prosthesis for the Treatment of Failed Hemiarthroplasty for Proximal Humeral Fracture. *The Journal of Bone and Joint Surgery, 89,* 292–300.

Levy, J. C., Virani, N., Pupello, D., & Frankle, M. (2007). Use of the reverse shoulder prosthesis for the treatment of failed hemiarthroplasty in patients with glenohumeral arthritis and rotator cuff deficiency. *The Journal of Bone and Joint Surgery*, *89*, 189–195.

Molé, D., Wein, F., Dézaly, C., Valenti, P., & Sirveaux, F. (2011). Surgical Technique: The Anterosuperior Approach for Reverse Shoulder Arthroplasty. *Clinical Orthopaedics and Related Research®*, *469*, 2461–2468.

Nolan, B. M., Ankerson, E., & Wiater, J. M. (2011). Reverse Total Shoulder Arthroplasty Improves Function in Cuff Tear Arthropathy. *Clinical Orthopaedics and Related Research®*, *469*, 2476–2482.

Nové-Josserand, L., & Clavert, P. (2018). Glenoid exposure in total shoulder arthroplasty. *Orthopaedics & Traumatology: Surgery & Research*, *104*, S129–S135.

Rho, J. Y., Ashman, B. A., & Turner, C. H. (1993). Young's modulus of trabecular and cortical bone material: Ultrasonic and microtensile measurements. *Journal of Biomechanics, 26,* 111-119.

Sakoma, Y., Sano, H., Shinozaki, N., Itoigawa, Y., Yamamoto, N., Ozaki, T., & Itoi, E. (2011). Anatomical and functional segments of the deltoid muscle: Anatomical and functional segments of deltoid. *Journal of Anatomy*, *218*, 185–190.

Schairer, W. W., Nwachukwu, B. U., Lyman, S., Craig, E. V., & Gulotta, L. V. (2015). Reverse shoulder arthroplasty versus hemiarthroplasty for treatment of proximal humerus fractures. *Journal of Shoulder and Elbow Surgery*, *24*, 1560–1566.

Schwartz, D. G., Kang, S. H., Lynch, T. S., Edwards, S., Nuber, G., Zhang, L.-Q., & Saltzman, M. (2013). The anterior deltoid's importance in reverse shoulder arthroplasty: a cadaveric biomechanical study. *Journal of Shoulder and Elbow Surgery*, *22*, 357–364.

Sebastiá-Forcada, E., Cebrián-Gómez, R., Lizaur-Utrilla, A., & Gil-Guillén, V. (2014). Reverse shoulder arthroplasty versus hemiarthroplasty for acute proximal humeral fractures. A blinded, randomized, controlled, prospective study. *Journal of Shoulder and Elbow Surgery*, *23*, 1419–1426.

Walker, M., Willis, M. P., Brooks, J. P., Pupello, D., Mulieri, P. J., & Frankle, M. A. (2012). The use of the reverse shoulder arthroplasty for treatment of failed total shoulder arthroplasty. *Journal of Shoulder and Elbow Surgery*, *21*, 514–522.

Wellmann, M., Petersen, W., Zantop, T., Schanz, S., Raschke, M. J., & Hurschler, C. (2008). Effect of Coracoacromial Ligament Resection on Glenohumeral Stability Under Active Muscle Loading in an In Vitro Model. *Arthroscopy: The Journal of Arthroscopic & Related Surgery*, *24*, 1258–1264.

Willis, M., Min, W., Brooks, J. P., Mulieri, P., Walker, M., Pupello, D., & Frankle, M. (2012). Proximal humeral malunion treated with reverse shoulder arthroplasty. *Journal of Shoulder and Elbow Surgery*, *21*, 507–513.

Chapter 5

5 Thesis Conclusions

Acromial insufficiency fractures following reverse total shoulder arthroplasty (RTSA) are poorly understood, a challenge to diagnose, and associated with inferior clinical outcomes. As RTSA becomes an increasingly utilized surgical procedure in the aging population, the incidence of this complication will likely increase. There is a paucity of literature focusing on factors to prevent or minimize acromial stress fractures. The purpose of this thesis was to utilize a cadaveric, biomechanical model to evaluate the role of RTSA implant configuration on acromial strain.

The primary objectives of this thesis were:

1. To evaluate the role of glenoid lateralization on acromial strain following reverse total shoulder arthroplasty implantation (Chapter 2).

2. To evaluate the role of humeral lateralization on acromial strain following reverse total shoulder arthroplasty implantation (Chapter 2).

3. To evaluate the role of neck-shaft angle on acromial strain following reverse total shoulder arthroplasty implantation (Chapter 3).

4. To evaluate the role of the coracoacromial ligament following reverse total shoulder arthroplasty implantation (Chapter 4).

5.1 *Summary of Chapter 2:* The Role of Glenoid and Humeral Lateralization on Acromial Strain

The purpose of this study was to evaluate the role of both glenoid lateralization and humeral lateralization on acromial strain following RTSA implantation. Total deltoid force was also measured as a secondary outcome.

In regards to glenoid lateralization, the hypothesis of this study was that increasing glenoid lateralization would correlate with an increase in acromial strain. This was based on previous biomechanical and computational literature, although no previous studies have evaluated acromial strain directly. The rationale was that with increased glenoid lateralization, the center of rotation (COR) is also lateralized, causing a decrease in deltoid moment arm, decreased deltoid efficiency, and a resultant increase in deltoid force required for range of motion. The results of this study showed that with increasing glenoid lateralization, there was a significant increase in acromial strain when the arm was in 0° forward flexion. There was a concurrent trend towards increased total deltoid force however this did not reach statistical significance. With the arm in other planes of elevation, a significant change in acromial strain was not measured.

For humeral lateralization, the hypothesis of this study was that increasing humeral lateralization would correlate with an increase in acromial strain. This was also based on previous literature, specifically a finite element analysis which found increased acromial stress with increased humeral lateralization. The biomechanical effect of humeral lateralization is difficult to interpret in a cadaver model. Multiple factors are at play, including deltoid tension which was not able to be assessed in this study. In fact, the results of this study found that increasing humeral lateralization lead to a decrease in acromial strain with the arm in abduction. This finding is supported by biomechanical literature which suggests that increased humeral lateralization causes a decrease in deltoid force required for abduction. In this study, increased humeral lateralization did not cause a significant change in total deltoid force.

This is the first biomechanical study to investigate the effect of glenoid and humeral component lateralization on acromial strain following RTSA implantation. The findings of this study provide an important contribution to the existing literature and are relevant for the future design and manufacturing of RTSA implants.

5.2 *Summary of Chapter 3*: The Role of Neck-Shaft Angle on Acromial Strain

The purpose of this study was to assess the role of neck-shaft angle (NSA) on acromial strain following RTSA implantation. Total deltoid force was measured as a secondary outcome.

The hypothesis of this study was that changing NSA would have no significant effect on acromial strain. This was assessed using a custom modular prosthesis system with neck-shaft angles of 135°, 145°, and 155° and all other implant parameters held constant. The rationale behind this hypothesis was that changing NSA results in a very small change in humeral offset, which is negligible for its effect on deltoid moment arm and acromial strain. Additionally, altering the inclination of the humeral stem has an implicated role in arm lengthening and deltoid tensioning, however this was not assessed in this study as the deltoid was released from its distal insertion. In fact, the results of this study found that changing NSA had no significant effect on acromial strain or total deltoid force required for range of motion.

This is the first biomechanical cadaveric study to investigate the effect of NSA on acromial strain following RTSA implantation. Again, the findings of this study have an important application for surgeons and implant manufacturers as the optimal implant configuration continues to be studied.

5.3 *Summary of Chapter 4:* The Effect of Coracoacromial Ligament State on Acromial Strain

The purpose of this study was to assess the effect of coracoacromial (CA) ligament state on acromial strain in the setting of RTSA. Total deltoid force was measured as a secondary outcome.

The hypothesis of this study was that disruption of the CA ligament would not cause a significant change in acromial strain or total deltoid force. The rationale behind this hypothesis is that the RTSA construct has a constrained COR. While the native shoulder relies on the CA ligament as a soft tissue stabilizer for superior and anterior head migration, the RTSA construct does not. The results of this study found that with disruption of the CA ligament, there was no change in strain or total deltoid force required for range of motion.

This is the first biomechanical study to investigate the role of the CA ligament in the RTSA construct. The results of this study provide an important and relevant contribution to the literature and to surgeons who employ this procedure.

5.4 Future Directions

The current study was able to evaluate 3 specific modifiable implant parameters and their effect on acromial strain: glenoid lateralization, humeral lateralization, and neck-shaft angle. Throughout the testing protocol, all other implant parameters remained constant. As such, the opportunity exists to continue exploring the topic of acromial strain through the assessment of other implant parameters, such as glenoid inferiorization, glenosphere diameter, and polyethylene thickness. Overall, a better understanding of acromial insufficiency fractures beyond implant configuration is warranted.

5.5 Significance

Reverse total shoulder arthroplasty is becoming a more widely used surgical procedure in the setting of rotator cuff tear arthropathy, proximal humerus fractures, and revision arthroplasty. Its use is continuing to grow and be adopted worldwide. With its increasing popularity comes a resultant increase in complications and adverse outcomes. Acromial insufficiency fractures are reported to occur in up to 10% of patients, usually within the first 3 to 10 months following surgery. Often underdiagnosed, this complication causes increased patient morbidity and poor clinical outcomes. With a wealth of literature focused on RTSA indications, biomechanics and outcomes, few studies have focused on acromial insufficiency fractures.

This study highlights the importance of how implant parameter selection can alter the biomechanics of the shoulder. It is important to take this into consideration when choosing a surgical implant. Considerations include functional range of motion, implant stability, contact mechanics, and acromial strain. While some of the implant parameters that were evaluated in this study are not able to be modified at time of surgery, they may be addressed at the manufacturing level, highlighting the significance of this study in future RTSA implant design. Table 5-1 outlines some commonly used commercial implants and their associated implant parameters as a reference.

Additional significant conclusions can be drawn from this study. The CA ligament has been shown to provide no additional stability to the RTSA construct, which may be of interest to surgeons as they plan their surgical approach and soft-tissue dissection. It was also concluded from this study that greater acromial strain and total deltoid force occurred with the arm in forward flexion, suggesting that excessive loading in this position should be limited during the post-operative period. Furthermore, the highest strain values were measured in the region of Levy type II acromial fractures in all implants tested, supporting the existing literature. Finally, when converting the measured strain in this study to stress at physiologic levels, these values approached if not exceeded the traumatic fracture yield of cortical bone. This suggests that the etiology of acromial fractures may be more of a traumatic fracture mechanism than was previously believed.

Manufacturer	Implant	Neck-Shaft Angle	Glenoid Lateralization (mm)	Humeral Lateralization (mm)
Arthrex	Univers 135°	135°	0	-5
Arthrex	Univers 155°	155°	0	-3
Aston	Duocentric	145°	5	7.7
Biomet	Comprehensive	147°	5	7.2
Biomet	TESS	150°	7	-1
DJO	Altivate	135°	4	-1.8
DePuy	Delta III	155°	2	-3.5
DePuy	DeltaXtend	155°	1.5	1
Exactech	Equinoxe	145°	2	4.8
FH Ortho	Arrow	155°	8.7	12.7
FH Ortho	Arrow II	155°	8.5	10.1
Fx Solutions	Humelock Reverse	145°	3.5	2
Fx Solution	Easytech	145°	3.5	4.9
Lima	SMR	150°	5	-3.5
Lima	SMR Stemless	140°	5	-2.2
Mathys	Affinis Reverse	155°	1.5	-5.4
Medacta	Shoulder System 145°	145°	4	1.7
Medacta	Shoulder System 155°	155°	4	2.6
Strkyer	ReUnion RSA	135°	2	7.1
Tornier	Aequalis	155°	0	1
Tornier	Aequalis II	155°	0	1
Tornier	Aequalis II + BioRSA	155°	7	1
Tornier	Ascend Flex 127.5°	145°	0	6.8
Tornier	Ascend Flex 132.5°	145°	0	4.6
Tornier	Ascend Flex 137.5°	145°	0	3.8
Tornier	Ascend Flex 132.5° + BioRSA	145°	7	4.6
Zimmer	Inverse Reverse	155°	6	6.4
Zimmer	Trabecular Metal	150°	2.5	0.5

Table 5-1: Commercial Implant Parameters

Adapted from Werthel et al., 2018.

APPENDIX A: Glossary of Terms

ABDUCTION	Movement away from the midline of the body
ADDUCTION	Movement towards the midline of the body
AMERICAN SHOULDER AND ELBOW SURGEON (ASES) SCORE	A standardized outcome score for the shoulder graded on a 100-point scale to assess pain and function
ANTERIOR	Located towards the front of the body in the sagittal plane
ARTHROPATHY	Disease of a joint
ARTHROPLASTY	Surgical reconstruction or artificial replacement of a joint
ARTICULAR CARTILAGE	Highly specialized connective tissue covering the articular surface of synovial joints
ARTICULATION	A joint; a connection between two or more bones

AVULSION FRACTURE	When a fragment of bone tears away from the main mass of bone by attached soft tissues
BURSA	A fluid-filled sac, usually around a joint
CADAVERIC	A part of a dead body used for scientific or medical research
CASE-CONTROL STUDY	Retrospective study to determine whether an exposure is associated with an outcome
CIRCUMDUCTION	Circular movement of a limb
COMPUTATIONAL MODEL	Use of a computer program to study a material
CONSTANT SCORE	A standardized outcome score for the shoulder graded on a 100-point scale to assess pain and function
COMPUTED TOMOGRAPHY (CT)	Cross-sectional imaging of the body using a series of x-rays
DISTAL	Located away from the trunk of the body

ELEVATION	Movement away from the body in any plane
EXTENSION	As it pertains to the arm, movement of the limb in a posterior direction in the sagittal plane
EXTERNAL ROTATION	Rotation away from the midline of the body, or laterally
FINITE ELEMENT ANALYSIS (FEA)	Computer analysis of a material using finite elements
FORWARD FLEXION	As it pertains to the arm, movement of the limb in an anterior direction in the sagittal plane
IMPINGEMENT	Abnormal contact of two or more bones or structures
INFERIOR	Located below
INTERNAL ROTATION	Rotation towards the midline of the body, or medially
IN-VITRO	Outside a living organism
IN-VIVO	Within a living organism

KINEMATICS	Mechanics focusing on the motion of objects without considering the contributing forces
LATERAL	Located away from the midline of the body in the coronal plane
MAGNETIC RESONANCE IMAGING (MRI)	Detailed imaging of the body using high-frequency radio waves from a strong magnetic field
MECHANICAL ADVANTAGE	Advantage gained by improving the effectiveness of a force
MEDIAL	Located towards the midline of the body in the coronal plane
MOMENT	Turning effect of a force (torque)
MOMENT ARM	Measured length between a joint axis and the force acting on that joint
MULTI-AXIAL	Movement in a number of axes
PERIPROSTHETIC	In close proximity to or surrounding a joint
PHYSIOLOGIC	Considered normal, not pathologic

PLANE OF ELEVATION	Degree of freedom in which a limb elevates
POSTERIOR	Located towards the back of the body in the sagittal plane
PROSPECTIVE STUDY	Longitudinal study that follows an outcome over time
PROXIMAL	Located towards the trunk of the body
RADIOGRAPH	An image produced by x-ray
RANDOMIZED CONTROLLED TRIAL (RCT)	A clinical trial in which interventions are allocated at random
RETROSPECTIVE STUDY	A study that looks back in time
RETROVERSION	Tilting or tipping backwards
SCAPTION	Abduction of the humerus in the scapular plane
SHEAR	Line of force parallel to an object
STRAIN	Change in length of a material over its original length

STRAIN GAUGE	A device used to measure strain of an object
STRESS	Force applied to a material per unit area
SUPERIOR	Located above
TRANSEPICONDYLAR AXIS	Axis in line with the medial and lateral epicondyles
ULTRASOUND (US)	Form of medical imaging used to examine anatomic structures using ultrasound waves
YOUNG’S MODULUS	Measure of elasticity or stiffness of a material

Curriculum Vitae

Alicia Kerrigan
Department of Surgery, Division of Orthopaedic Surgery
Western University
London, ON

EDUCATION

2017-2018	**Western University** *Department of Surgery* London, Ontario ▪ Master's of Surgery Program
2015-present	**Western University** *London Health Sciences Centre* London, Ontario ▪ Orthopaedic Surgery Residency Training Program
2011-2015	**Western University** *Schulich School of Medicine and Dentistry* London, Ontario ▪ Doctor of Medicine
2007-2011	**McGill University** *Anatomy and Cell Biology* Montreal, Quebec ▪ Bachelor of Science

MEDICAL LICENSURES

2015-present	College of Physicians and Surgeons of Ontario
2015-present	Canadian Medical Protective Association

PROFESSIONAL MEMBERSHIPS

2015-present	Canadian Orthopaedic Association
2015-present	Canadian Medical Association
2015-present	Ontario Medical Association

HONORS AND AWARDS

2017 **SANDY KIRKLEY AWARD**
- Top clinical science research paper presentation
- Awarded at the annual Western Orthopaedic Surgery Resident Research Day
- $1000

2013 **HIPPOCRATIC COUNCIL CLUB EXECUTIVE AWARD**
- Teddy Bear Hospital Project
- Recognizes exemplary club executives, specifically in the areas of budgeting, innovation and leadership

2008 **CANADIAN INTERUNIVERSITY SPORT ACADEMIC ALL-CANADIAN HONOUR ROLL**
- Awarded to University-level varsity athletes who achieve academic excellence

2003-2007 **DUKE OF EDINBURGH AWARD**
- A youth leadership program designed to promote personal development in four distinct areas: community service, personal skills, physical recreation and adventurous journey
- Received bronze, silver and gold awards

2007 **ONTARIO SCHOLAR**
- Awarded to high school graduates who achieve an average of 80% or greater

2007 **BILINGUAL DIPLOMA**
- Awarded to high school graduates who complete a select number of course studies in French

RESEARCH EXPERIENCE

Acromial Insufficiency Fractures in Reverse Total Shoulder Arthroplasty: A Biomechanical Study

- *Supervisors: Dr. George Athwal, Dr. Jim Johnson, Orthopaedic Surgery*
- Current Master's of Surgery Project

Review Article: Developmental Hip Dysplasia in Connective Tissue Disorders

- *Supervisor: Dr. Waleed Kishta, Paediatric Orthopaedic Surgery*
- Pending publication in The Journal of Bone and Joint Surgery

Clinical Features & Debates: Paediatric Femoral Shaft Fracture Management – Rigid Nailing

- *Supervisor: Dr. Debra Bartley, Paediatric Orthopaedic Surgery*
- Published in the Canadian Orthopaedic Association Bulletin (Spring 2018)

Magnetic Resonance Imaging Assessment of Acute Achilles Tendon Rupture Healing in Non-Operative Patients

- *Supervisor: Dr. Kevin Willits, Orthopaedic Surgery*
- Winner of Sandy Kirkley Award for best clinical research paper
- Podium Presentation at Western Department of Orthopaedic Surgery Resident Research Day, London, ON, October 2017
- Podium presentation at Ontario Medical Association Sport Medicine Conference, Toronto, ON, January 2018
- Podium presentation at Canadian Orthopaedic Resident Association Annual Conference, Victoria, BC, June 2018
- Poster presentation at Canadian Orthopaedic Research Society Annual Conference, Victoria, BC, June 2018

Radiographic Analysis of Surgically Treated Flatfoot Deformity in Children with Cerebral Palsy

- *Supervisors: Dr. Waleed Kishta, Dr. Megan Cashin, Paediatric Orthopaedic Surgery*
- Poster presentation at Western Orthopaedic Surgery Resident Research Day, London, ON, October 2016
- Podium presentation at Western Paediatric Surgery Research Day, London, ON, February 2017
- Poster presentation at The American Orthopedic Foot and Ankle Society Annual Meeting, Boston, MA, July 2018
- Accepted for podium presentation at the SICOT Orthopaedic World Congress, Montreal, QC, October 2018

PROFESSIONAL DEVELOPMENT

May 2016	AO North American, Continuing Medical Education; Principles of Fracture Management, Basic Course – Chicago, IL
Dec 2017	International Paediatric Orthopaedic Society Annual Meeting – Orlando, FL
Jan 2018	Ontario Medical Association Sport Medicine Conference – Toronto, ON
June 2018	Canadian Orthopaedic Association Annual Meeting – Victoria, BC
July 2018	American Orthopaedic Foot and Ankle Association Annual Meeting – Boston, MA

LANGUAGES

English – native language

French – speak and read at high proficiency, write at an intermediate level

Spanish – speak, read and write with basic competence